The inner Earth's magnetosphere: fields, currents and particles

Lecture given by Natalia Ganushkina

Research seminar on Sun-Earth connections

Friday February 10, 2006
12-14 a.m., D115

Introductory words

Size vs importance: Lyrics

All great (both bad and good) things start from something small…

Napoleon

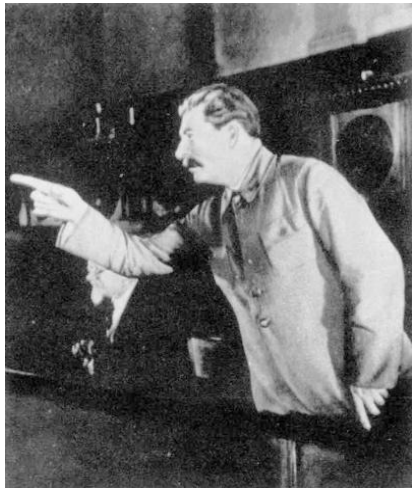

Stalin

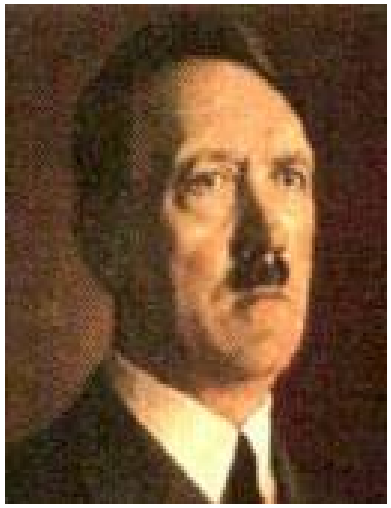

Hitler

They were not big men by size and, probably,
not very much impressive by appearance,
BUT, imagine,
how enormous was their
influence on our history…!!!

Size vs importance: Physics

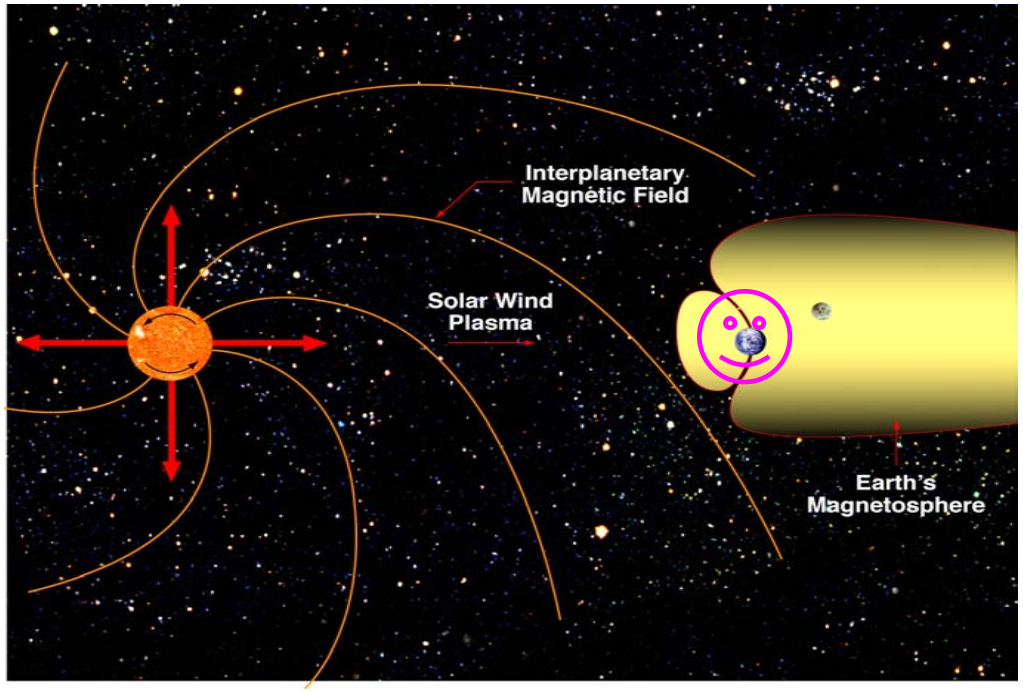

Inner magnetosphere has rather ***modest size***, with about 10 Re radius,

BUT the ***significance of the occurring processes*** is ENORMOUS

Although quite a significant progress has been made, inner magnetosphere is definitely ***worth of studying***

Dynamical inner magnetosphere: Overview

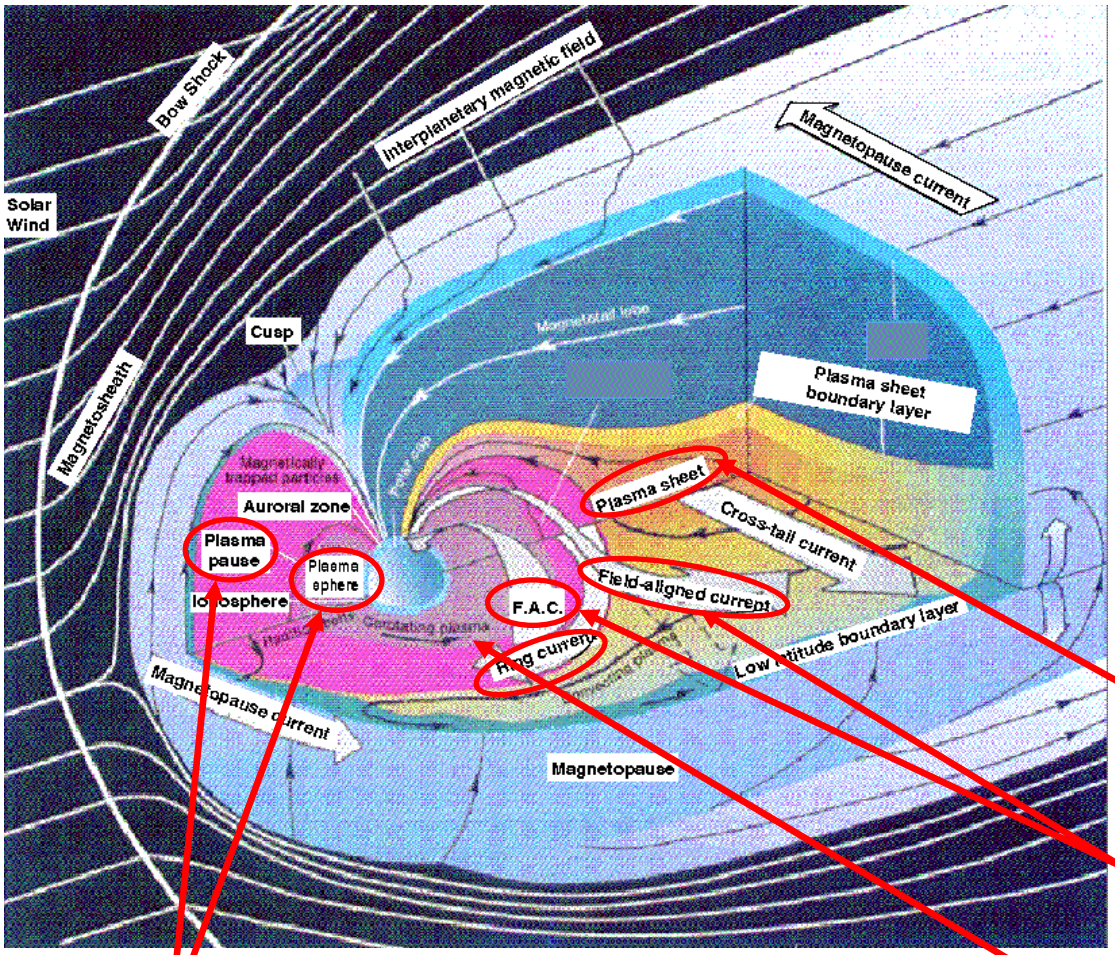

Plasma in magnetosphere:
mainly electrons and ions.

Sources of particles:
solar wind and ionosphere.

Plasma is grouped into different regions with different densities and temperatures.

Main regions:

- near Earth plasma sheet
(7-10 Re, n = 0.1-1 cm^{-3}, T=5 keV)

- field-aligned currents (~ 10^6 A)

- ring current (20-300 keV)
- radiation belts (up to MeVs) (2-7 Re)

- plasmasphere (< 4 Re, 10^3 cm^{-3}, 1 eV)
- plasmapause (sharp at 4 Re, drop to 1 cm^{-3})

Dynamical inner magnetosphere: Storms and substorms

The magnetosphere changes in a wide range of ***spatial and temporal*** scales.

Two characteristic dynamic processes

-account for most of the energy, momentum and plasma transport
- both from solar wind into the magnetosphere
- within the magnetosphere -- ionosphere system.

Magnetic storms

(several per month, associated with large
disturbances in the solar wind caused by solar eruptive events)
- lasting 1-5 days,
- ring current strongly enhanced,
- surface magnetic field at equator decreased up to 300 nT,
- significant auroral activity is observed.

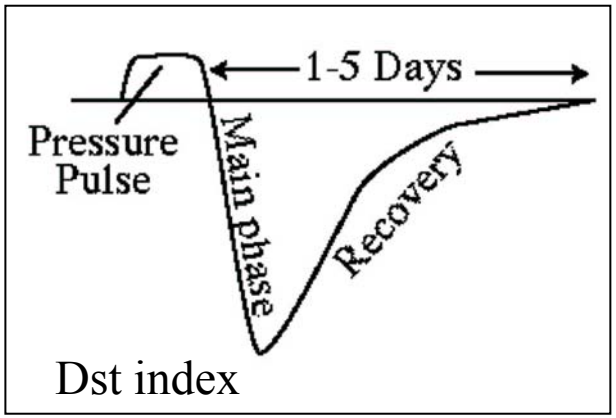

Magnetospheric substorms

(daily, under regular solar wind conditions)
- lasting 1-3 hours,
- injection of energetic particles into the inner magnetosphere,
- global reconfiguration of the magnetospheric magnetic field,
- intense auroral activity.

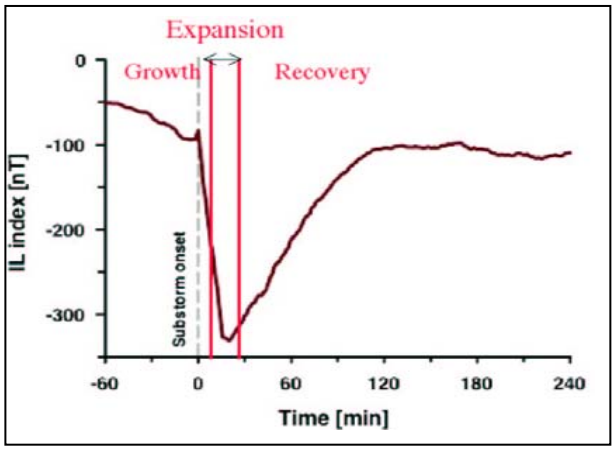

Magnetic storms, event overview

May 1-7, 1998 storm event overview

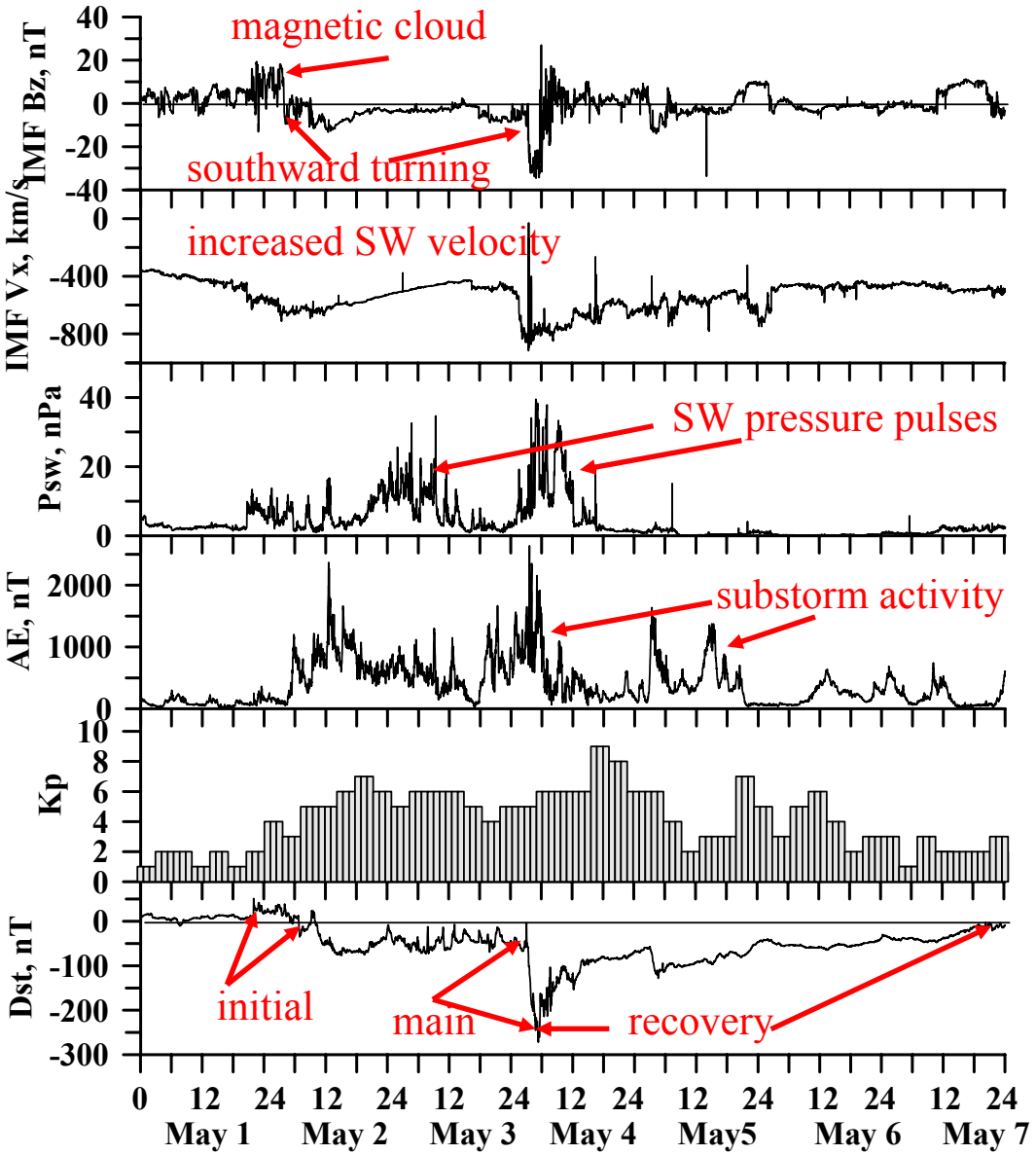

Initiated from extended period of solar activity started on April 29, 1998.
Several coronal mass ejections:
April 29th 1700 UT, May 1st 2340 UT,
May 2nd 0530 UT, May 4th 0200 UT.

May 4th 0400-0800 UT magnetopause as close as 5 Re.

The magnetospheric response
AE index

High Kp index

3 distinct Dst-enhancements:
May 2nd 0400 UT, -80 nT,
May 4th 0400 UT, -250 nT,
May 5th 0200 UT, -110 nT.

Magnetic storms, magnetospheric response

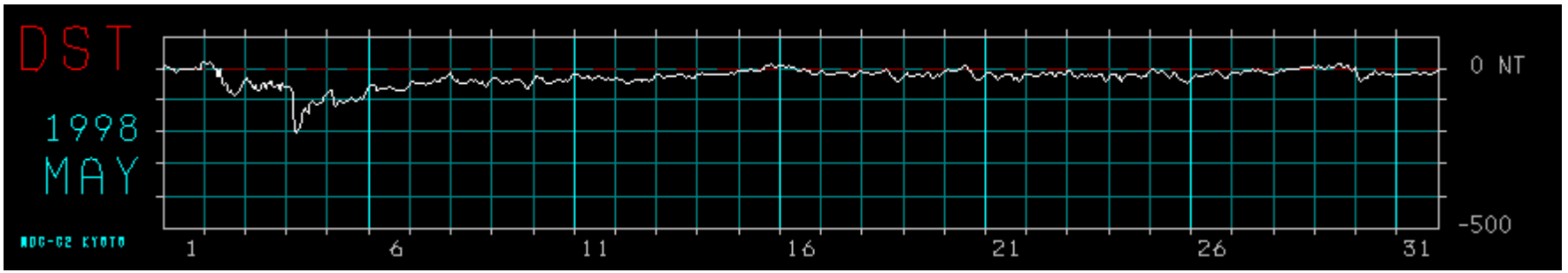

lasting 1-5 days, surface magnetic field at equator decreased up to 300 nT

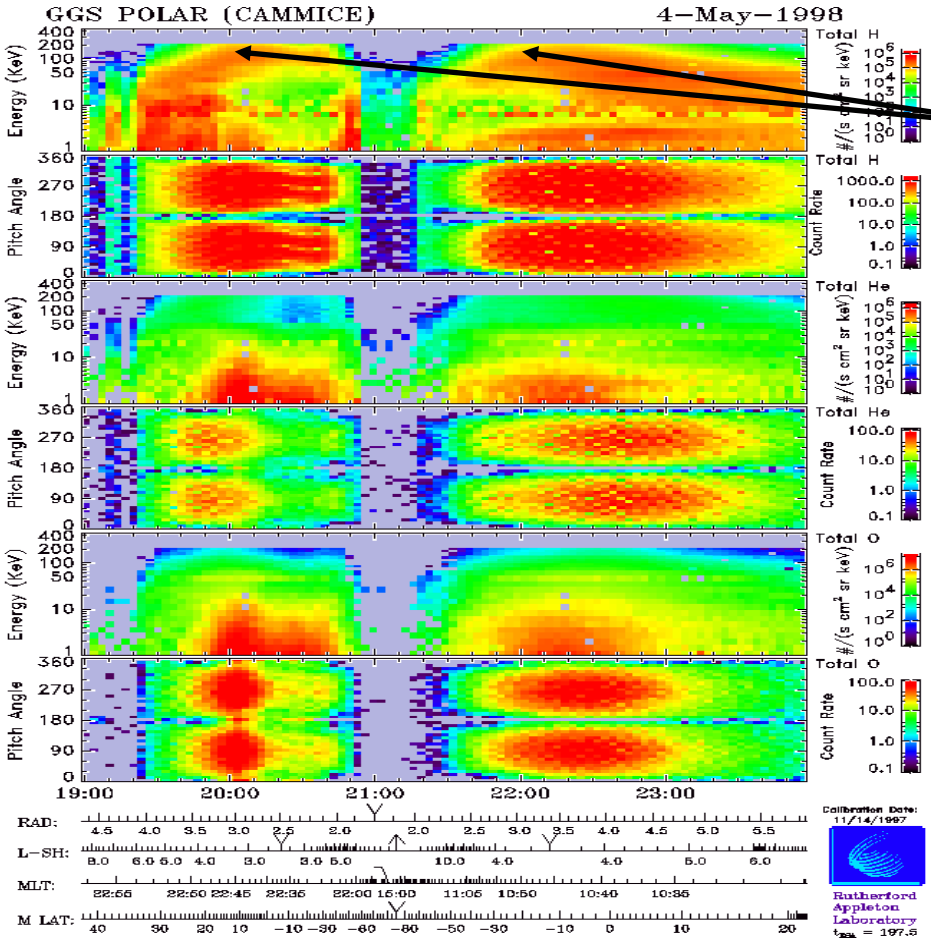

ring current strongly enhanced

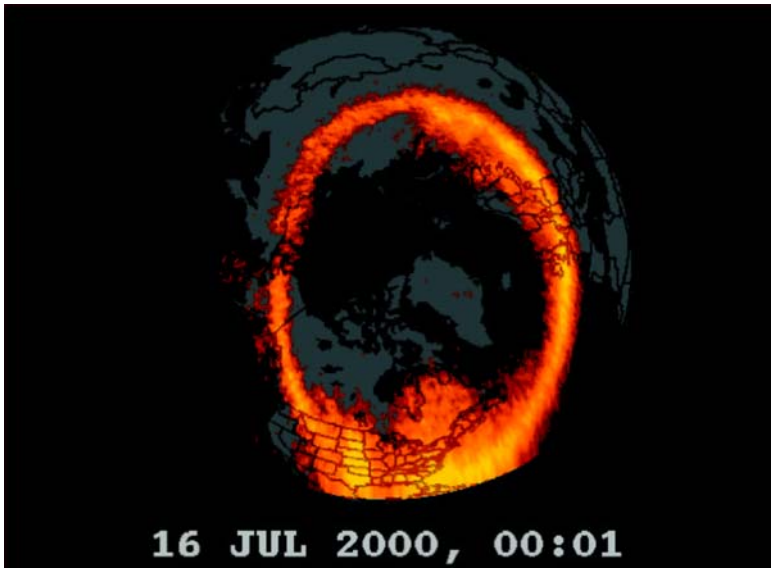

significant auroral activity is observed

Magnetospheric substorms

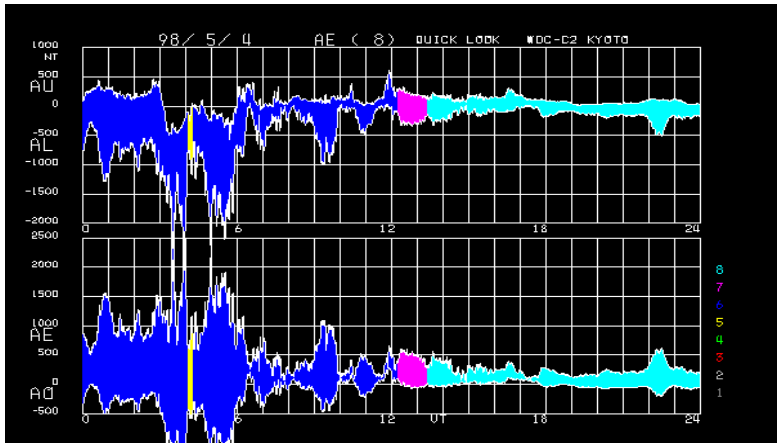

occur daily, lasting 1-3 hours

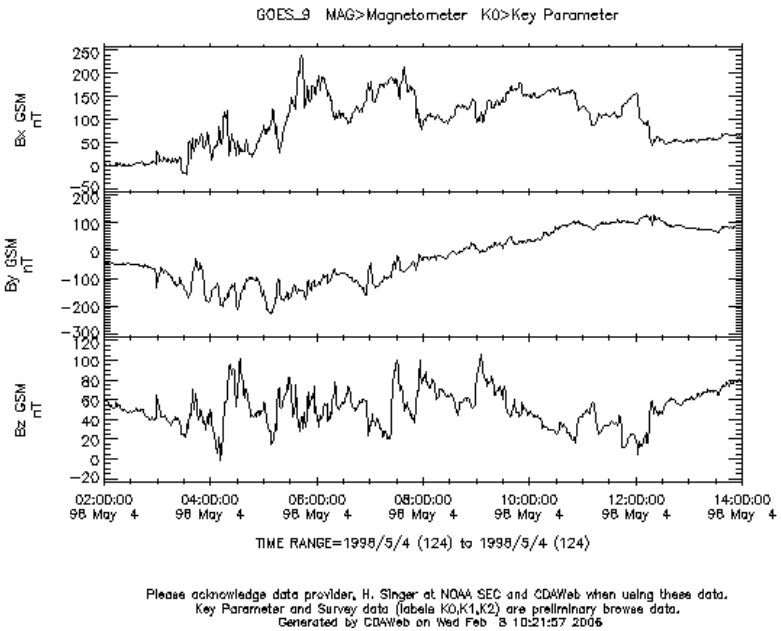

global reconfiguration of magnetic field

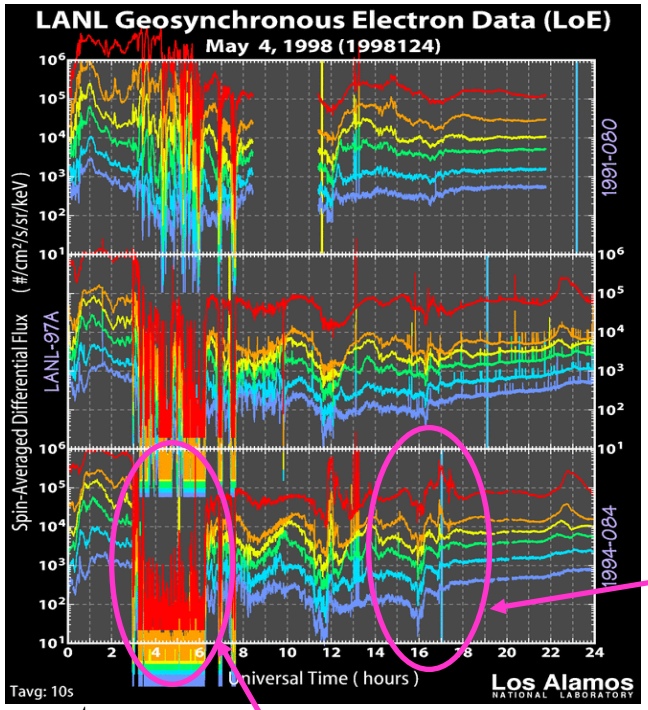

magnetopause crosses 6.6 Re orbit

injection of energetic particles into the inner magnetosphere

Intense auroral activity

Lecture logic

Charged ***particles move under Lorentz force*** in variable magnetic and electric fields.

Magnetic field models:
- accuracy and applicability for disturbed conditions are open questions.

Electric field models:
- **observations** are much fewer;
- electric field **nature** is still an open question;
- separation between **electric fields of different scales** is an open question;
- no comprehensive **models** exist for **smaller-scale fields and for distrubed conditions**.

Most important large-scale current system in the inner magnetosphere: ***ring current***.
- prediction of temporal changes in ring current - efforts in research on **space weather**;
- **processes of ring current formation and development** during storms are far from being fully understood;
- relative **importance of large-scale and smaller scale electric fields** in energization and transport of ions into the ring current is still an open question.

In this lecture these open questions will be addressed by using extensively the existing multi-satellite data sets as well as ground-based measurements and modern theoretical models.

Magnetospheric magnetic field modelling

Magnetospheric magnetic field modelling: Global and event-oriented

Global magnetospheric magnetic field models

- Most widely used (*Tsyganenko [1987, 1989], Tsyganenko [1995]*)
  Good representation of average magnetospheric configuration,
  fine structure of magnetic field during substorms and large magnetic field changes during storms were not accounted for.
- Storm-time models (*Alexeev et al. [1996], Tsyganenko [2002]*)
  model parameters for current systems fitted to entire data set,
  model magnetic field defined by assumed dependence on input parameters.

Event-oriented magnetospheric magnetic field models

- An accurate representation of magnetospheric configuration is of key importance for a specific event
- Study the evolution of different current systems during different storms and their relative contribution to Dst

Ganushkina et al., JGR, 2002; Ganushkina et al., AnnGeo, 2004

Storm-time magnetic field modelling: Ring current representation

Symmetric ring current = eastward + westward:

$$J(R,B/B_0)^{SYM} = -J_{0east}\exp\left(-\frac{(R_{eq}-R_{0east})^2}{2\sigma_{R_{eq}}^{\ 2}}\right)(B/B_0)^{-A/2} + J_{0west}\exp\left(-\frac{(R_{eq}-R_{0west})^2}{2\sigma_{R_{eq}}^{\ 2}}\right)(B/B_0)^{-A/2}$$

Asymmetric ring current = partial + closing Region 2 field-aligned currents :

$$J(R,B/B_0,\phi)^{ASYM} = J_{0part}\exp\left(-\frac{(R_{eq}-R_{0part})^2}{2\sigma_{Req}^2}\right)(B/B_0)^{-A/2}(1-C\cos(\phi-\delta))$$

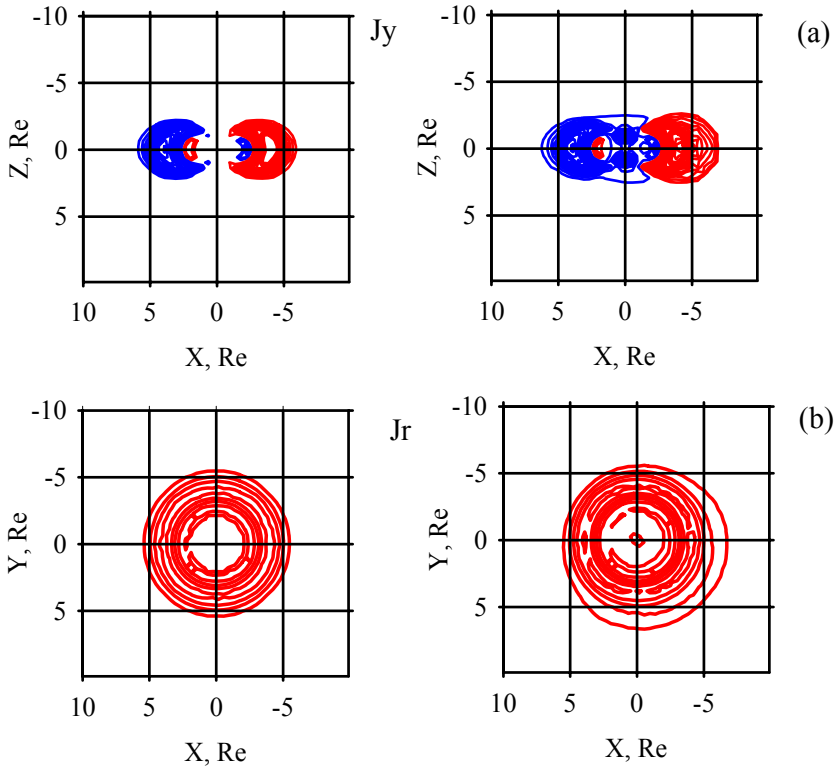

Local time asymmetry gives rise to field-aligned currents (calculated numerically)

Free parameters:

R_{0east}, R_{0west}, R_{0part},	mean radius
J_{0east}, J_{0west}, J_{0part},	maximum current density
σ_R,	width of current distribution
A,	anisotropy index
C,	constant
δ	duskward shift angle for partial RC

Storm-time magnetic field modelling: Addition of a new tail current sheet

Global changes:
intensification of the tail current (T89)
as a whole with amplification factor (1+ATS).
Local changes:
Adding a new thin tail current sheet.

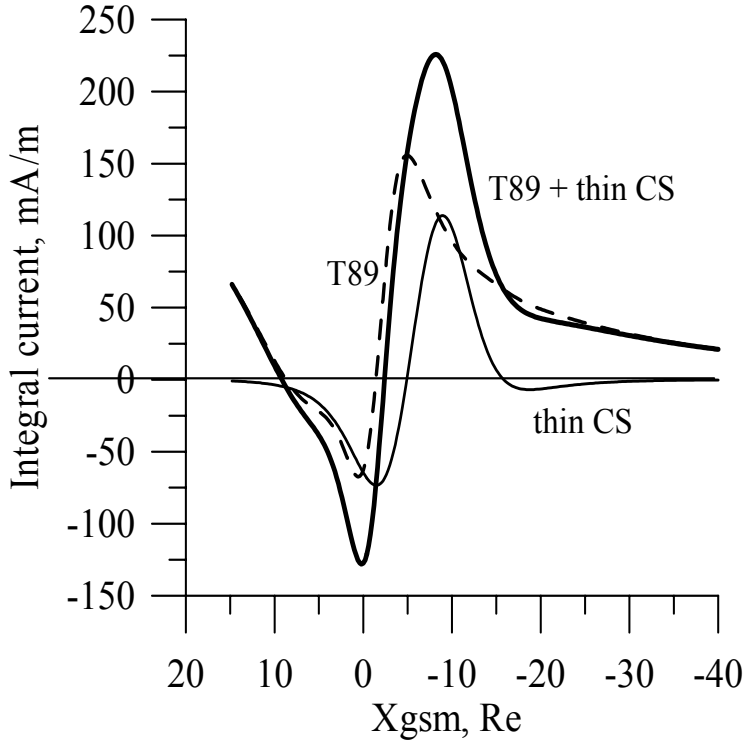

Two vector potentials, similar to T89:

$$A_1^T = \frac{W_2(x,y)}{S_T(z,a_T,D_0)+a_T+\xi_T(z,D_0)}\left(C_1+\frac{C_2}{S_T(z,a_T,D_0)}\right),$$

$$A_2^T = \frac{W_2(x,y)}{S_T(z,a_T,D_0)+a_T+\xi_T(z,D_0)}\left(C_1+\frac{C_2}{S_T(z,a_T,D_0)}\right),$$

With truncation factors:

$$W_1(x,y) = A_{ntc}\left(1-\frac{x-x_{1ntc}}{\left[\left(x-x_{1ntc}+D_x^2\right)\right]^{1/2}}\right)\left(1+y^2/D_y^2\right)^{-1}, \quad W_2(x,y) = A_{ntc}\left(1-\frac{x-x_{2ntc}}{\left[\left(x-x_{2ntc}+D_x^2\right)\right]^{1/2}}\right)\left(1+y^2/D_y^2\right)^{-1},$$

Subtracting $A_1^T - A_2^T \approx W_1(x,y) - W_2(x,y)$ gives a thin current sheet with finite x-scale, zero outside 25 Re.

Free parameters:

A_{ntc},	thin current sheet intensity
x_{1ntc}, x_{2ntc},	X_0 - location of steepest decrease of W(x,y)
D_0	D_0 - half-thickness of current sheet

Storm-time magnetic field modelling: Magnetopause currents

Scaling factor AMP=χ^3 for the magnetic field of Chapman-Ferraro currents at magnetopause, determined from solar wind pressure variations P_{SW}:

$$B_{CF} = \chi^3 B_{CF_{T89}}, \chi = \left(P_{SW} / \langle P_{SW} \rangle\right)^k, k \approx 1/6.$$

Parameter R_T , characteristic scale size of magnetotail, defined by solar wind parameters:

$$R_T = 30 R_E \frac{Z_{T,Shue}}{Z_{T,T89}},$$

30 R_E - parameter R_T in T89 Kp=4,

$Z_{T, Shue}$ - magnetopause position given by *Shue et al [1998]* model dependent on P_{SW} and IMF Bz at X= - 20 R_E , Y = 0,

$Z_{T, T89}$ - 'magnetopause' position given by T89 Kp= 4 model at X= - 20 R_E , Y = 0.

Event-oriented magnetospheric magnetic field modelling

Baseline model: Tsyganenko T89 Kp=4

Current system	Parameter	Status
Eastward RC	Roeast	2 Re
	Joeast	1.5 nA/m^2
Westward RC	Rowest	2.5 – 4.5 Re
	Jowest	1.5 – 15 nA/m^2
Partial RC	Ropart	5 – 6.5 Re
	Jopart	0.5 - 7 nA/m^2
	C	1
	σ	From Dst
Tail current	ATS	-0.5 – 2
	Antc	0.1 – 2.4
	X1ntc	- 2 Re
	X2ntc	- 10 Re
	Do	0.2 Re
Magnetopause currents	AMP	From SW
	RT	From SW & IMF

$\sigma = 0.8$
$A = 1$

$$\delta = \frac{\pi}{2}\tanh\frac{|Dst|}{Dst_0}, \qquad Dst_0 = 40\ nT$$

$$AMP = \left(P_{SW}/\langle P_{SW}\rangle\right)^k, k \approx 1/6.$$

$$R_T = 30R_E\frac{Z_{T,Shue}}{Z_{T,T89}},$$

Varying free parameters, we find the set of parameters that gives the best fit between model and in-situ field observations by **GOES 8 and 9, Polar, Geotail and Interball Tail** satellites and **Dst** (SYM-index) measurements.

Overview of four modelled storm events

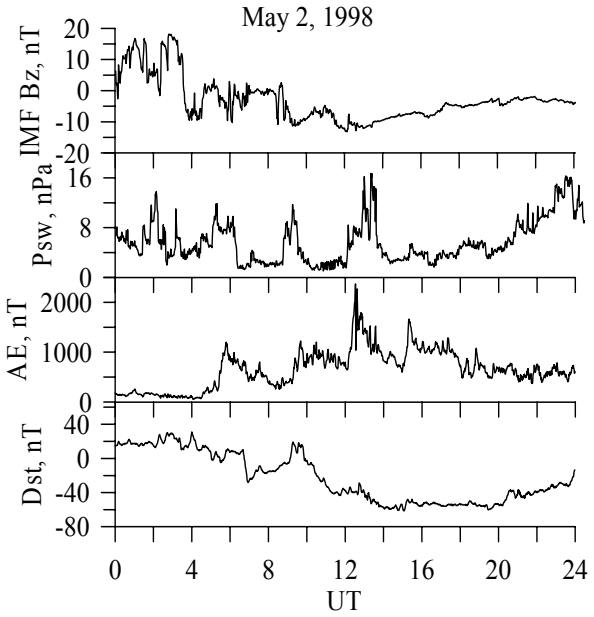

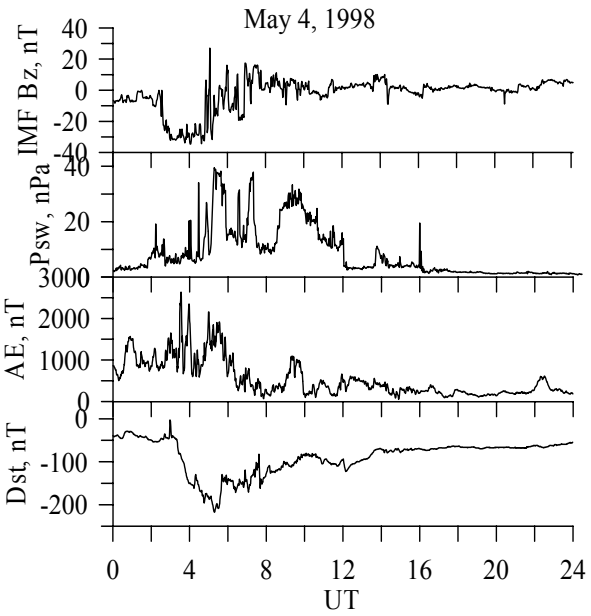

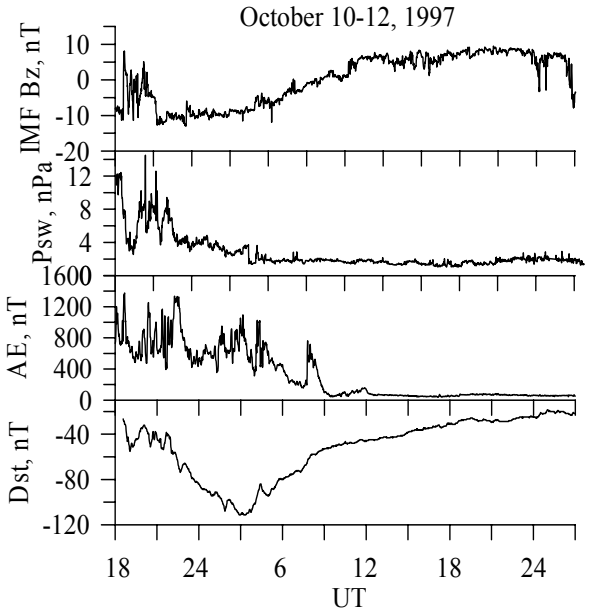

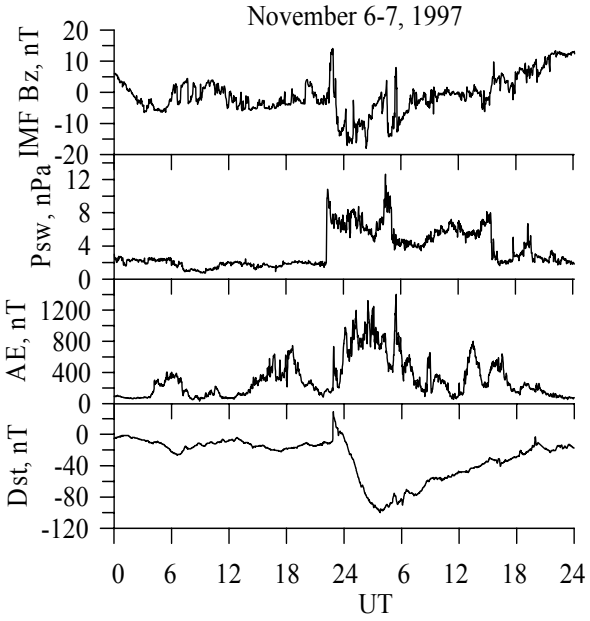

Modelling results: Magnetic field and Dst index (1)

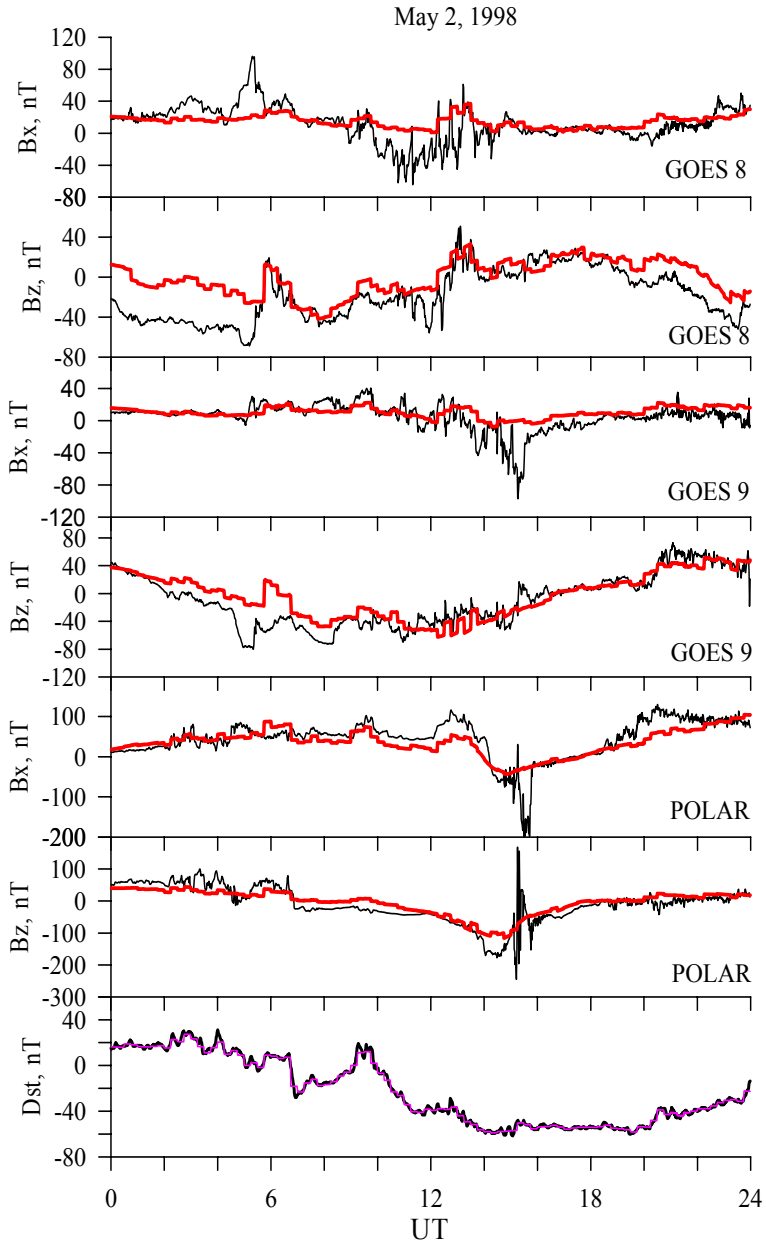

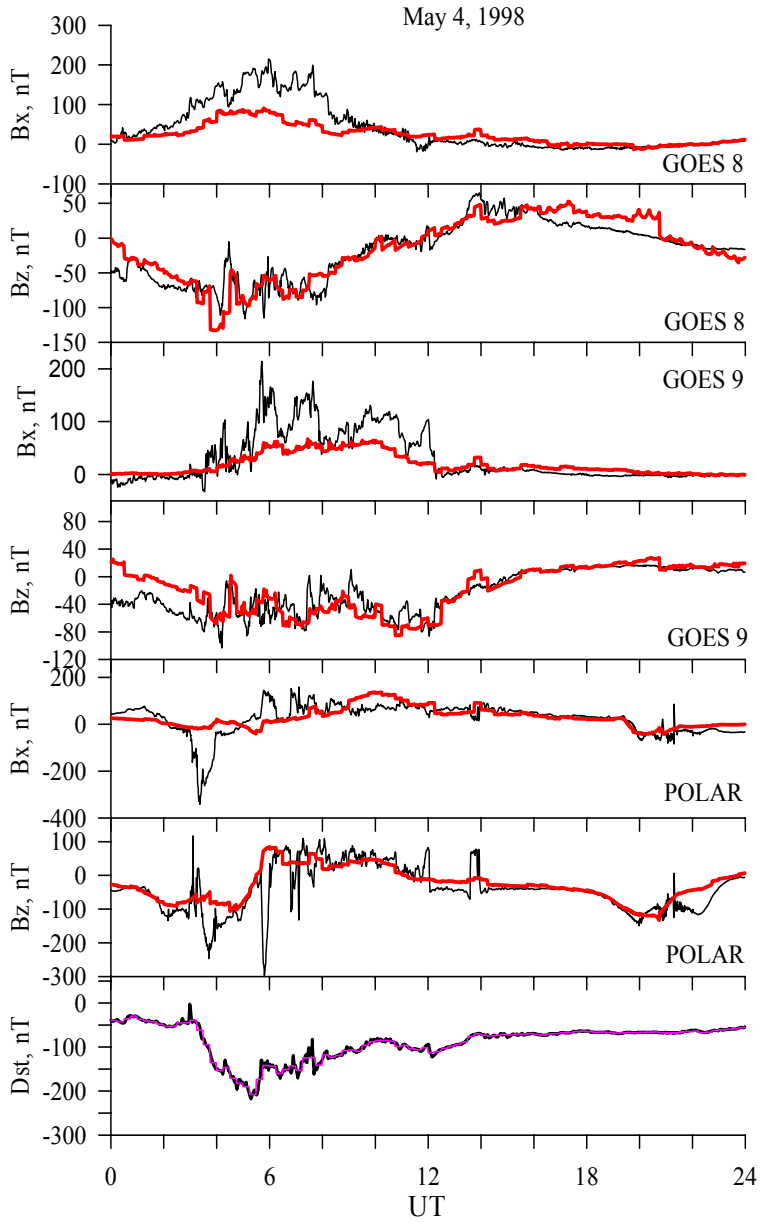

Modelling results: Magnetic field and Dst index (2)

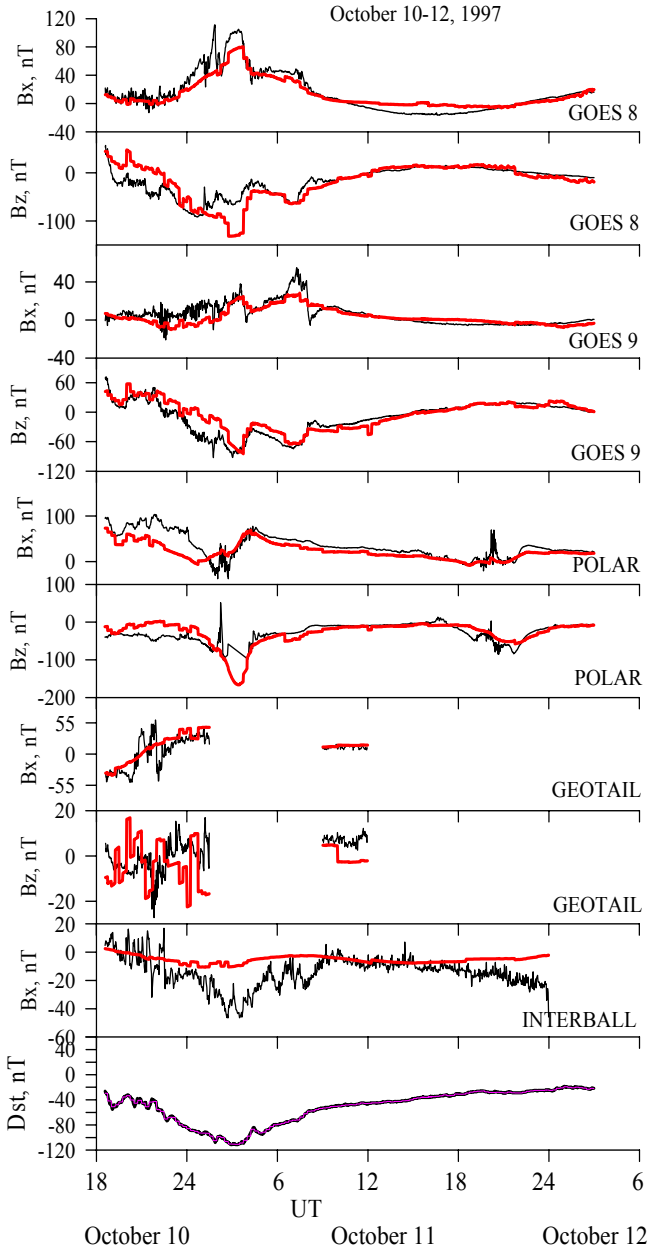

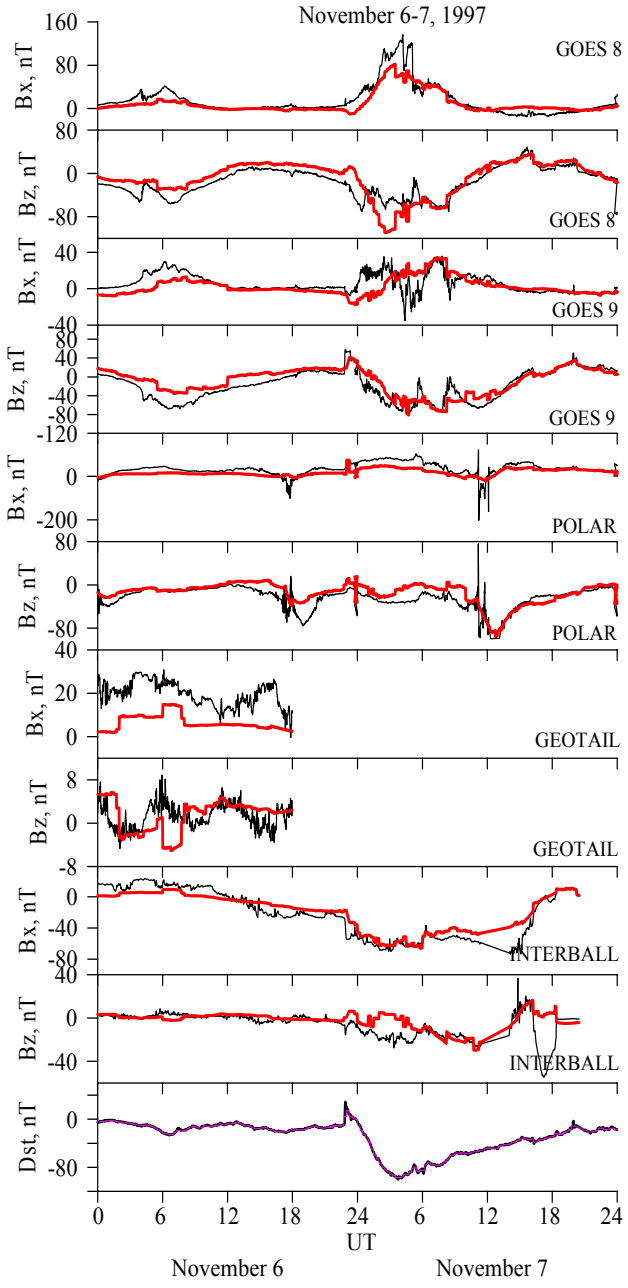

Model current density for May 4, 1998 storm event

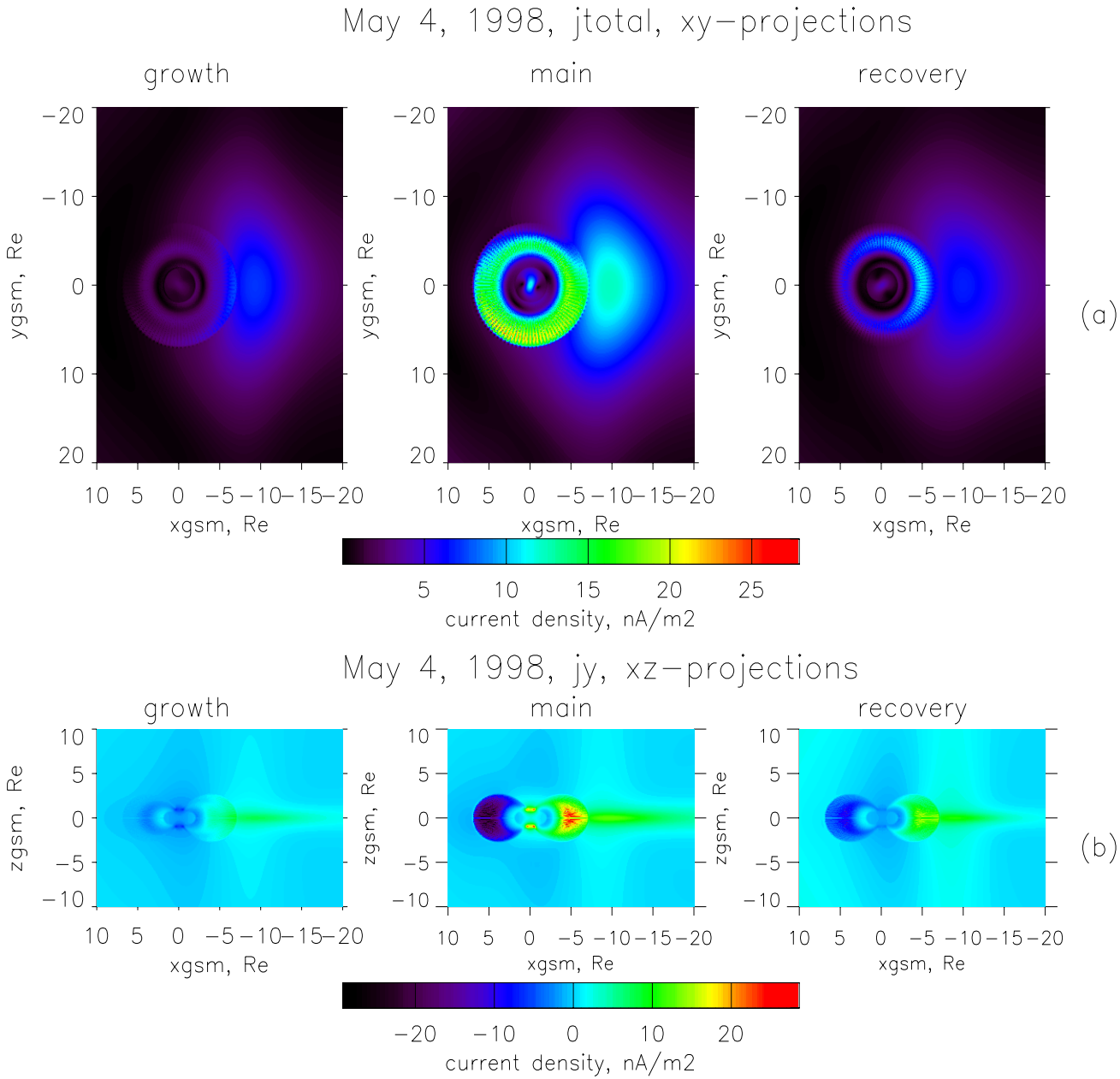

Modelling results: Contributions to Dst index

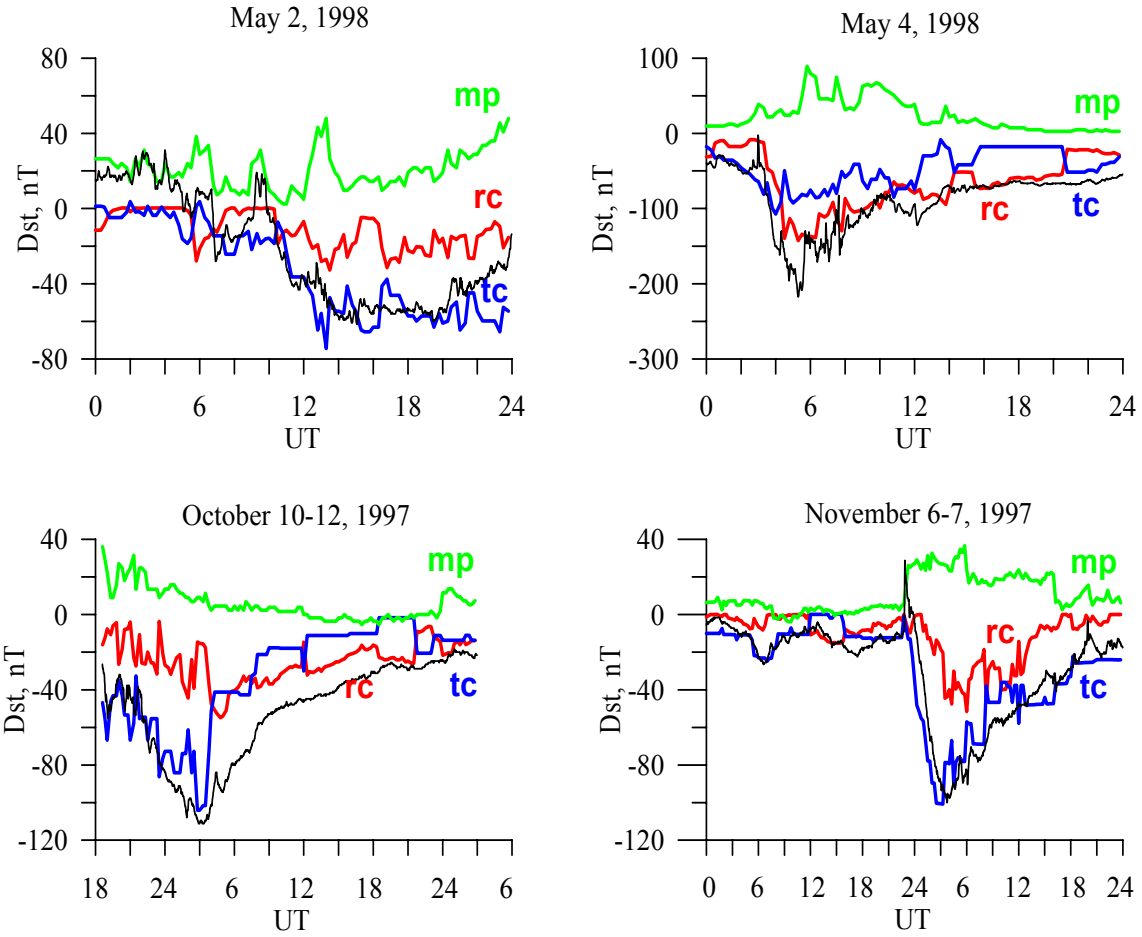

- tail current intensifies first and follows Dst drop,
- ring current develops later, stays longer increased,
- moderate storms: tail current contributes more than ring current,
- intense storm: ring current is dominant

Magnetospheric models used for comparison

- **T01 Model** (Tsyganenko, JGR, 2002)

  Parameterization by ψ, Dst, Psw, IMF By, IMF Bz, G1,G2 (history of IMF).

- **Event-oriented model G2004** (Ganushkina et al., JGR, 2002; AnnGeo, 2004)

  T89+ Storm-time current systems

Kalegaev, Ganushkina et al., AnnGeo, 2005

Overview of two modelled storm events

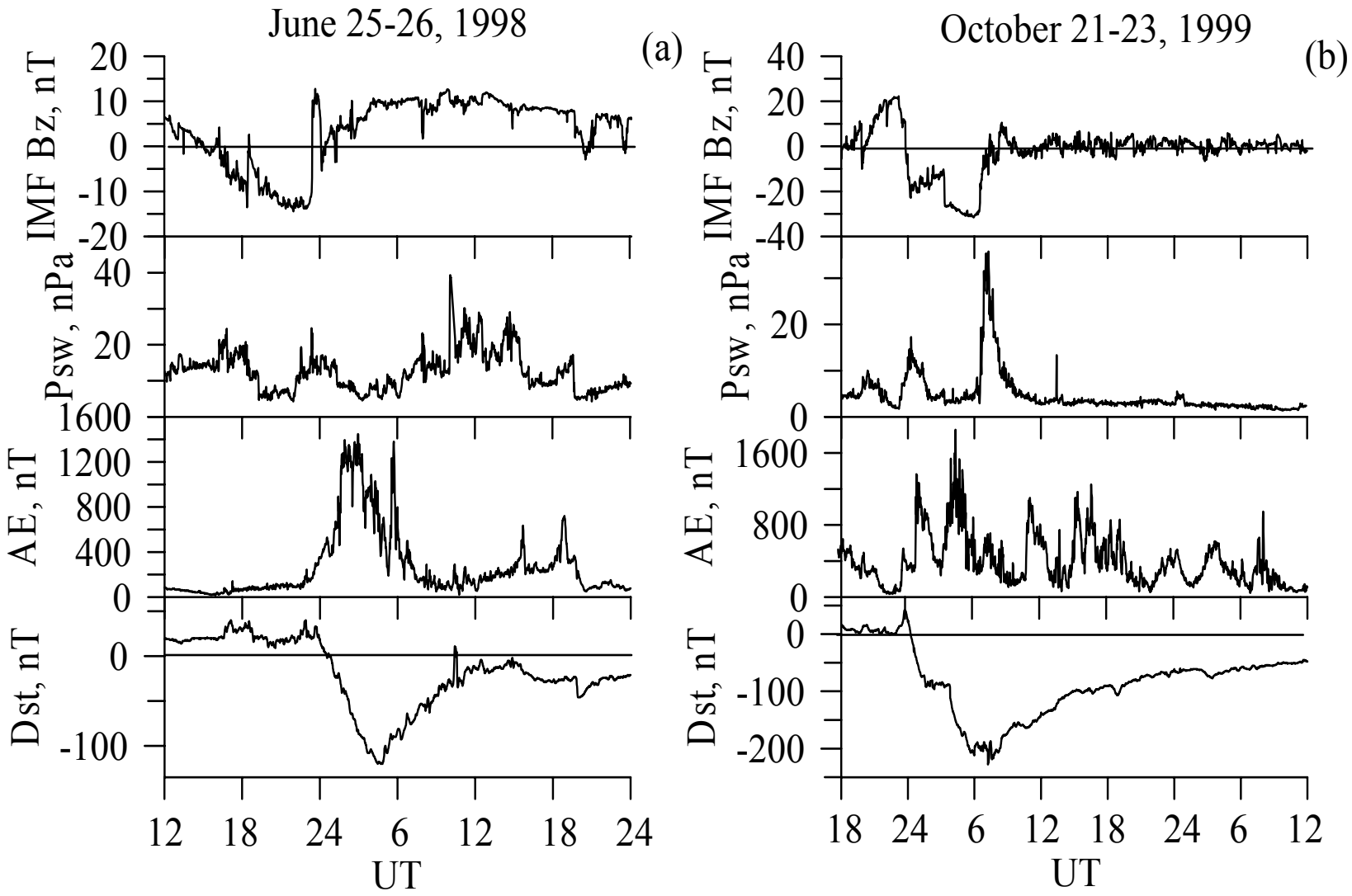

Modelling results: Magnetic field, T01

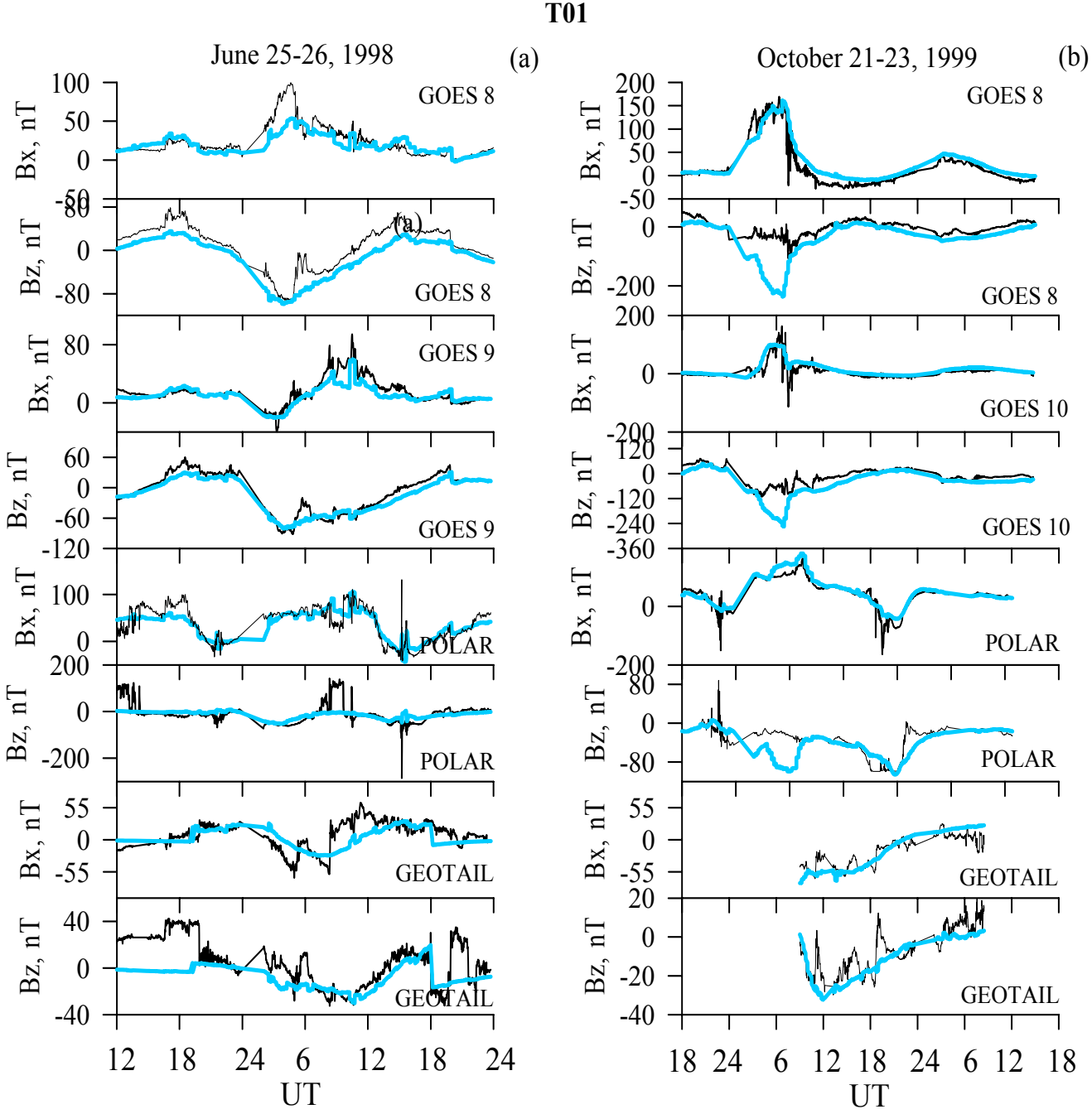

Modelling results: Magnetic field, event-oriented, G2004

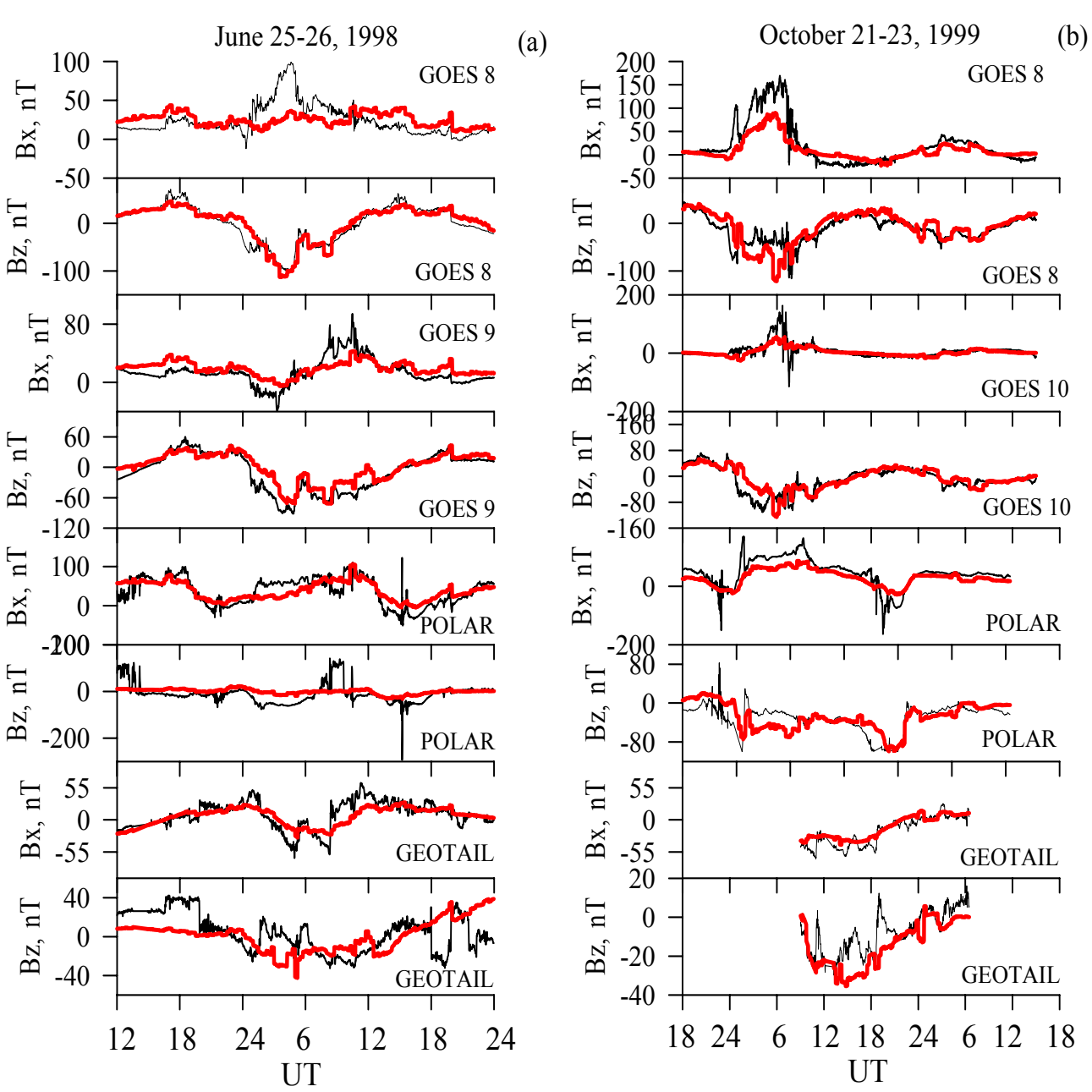

October 20-24, 2001 storm event

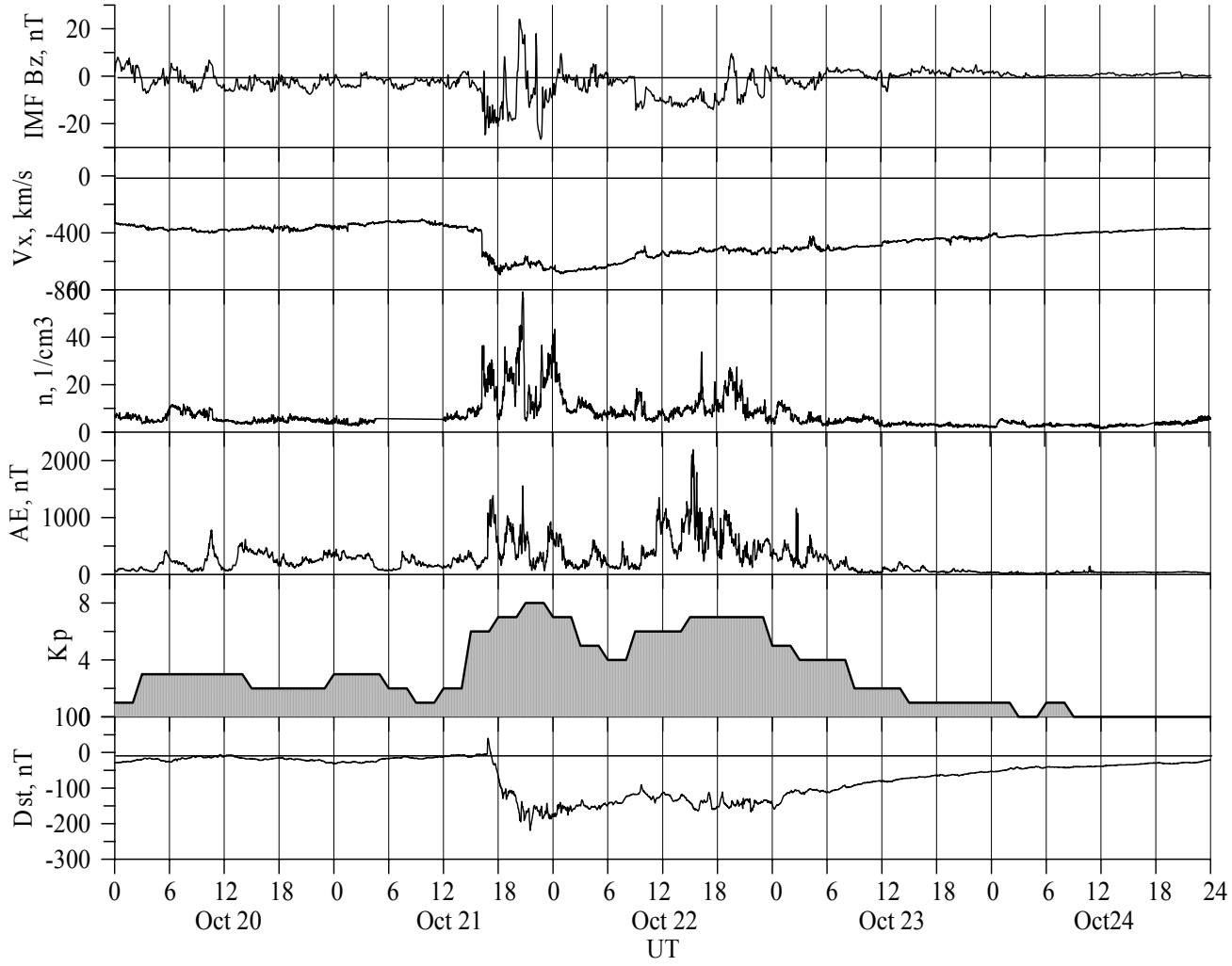

October 22, 1000-2000 UT: Magnetic field during saw-tooth event

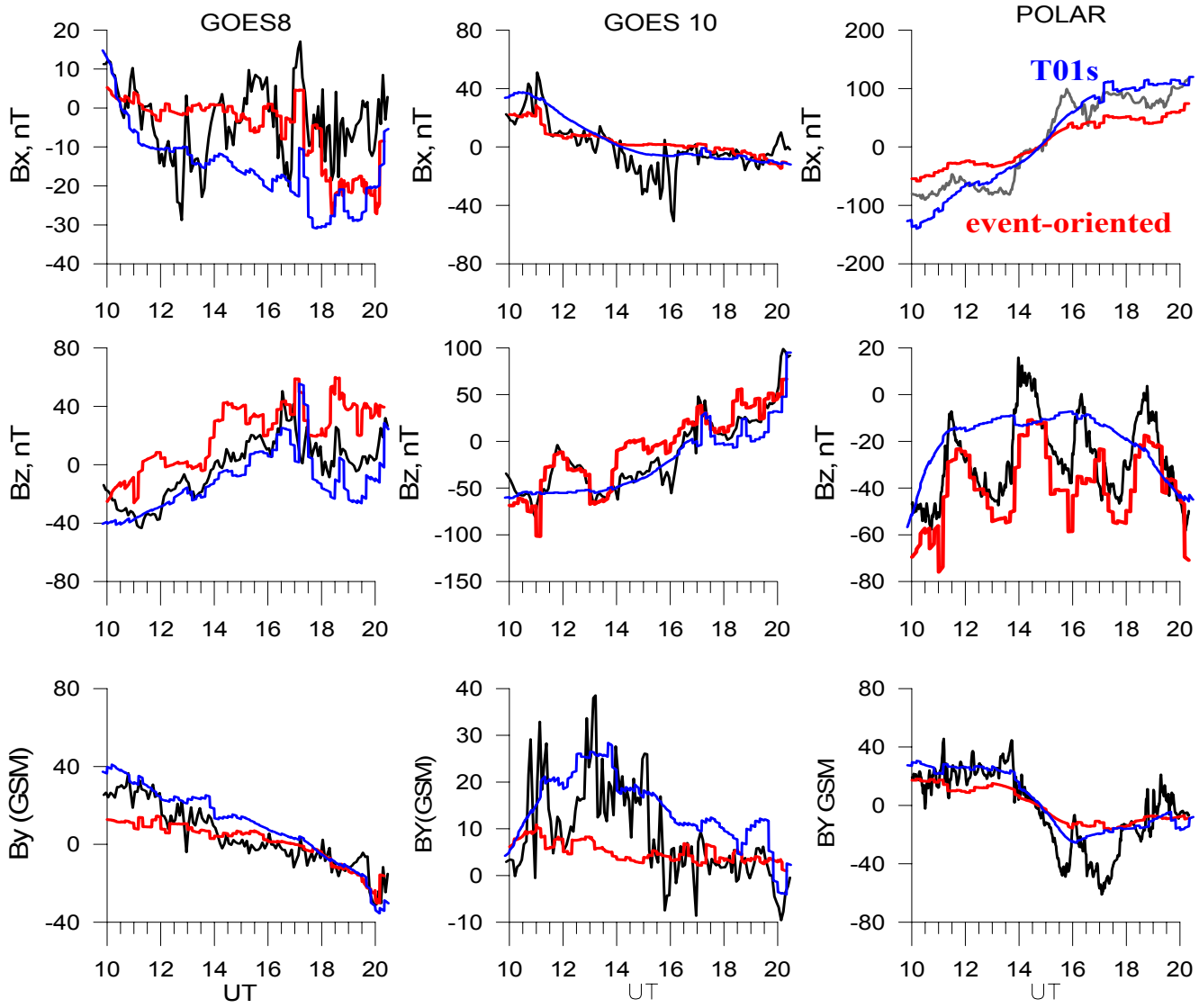

Event-oriented magnetospheric magnetic field modelling: Advantages and disadvantages

+ Allows to play easily with current systems, their location and parameters, to get better agreement with data
+ Good representation of smaller scale variations in magnetic field: substorm-associated, saw-tooth events
+ Good representation of local magnetic field variations (observations at a specific satellite)

To get detailed magnetic field variations for a specific event, time period, magnetospheric Region $\Rightarrow$ use event-oriented model

- Only for specific events, when magnetic field data are available at least at 3 satellites in different magnetospheric regions
- Requires some work for determination of model parameters
- Based on T89 version

To get magnetic field quickly, for several storms, over a large region in magnetosphere, good in average $\Rightarrow$ use T01s model

Particle transport from the plasma sheet to the ring current region and ring current development under the influence of substorm-associated electric fields

Particle transport from the plasma sheet to the inner magnetosphere regions

0.03 keV at L=10

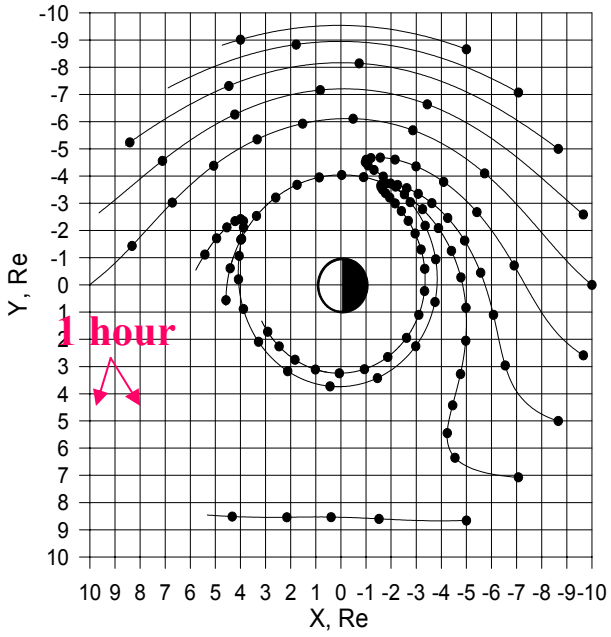

0.3 keV at L=10

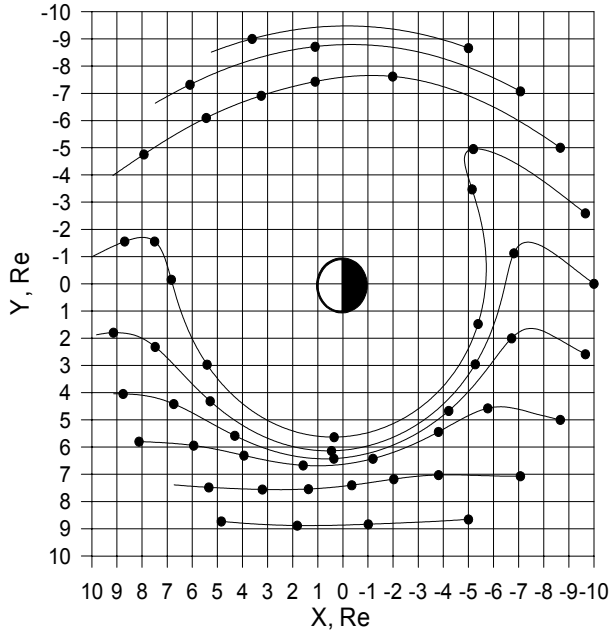

$$\text{Vdrift} = \underbrace{\frac{\vec{E}\times\vec{B}}{B^2}}_{\text{ExB-drift}} + \underbrace{\frac{mv_{\perp}^2}{2qB^3}\left(\vec{B}\times\nabla B\right)}_{\text{Gradient drift}} + \underbrace{\frac{mv_{II}^2}{q}\frac{\vec{R}_c\times\vec{B}}{R_c^2B^2}}_{\text{Curvature drift}}$$

Ring current energy density and total energy calculated from Polar CAMMICE/MICS measurements

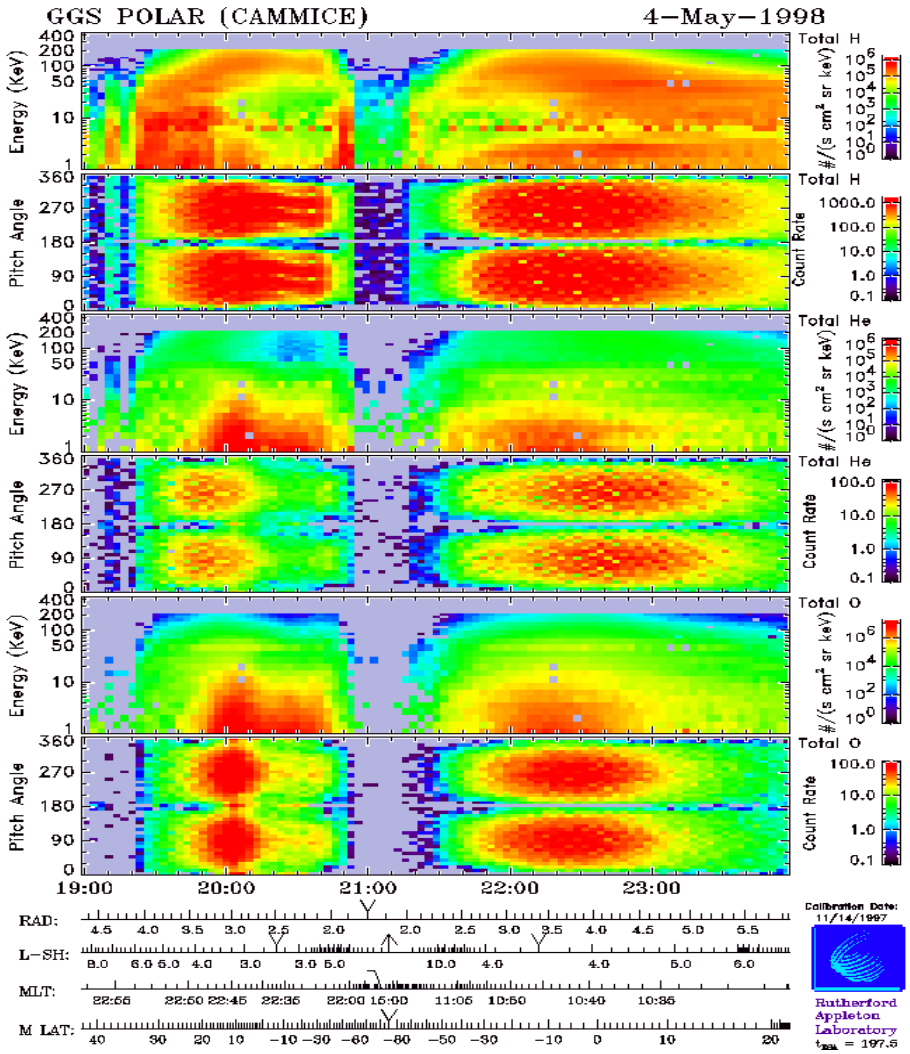

Polar orbit, years 1996-1998

- 1.8 x 9 Re, 86º incl.,
- 18 h period,
- spin axis ⊥ orbit plane,
- ions of 1-200 keV

Energy density of RC protons

$$w(L) = 2\pi\sqrt{2mq}\int_0^\infty dE\sqrt{E}\, j(E,L),$$

Total proton ring current energy

$$W_{RC} = \int_V w(L)\,dV,$$

Contributions to RC energy from protons with different energy ranges: 27 storms' statistics

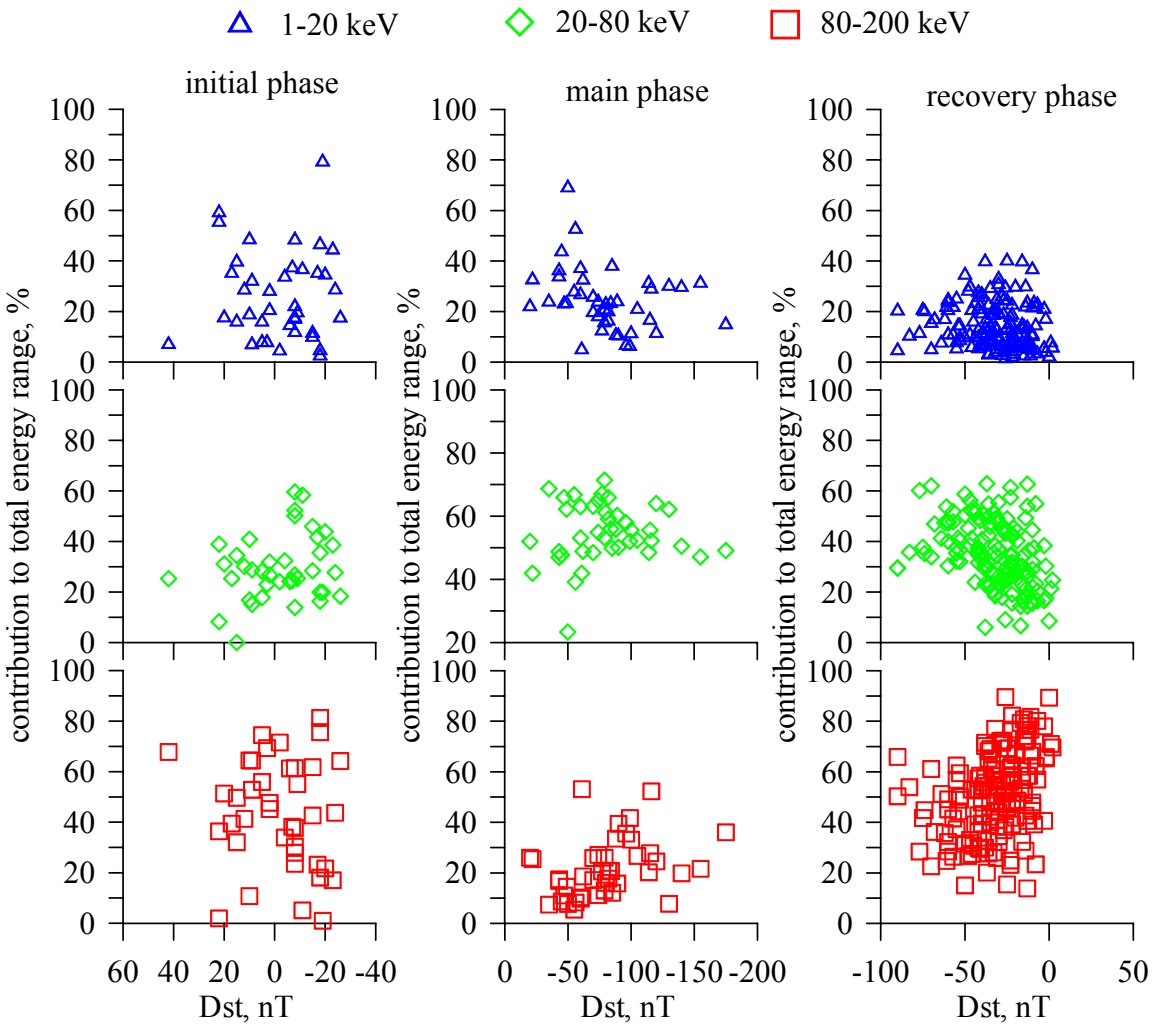

May 1-7, 1998: Storm event overview

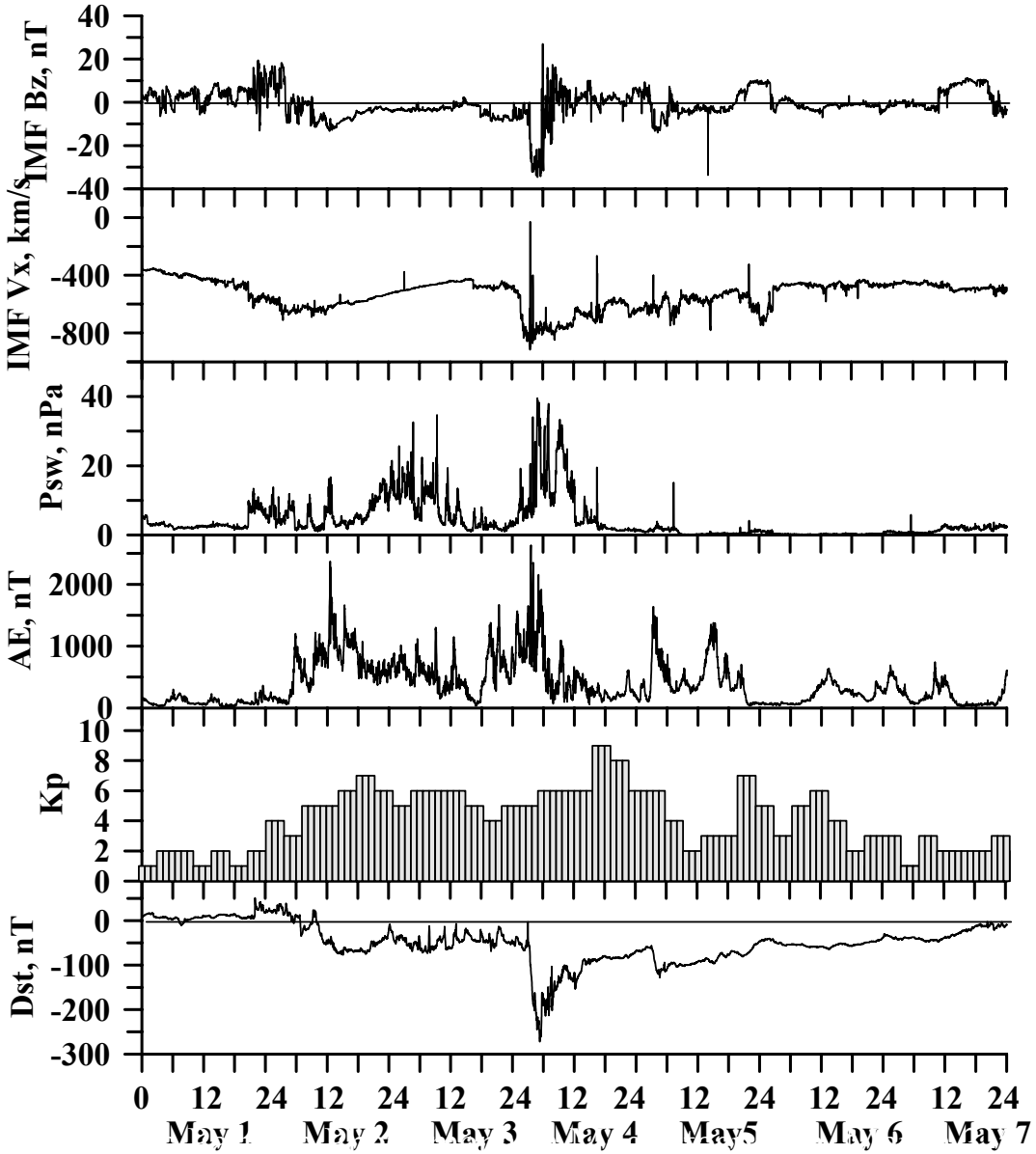

Contributions to RC energy from particles with different energy ranges: May 1-7, 1998 storm event

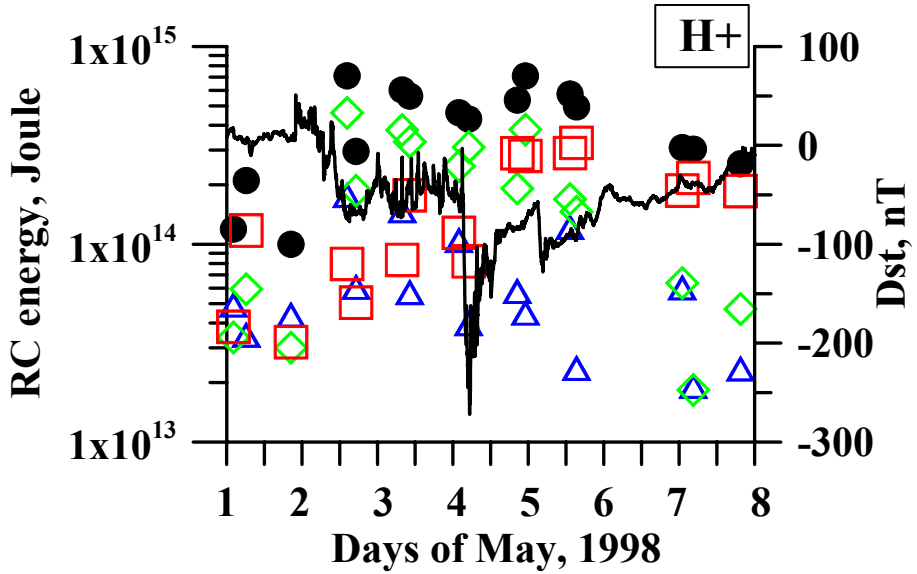

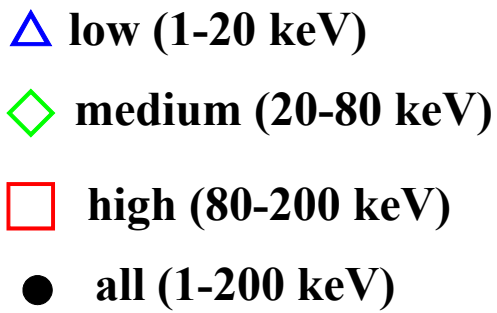

Storm main phase: main contribution from medium energies (20-80 keV)
Storm recovery phase: main contribution from high energies (80-200 keV)

Particle tracing procedure description

- Drift of protons with 90º±60ºpitch angles, 1st and 2nd invariants = const in time-dependent magnetic and electric fields, drift velocity as sum of ExB and magnetic (gradient and curvature) drifts
- *Maxwellian*-type distribution function at R=7 1900-0500 MLT with observed parameters (<Tps>, Nps)
- Changes in distribution function and flux calculations using *Liouville*'s theorem taking into account charge-exchange processes with cross section by *Janev and Smith, 1993* and number density of neutrals by thermosphere model MSISE 90 (*Hedin, 1991*)
- Magnetic field models:
  - dipole,
  - *Tsyganenko* T89, Kp-dependent
  - *Tsyganenko* storm-time T01s, Dst, Psw, By, Bz IMF, G2, G3 dependent
- Electric field models:
  - Volland-Stern Kp-dependent
  - *Boyle et al., 1997* polar cap potential applied to Volland-Stern type convection
- Substorm-associated fields:
  - electric field pulses similar to *Sarris et al., 2002* at substorm onsets,
  - magnetic field from pulses

May 2-4, 1998 storm event: Modeling results (1a)

Magnetic field: Tsyganenko T89
Electric field: Kp-dependent Volland-Stern convection electric field

$$\Phi_{convection} = AR^{\gamma} \sin(\phi - \phi_0),$$

$$\gamma = 2, A = \frac{0.045}{1 - 0.159Kp + 0.0093Kp^2} kV / R_E^2$$

Boundary condition:
constant plasma sheet number density (Nps=0.4 cm^{-3}) and
average temperature (<Tps>=5 keV)

May 2-4, 1998 storm event: Modeling results (1b)

T89 magnetic field and Kp-dependent Volland-Stern convection electric field, Nps=0.4 cm^{-3}, <Tps>=5 keV

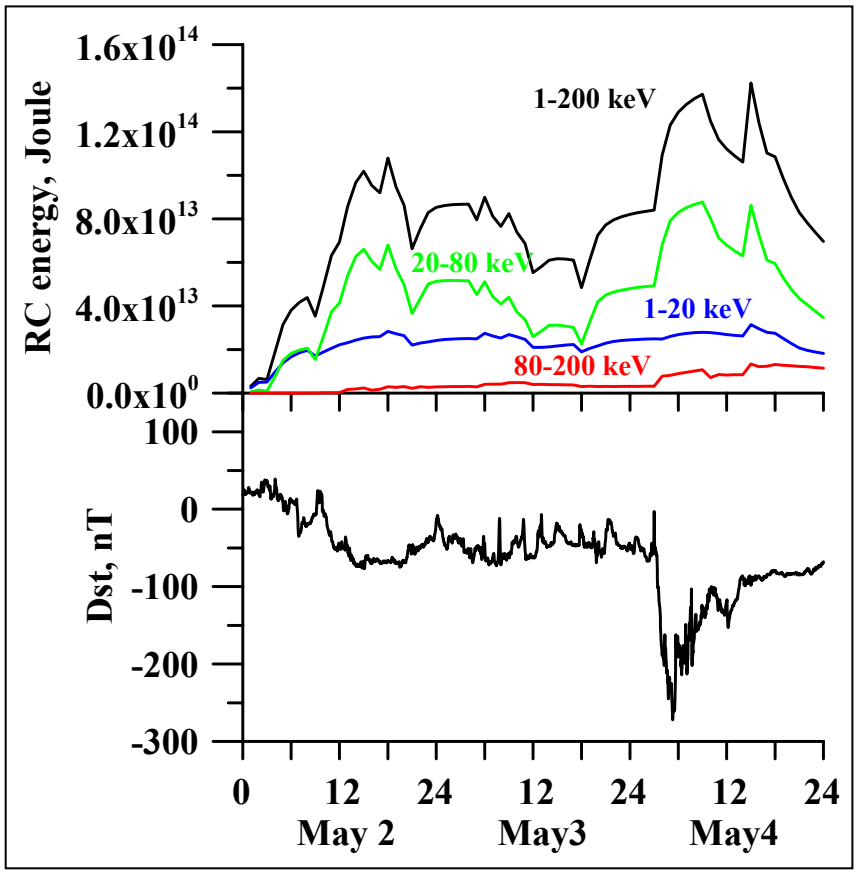

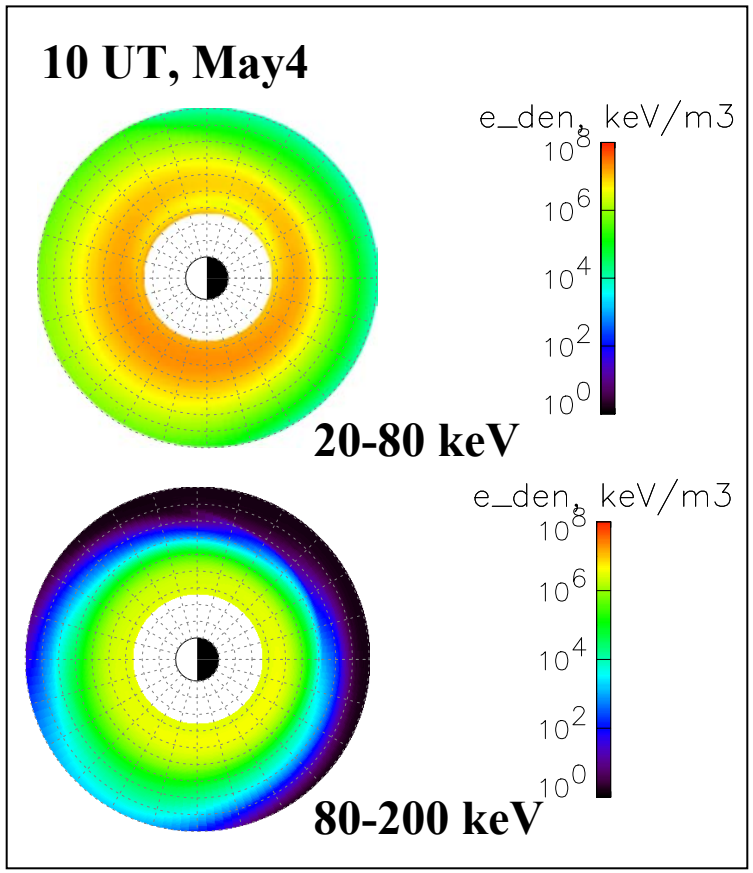

May 2-4, 1998 storm event: Modeling results (2a)

Magnetic field: Tsyganenko T89
Electric field: Boyle et al., 1997 polar cap potential dependent on solar wind and IMF parameters applied to Volland-Stern convection field

$$\Phi = \left[1.1\cdot 10^{-4} V_{sw}^{2} + 11.1 B_{IMF} \sin^{3}\left(\frac{\theta_{IMF}}{2}\right)\right] \frac{\sin\phi}{2} \left(\frac{R}{R_B}\right)^{2},$$

$$R_B = 10.47 R_E$$

Boundary condition:
plasma sheet number density Nps dependent on solar wind number density Nsw (Ebihara and Ejiri, 2001),
average temperature <Tps>=5 keV

$$N_{ps} = 0.025 N_{sw} + 0.395$$

May 2-4, 1998 storm event: Modeling results (2b)

T89 magnetic field and Boyle et al., 1997 polar cap potential dependent on solar wind and IMF parameters, Nps ~ Nsw, <Tps>= 5 keV

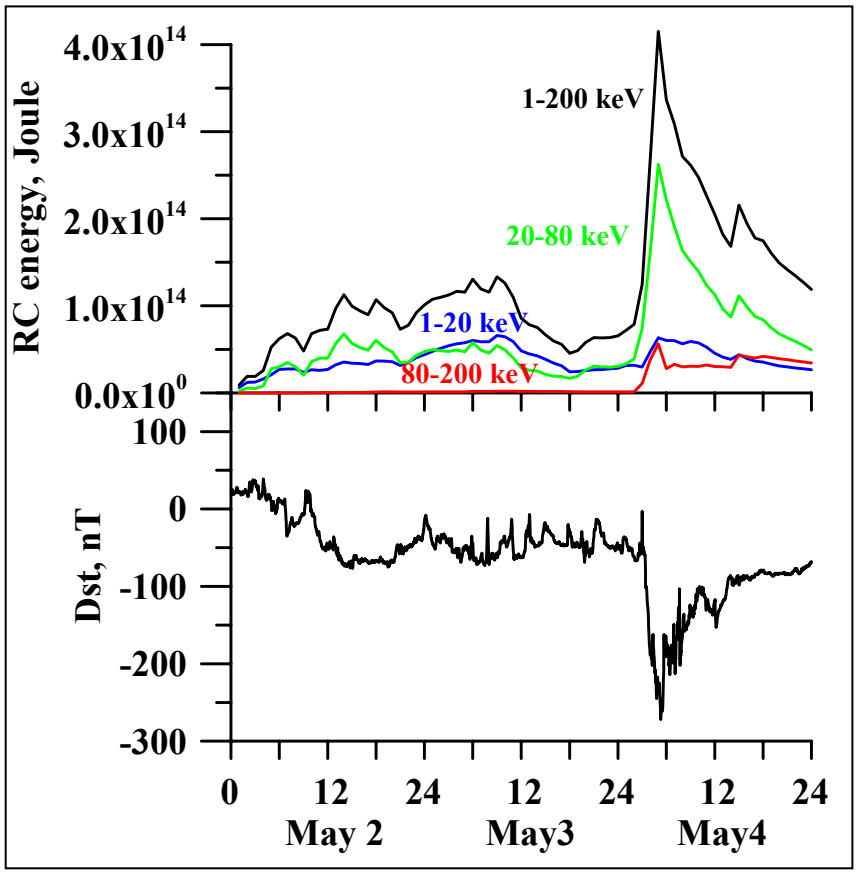

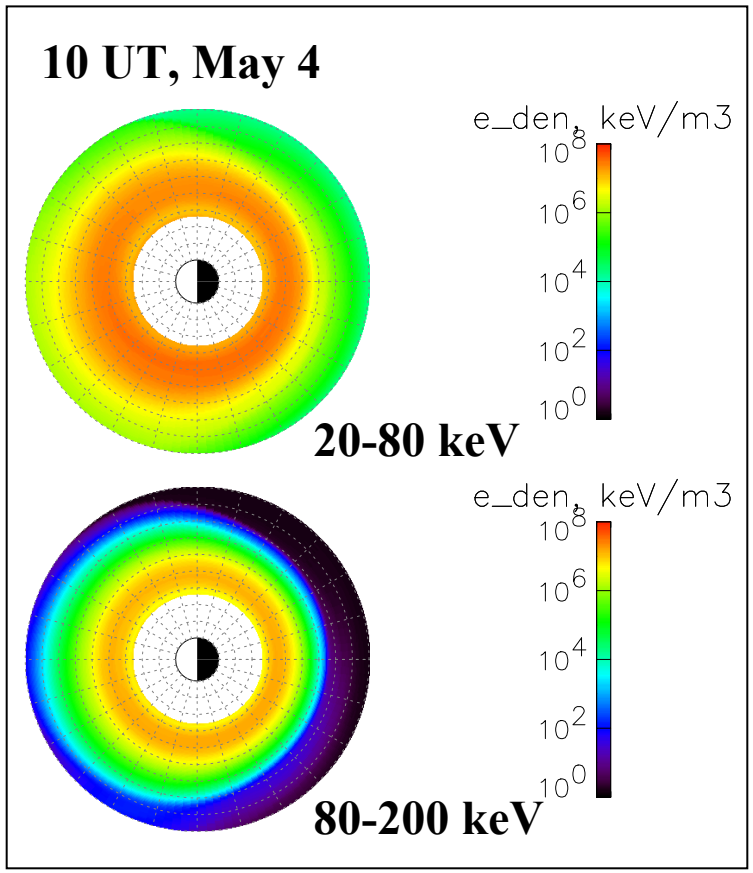

May 2-4, 1998 storm event: Modeling results (3a)

Magnetic field: Tsyganenko T89
Electric field: Boyle et al., 1997 polar cap potential dependent on solar wind and IMF parameters applied to Volland-Stern convection field
Boundary condition:
Nps and <Tps> from LANL MPA data (6.6 Re, 0500-1900 MLT)

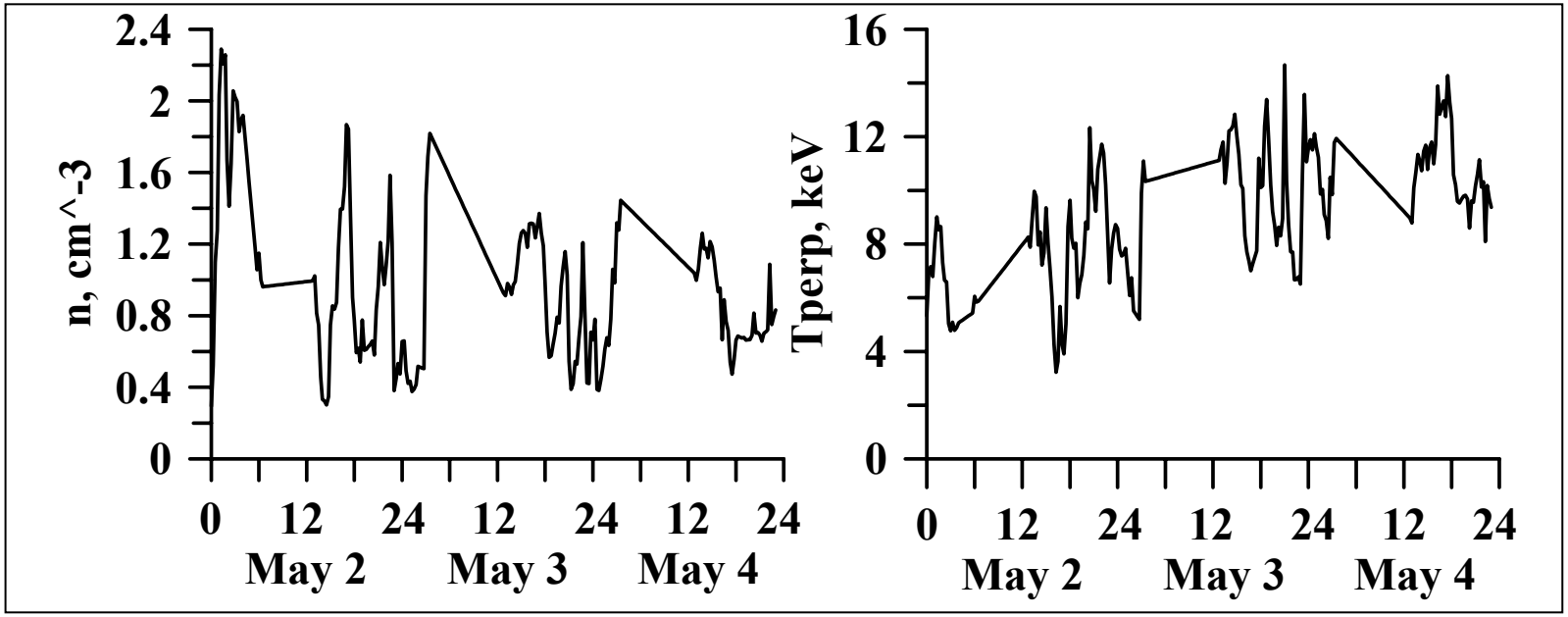

May 2-4, 1998 storm event: Modeling results (3b)

T89 magnetic field and Boyle et al., 1997 polar cap potential dependent on solar wind and IMF parameters, Nps from LANL MPA measurements

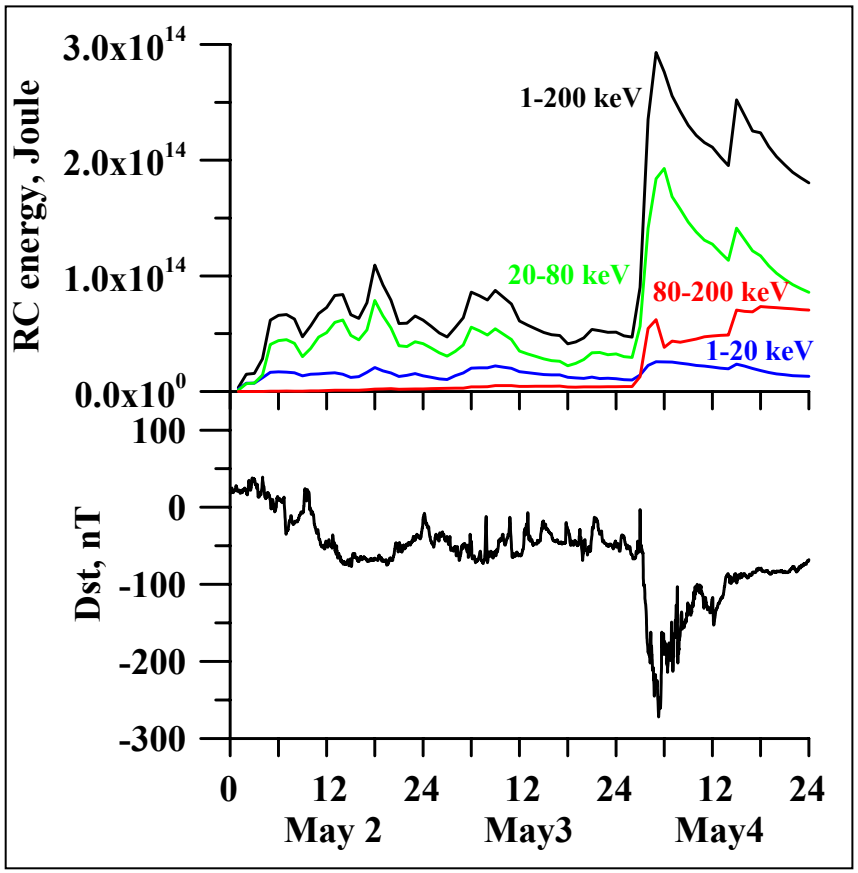

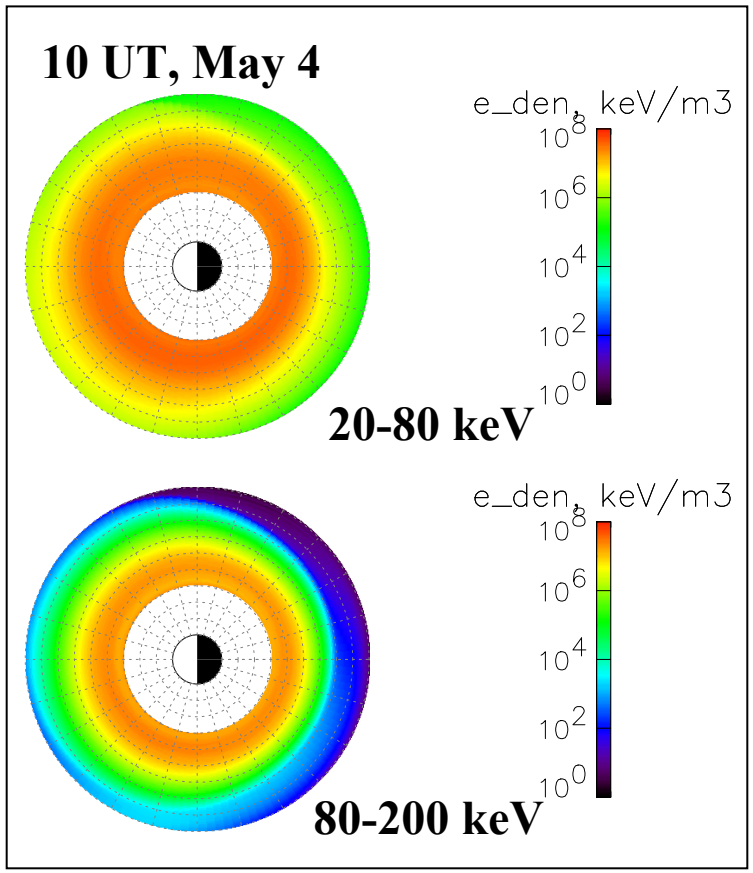

Electric field pulse model

Time varying fields associated with dipolarization in magnetotail, modeled as an electromagnetic pulse (*Li et al., 1998; Sarris et al., 2002*):

- Perturbed fields propagate from tail toward the Earth;
- Time-dependent Gaussian pulse with azimuthal E;
- E propagates radially inward at a decreasing velocity;
- decreases away from midnight.

Time-dependent B from the pulse is calculated by Faraday's law.

In spherical coordinates (r, θ, φ): $E_\phi = -E_0(1 + c_1\cos(\phi - \phi_0))^p \exp(-\xi^2)$,

$\xi = [r - r_i + v(r)(t - t_a)]/d$ - location of the pulse maximum, r_I determines pulse arrival time

$v(r) = a + br$ - pulse front velocity, d - width of pulse,
c_1 , p describe LT dependence of E amplitude, largest at ϕ_0,

$t_a = (c_2 R_E / v_a)(1 - \cos(\phi - \phi_0))$ - delay of pulse from ϕ_0 to other LTs,
c_2 - delay magnitude,
v_a - longitudinal propagation speed

Electric and magnetic fields in pulse model

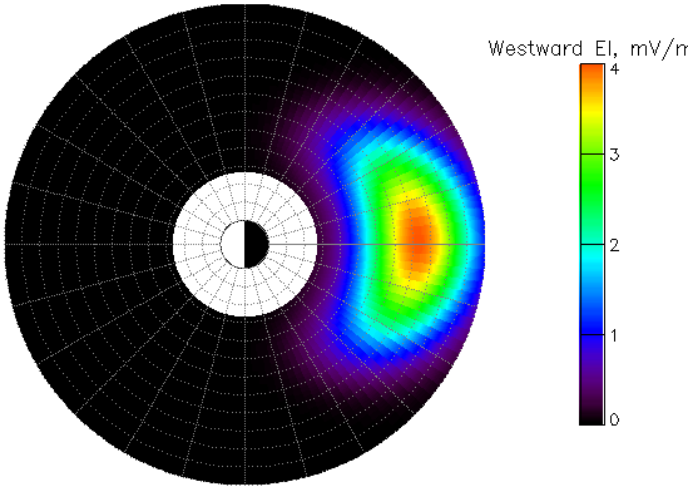

electric field

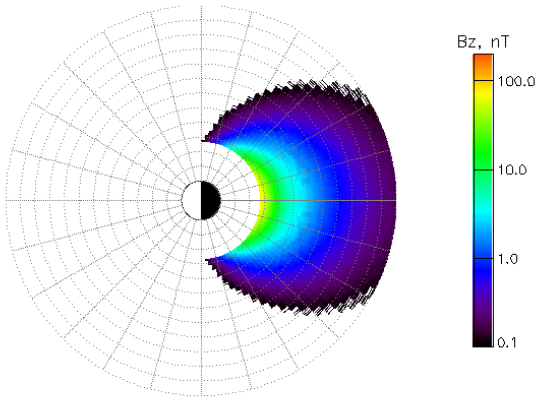

magnetic field

May 2-4, 1998 storm event: Modeling results (4a)

Magnetic field: Tsyganenko T89
Electric field: Boyle et al., 1997 polar cap potential dependent on solar wind and IMF parameters applied to Volland-Stern convection field
Boundary condition:
Nps and <Tps> from LANL MPA data

Electric field pulses at substorm onsets:

May 2		May 3		May 4	
0520 UT	4 mV/m	0500 UT	3 mV/m	0015 UT	6 mV/m
0910 UT	4 mV/m	1200 UT	3 mV/m	0240 UT	6 mV/m
1205 UT	8 mV/m	1800 UT	4 mV/m	0325 UT	8 mV/m
1600 UT	6 mV/m	2030 UT	6 mV/m	0430 UT	7 mV/m
				0900 UT	3 mV/m

May 2-4, 1998 storm event: Ring current energy

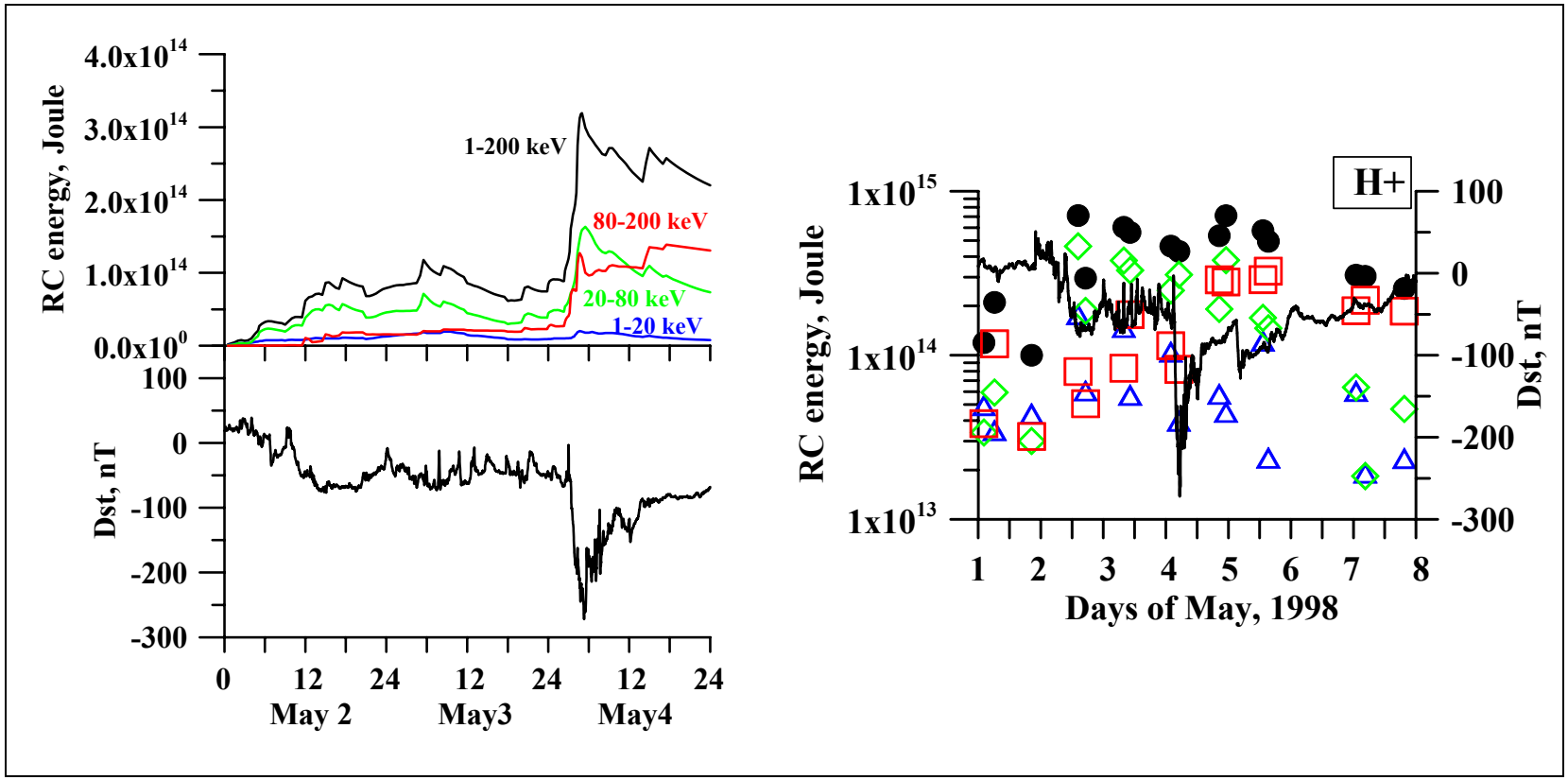

May 2-4, 1998 storm event: Pulse propagation

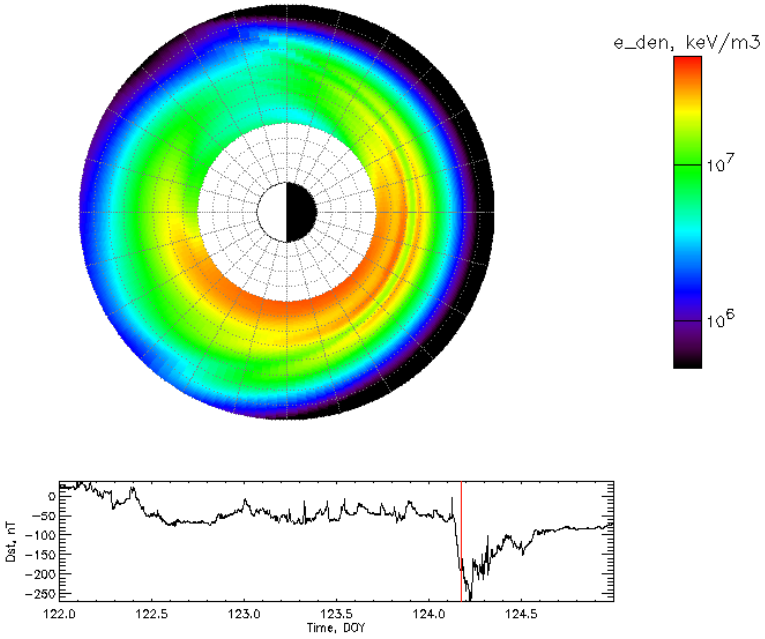

medium energies

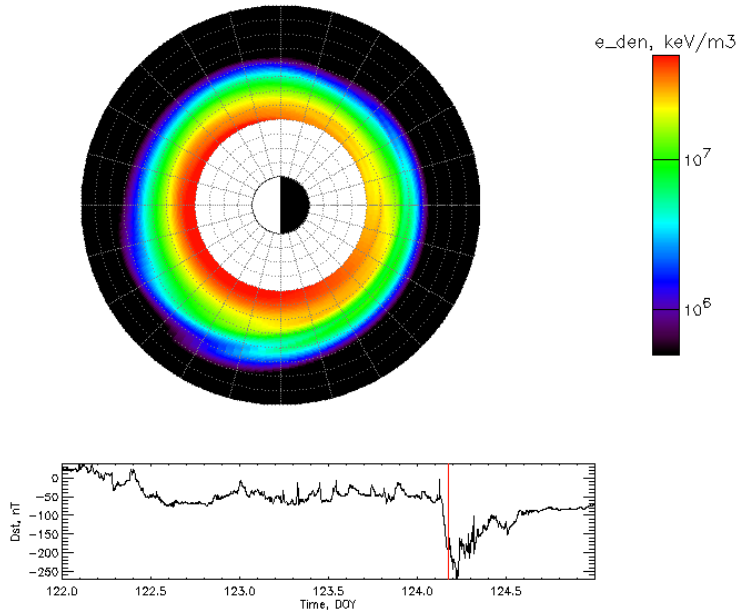

high energies

May 2-4, 1998 storm event: Energy density maps

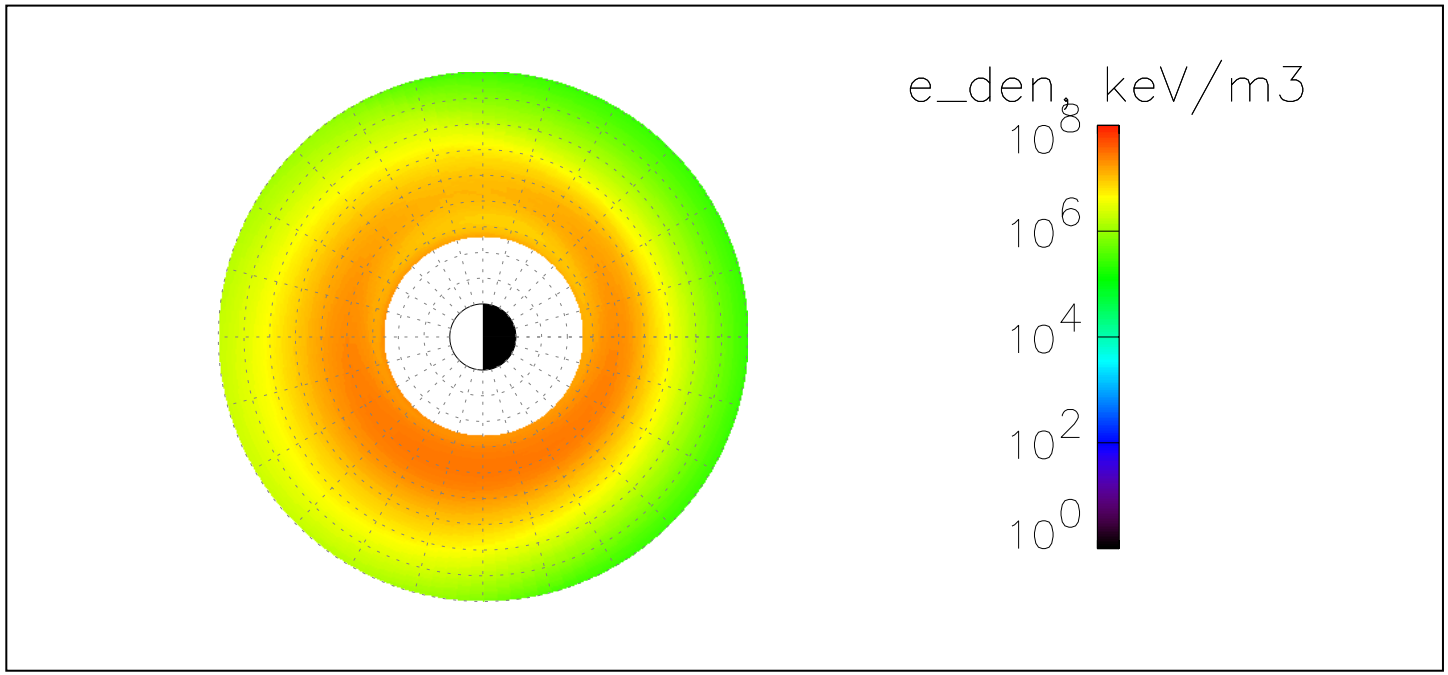

energy density

Transport and acceleration of plasma sheet protons into the ring current region

- **Protons with different energies contribute differently during different storms phases:**
  Statistics on Polar CAMMICE/MICS data:
  - during storm main phase medium energies (30-80 keV) contribute most,
  - more than high energies (80-300 keV), during recovery – opposite.

- **Right choice of magnetic field model in ring current modelling is important as much as that of electric field: more realistic model than dipole gives 2 times SMALLER values of proton RC energy.**

- **Only implementation of substorm-associated electric fields into particle tracing provides clear dominance of high energy protons during storm recovery phase for both modelled storm events.**

- **Ring current formation during storms is a combination of convection and inward shifts and energization due to pulsed electric field.**

Energy-dispersed structures of ions in the inner magnetosphere observed at high- and low-altitude satellites (Polar, Interball Auroral ION, Viking, CLUSTER CIS and Akebono)

Observations of energy-dispersed ion structures on Polar CAMMICE/MICS

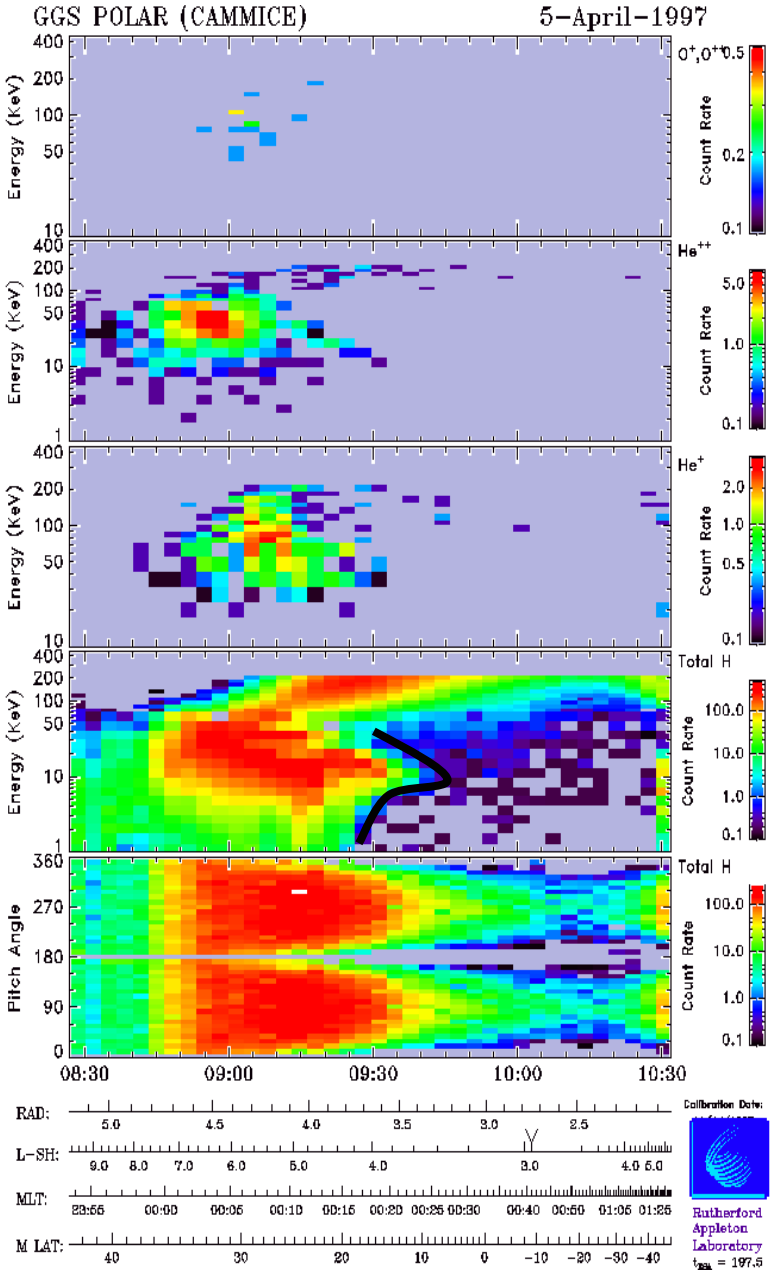

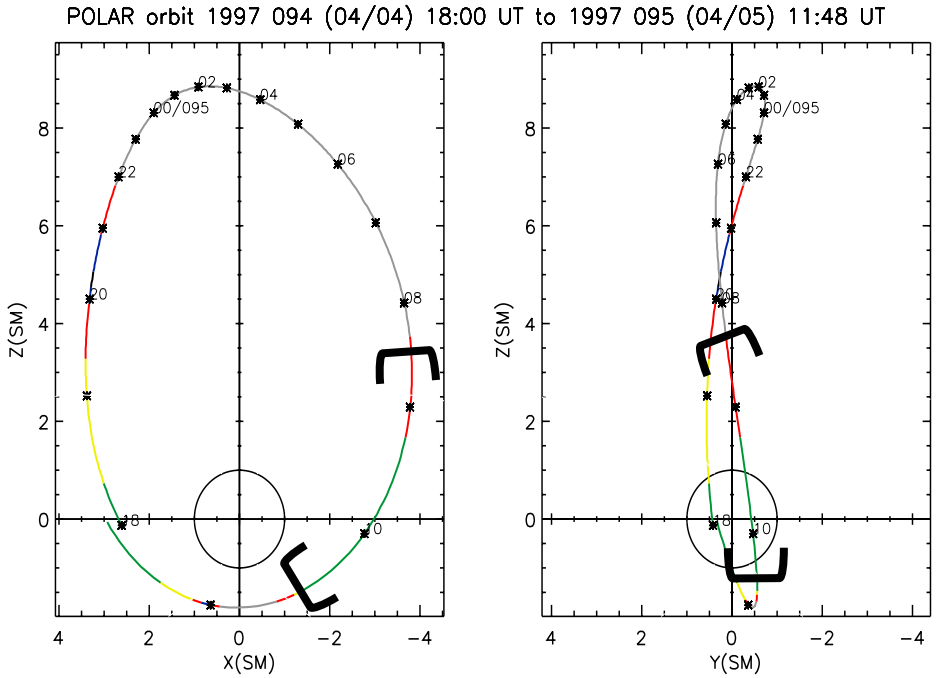

Polar orbit, years 1996-1998

- 1.8 x 9 Re elliptical,
- 86 deg inclination,
- 18 hours period,
- apogee over north polar reg.,
- spin axis normal to orbit plane

CAMMICE/MICS instrument

- ions (H+, He+, He++, O+,O++)
- 1-200 keV

Nose structures in the inner magnetosphere

- *Smith and Hoffman, 1974*, **Explorer 45**:

"There exist 'nose' structures in proton spectrograms beginning at lower L values with a flux increase in the energy range 15-20 keV. The flux increase spreads to both higher and lower energies at larger L values and remains at high intensity beyond L=5.3… It always extends into the plasmapause..."

Spatial structure, not temporal

- *Ejiri at al., 1978, 1980,* **Explorer 45**: time-dependent drift trajectories of ions coming from the near-Earth plasma sheet

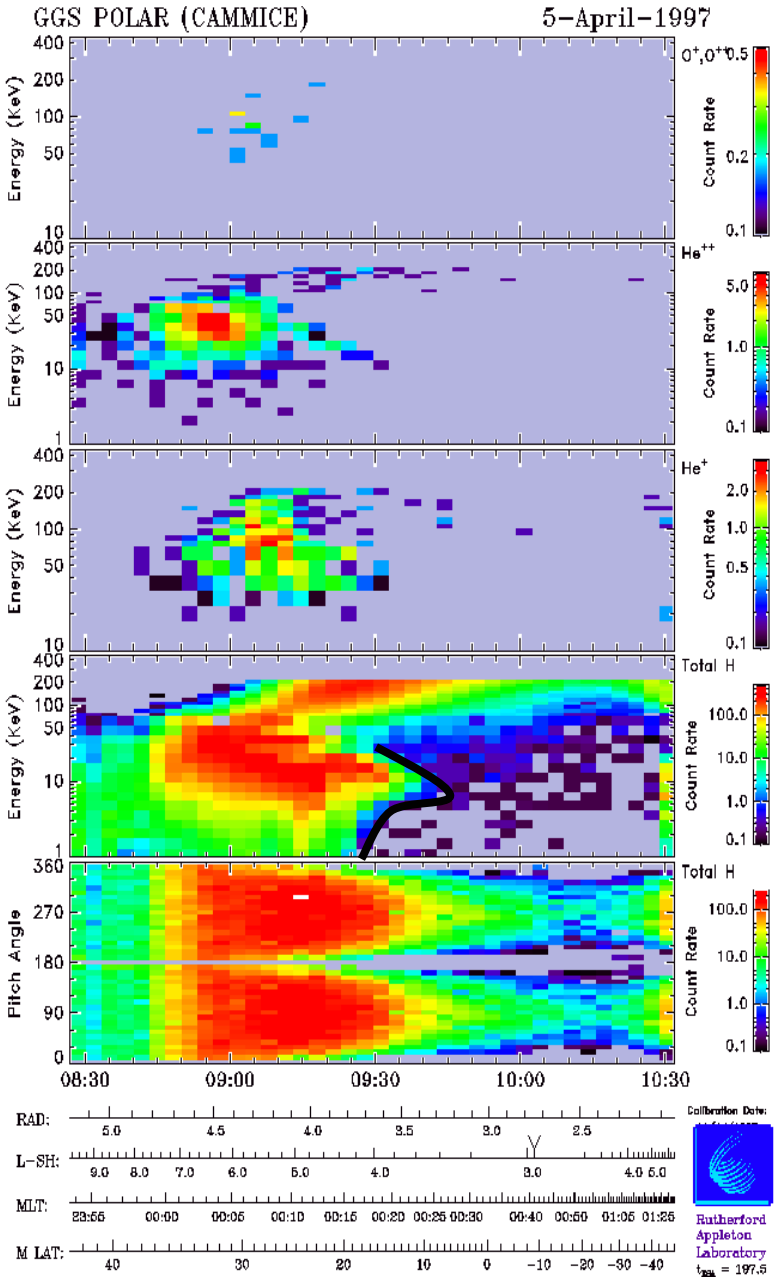

Stationary nose structures: Observations of Interball Auroral ION

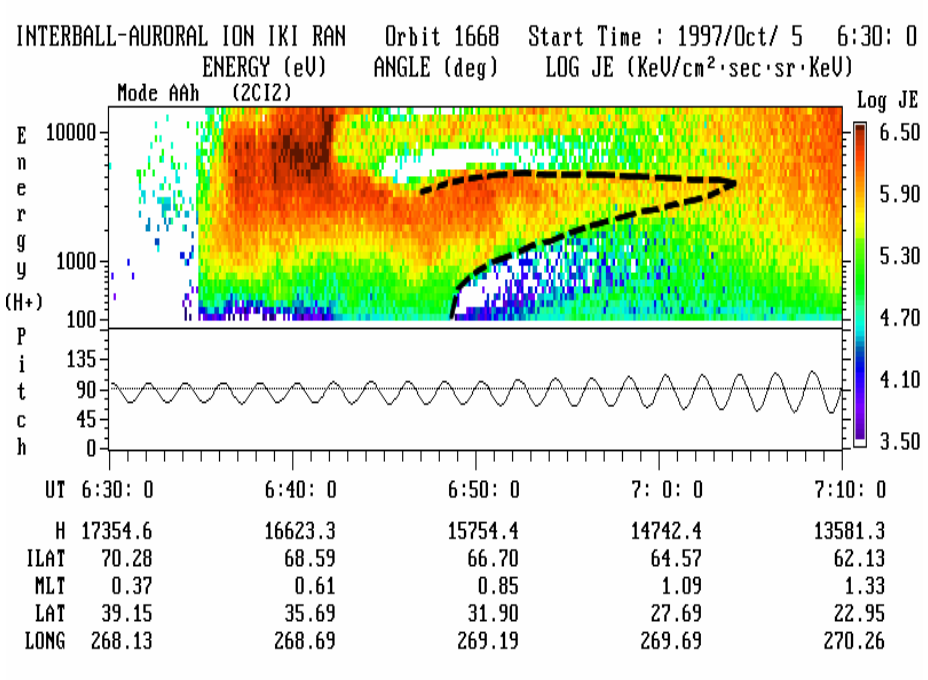

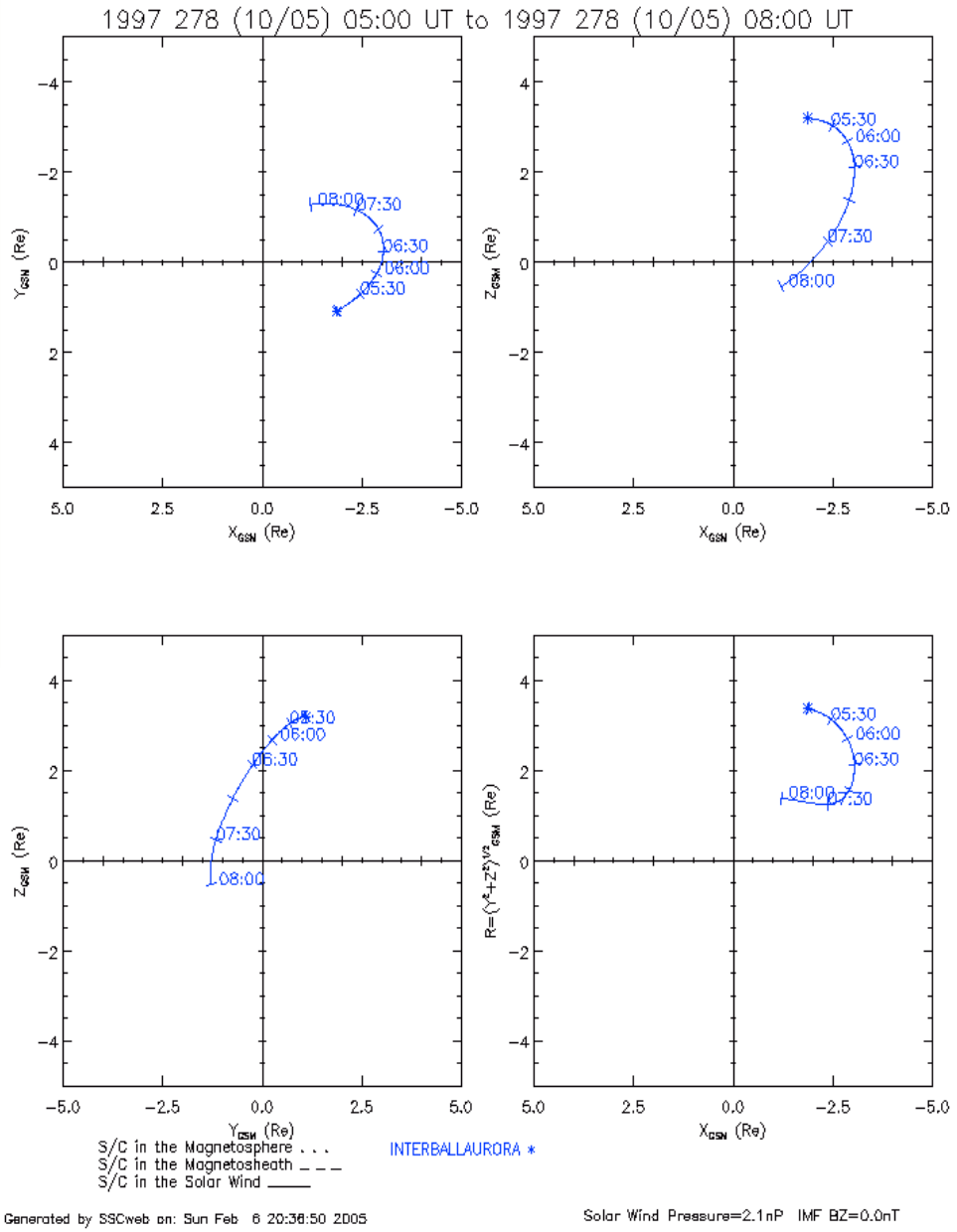

<u>The Interball Auroral probe</u>:

- **perigee at 770 km,**
- **apogee at 20,000 km**
- **65 deg inclination**

<u>ION instrument</u>:

ion measurements with energies from 10 eV to 20 keV.

Stationary nose structures: Conjugate observations by Polar and Interball

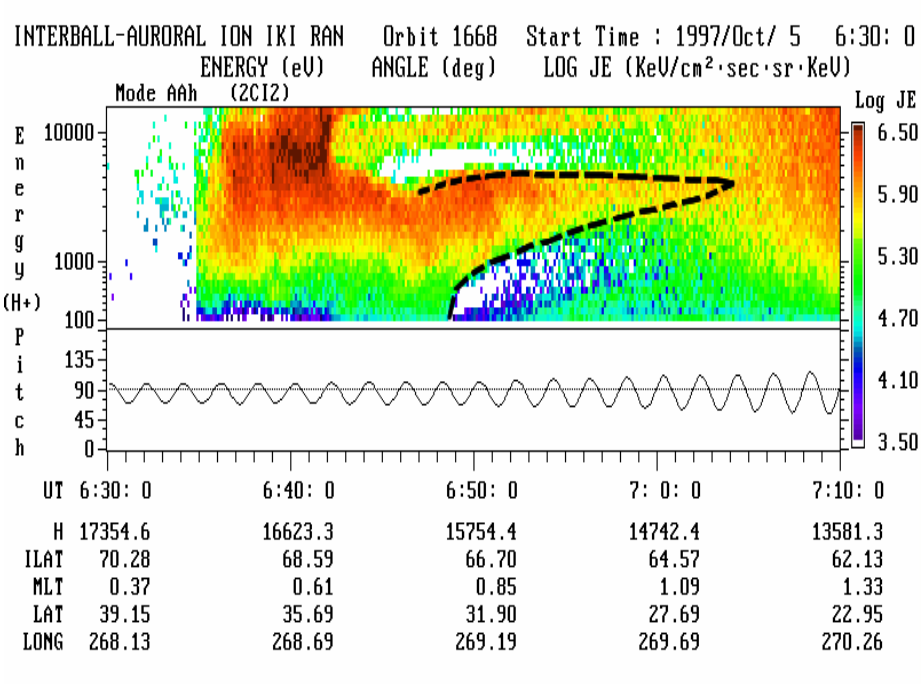

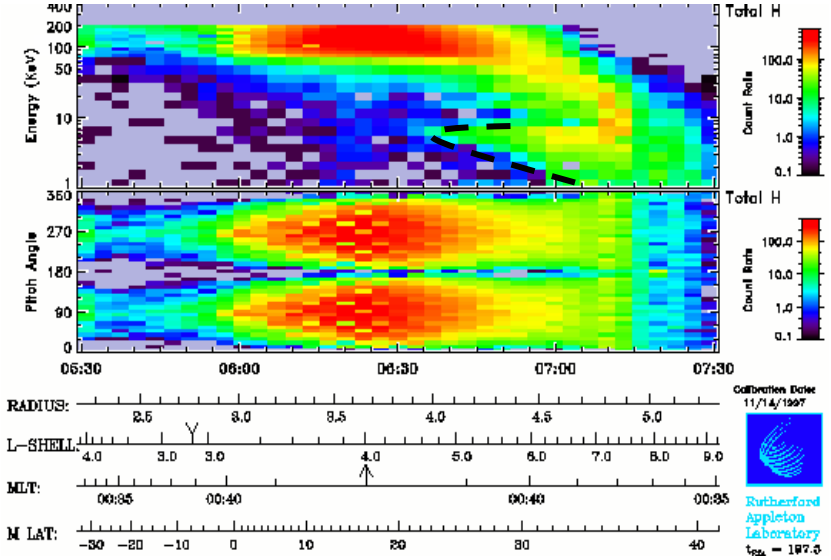

Interball Auroral ION data
October 5, 1997, 0640-0705 UT:
Stationary nose structure (dashed line)
in proton energy-time spectrogram
(energy flux)
in the nightside magnetosphere (00-01 MLT).

Characteristic energy below 10 keV

Polar CAMMICE/MICS data
0ctober 5, 1997, 0530-0730 UT
Stationary nose structure in proton energy-tim
spectrogram (count rates)
in the nightside magnetosphere (0000-0030 M

More than 10 hours for stationary nose structure formation

Intense nose structures: November 3, 1997 event

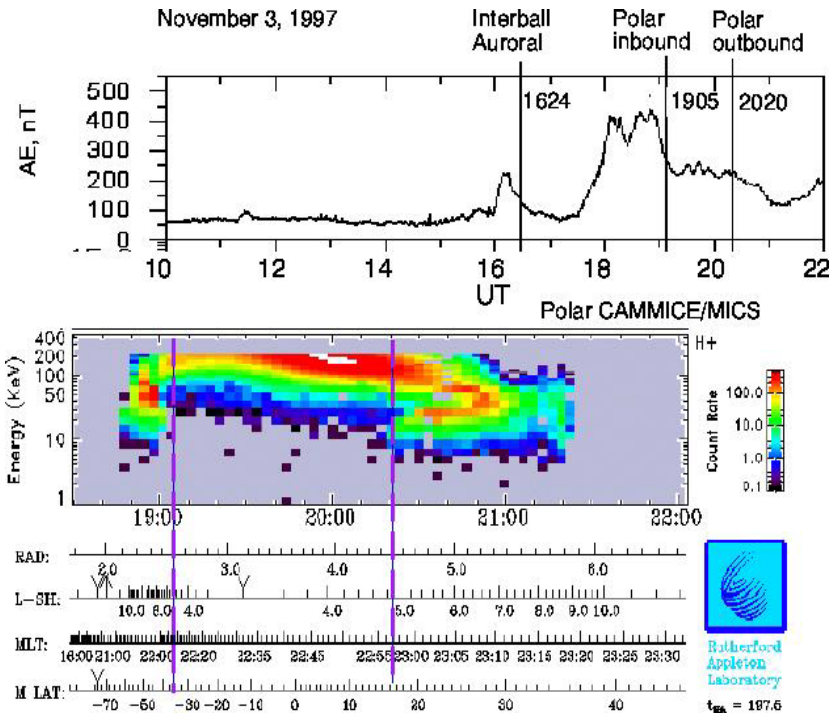

Satellite	UT	Req	MLT
Interball Auroral	1624	6.73	2200
LANL	1755	6.6	0100
Polar/ Inbound	1900	4.7	2158
Polar/ Outbound	2020	4.86	2254

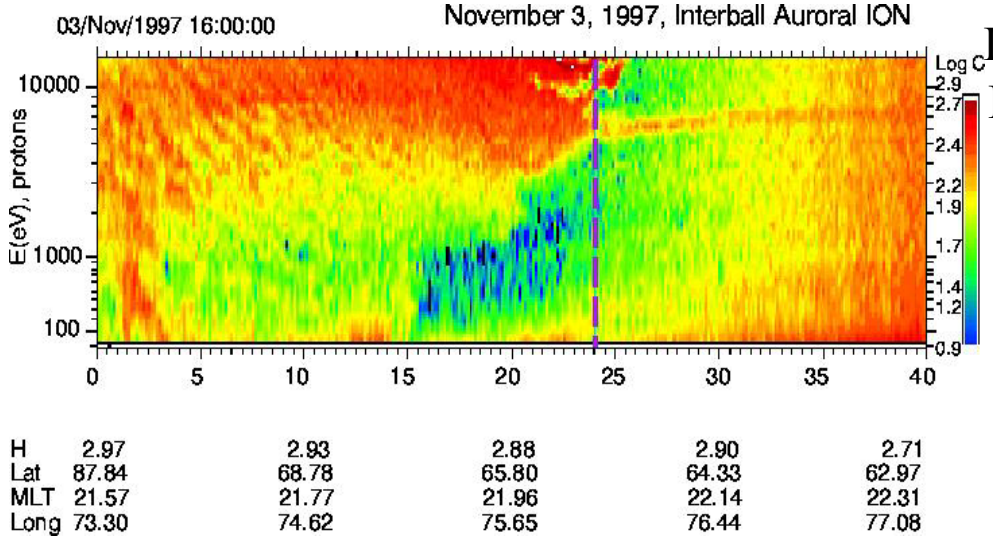

Interball Auroral nose: location of plasma for Polar/inbound nose formation 2.5 hours later.

LANL: indicator of inward plasma transport.

1755 UT, L=6.6 → 1900 UT, L=4.7 ⇒
2 Re inward motion within 1 hour.

Intense nose structures: November 3, 1997 event modeling

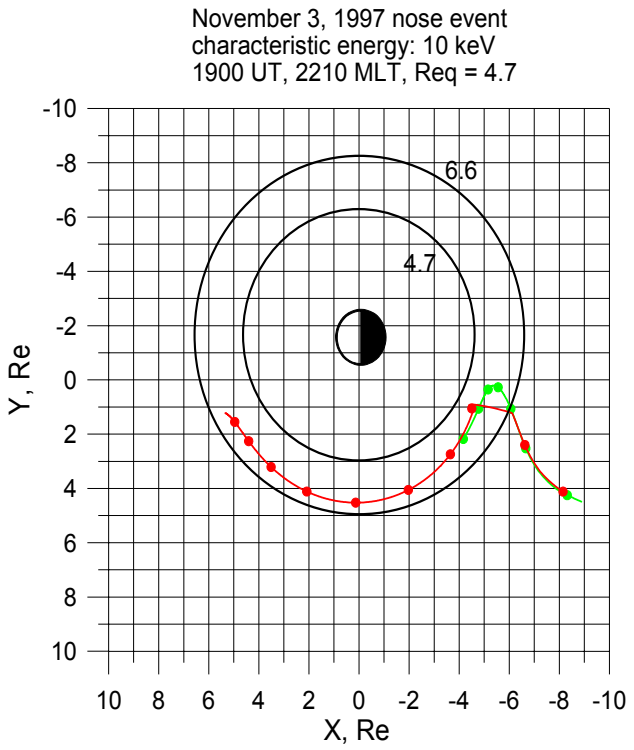

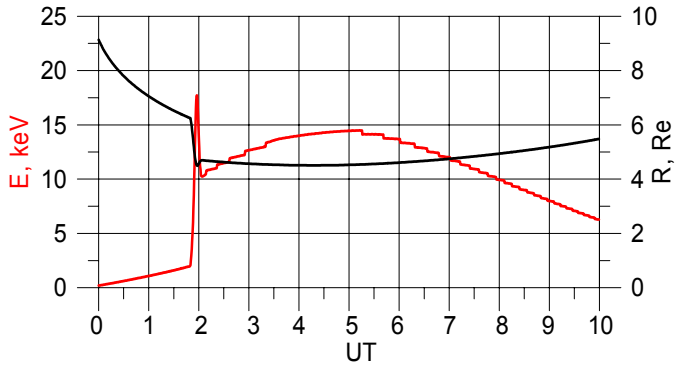

characteristic energy above 10 keV, fast earthward shift of previous population

VS+T89, Kp=1

2250 MLT

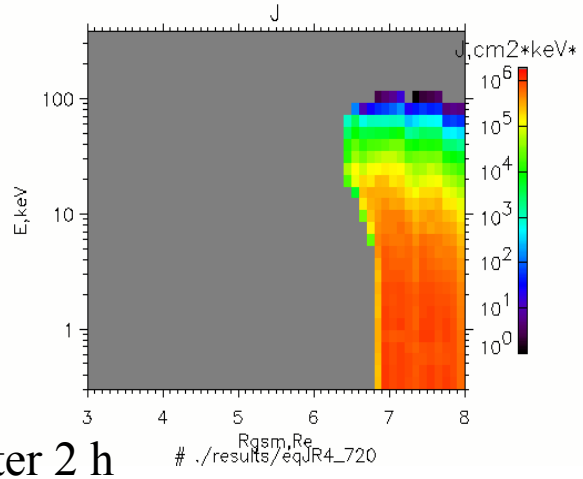

after 2 h

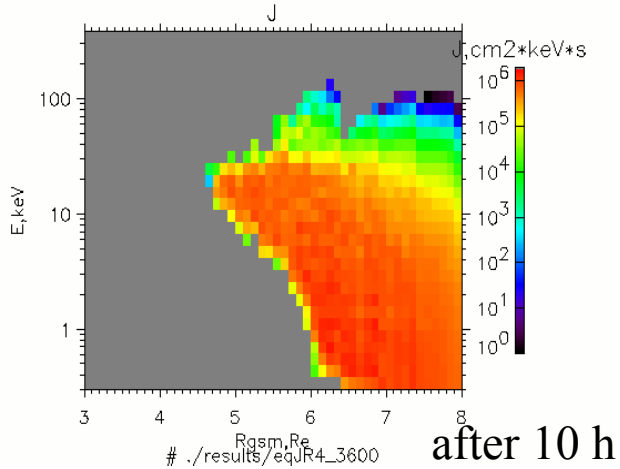

after 10 h

VS+T89+pulse (1mV/m), Kp=1

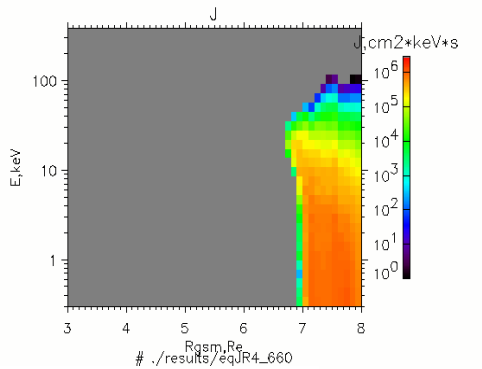

after 2 h

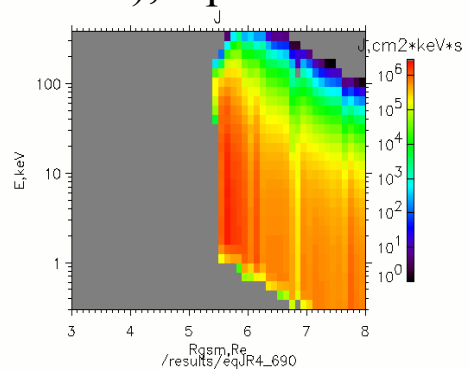

after 2 h 10 min

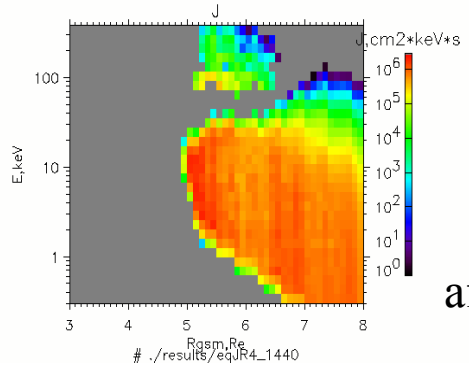

after 3 h 30 min

Wedge-like structures: Viking observations

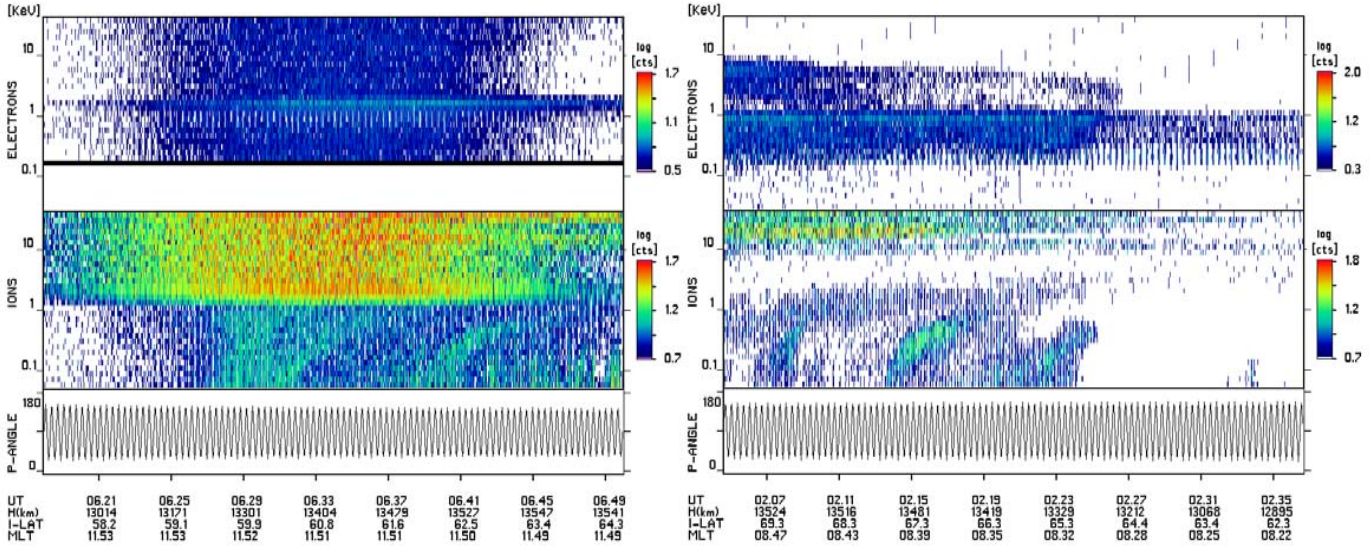

Viking satellite:

- elliptical orbit,
- apogee of 13500 km, perigee of 817 km,
- inclination of 98.8 deg, 262 min period

Positive Ion Energy Spectrometer

positive ions with 0.04 -1.25 keV for PISP 1

1.25-40 keV for PISP 2

Wedge-like structures in the inner magnetosphere

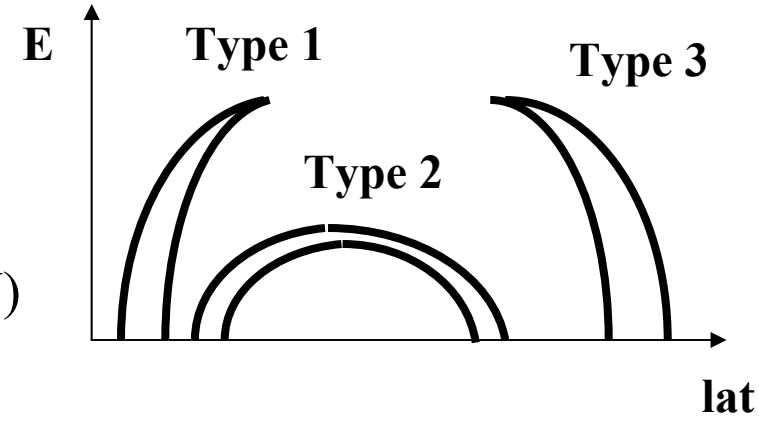

• Not many studies on the low-energy (< 1 keV) fine structures in the ring current region:

• *Yamauchi et al., 1996*: Viking and Freja data - wedge-like dispersed ions - energy-latitude dispersed structures of trapped sub-keV ions;

• *Ebihara et al., 2001*: determination of types of wedge-like structures and modeling.

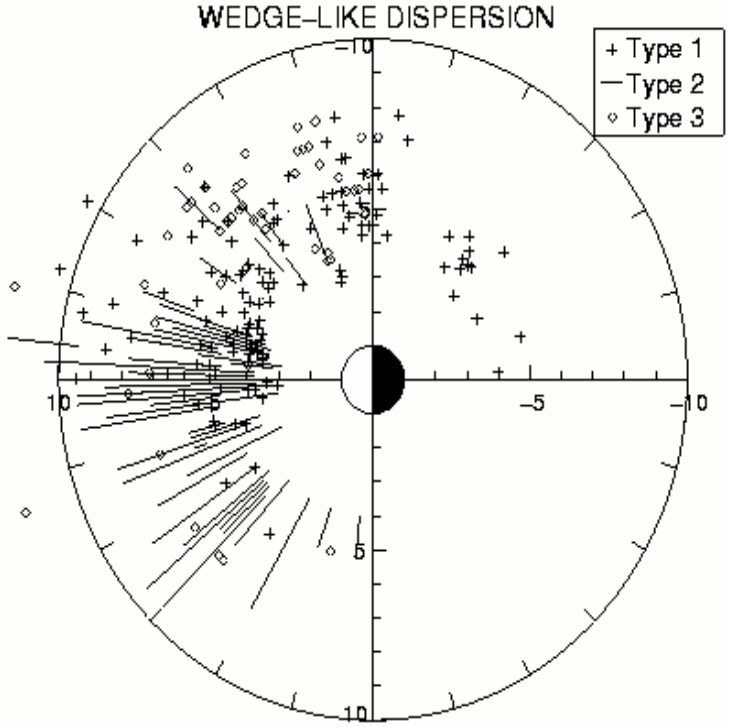

3 types of wedge-like structures: Viking observations

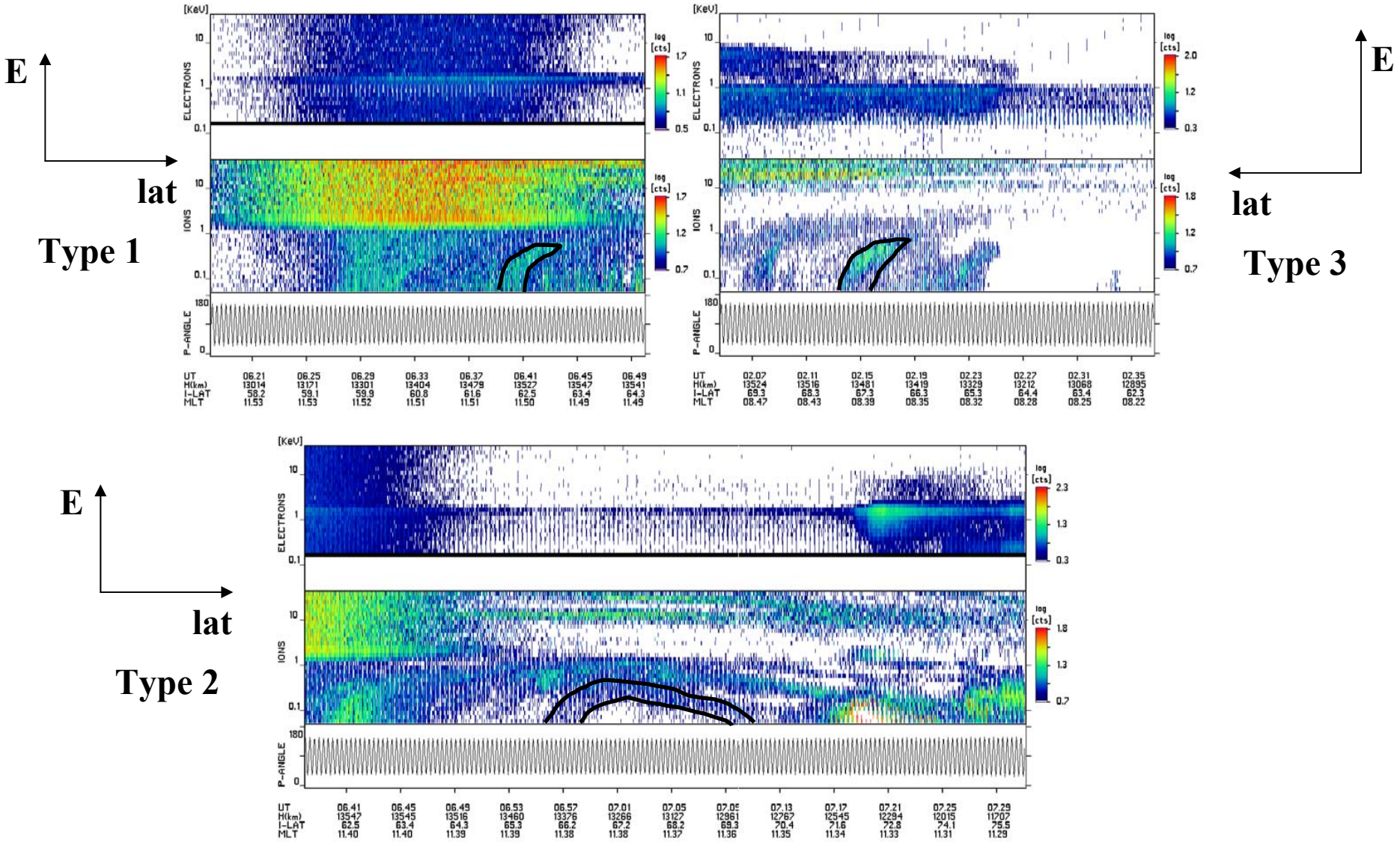

3 types of wedge-like structures: Modeling

(a) Type 1 and 2 dispersions

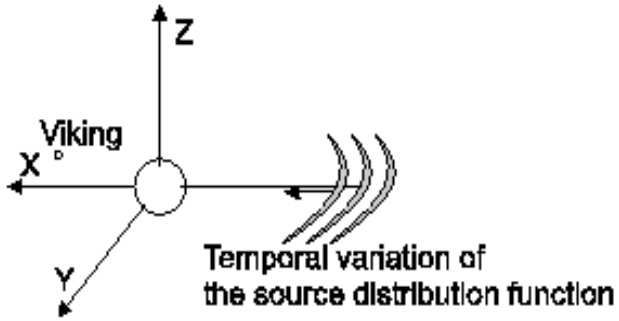

(b) Type 3 dispersion

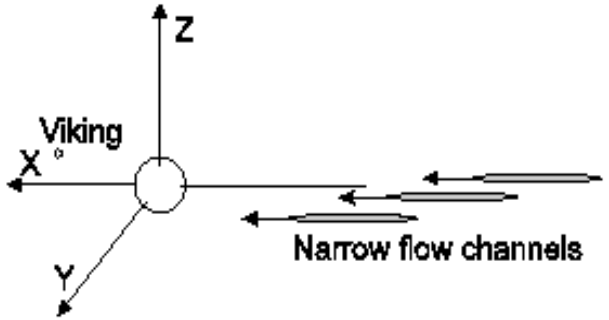

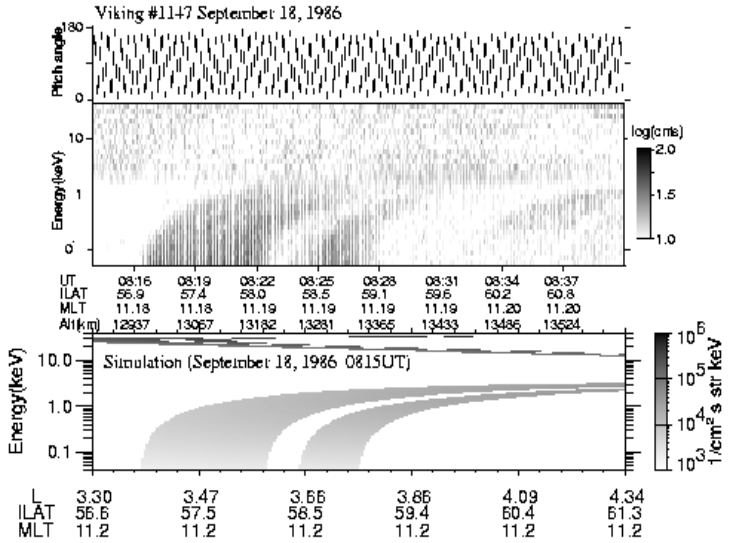

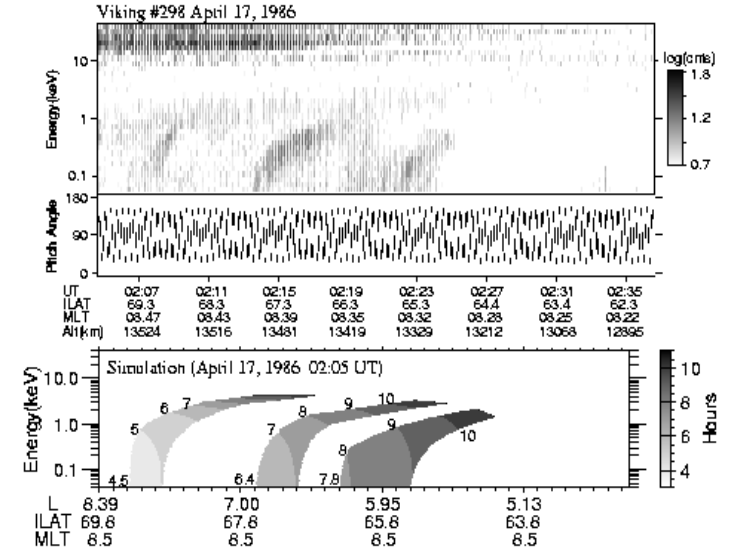

Wedge-like structures: Cluster CIS observations

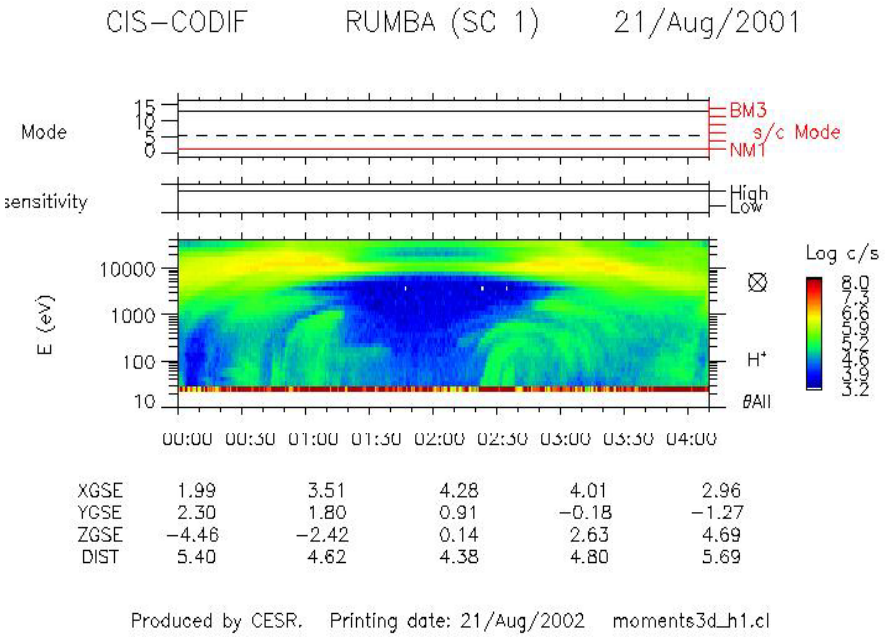

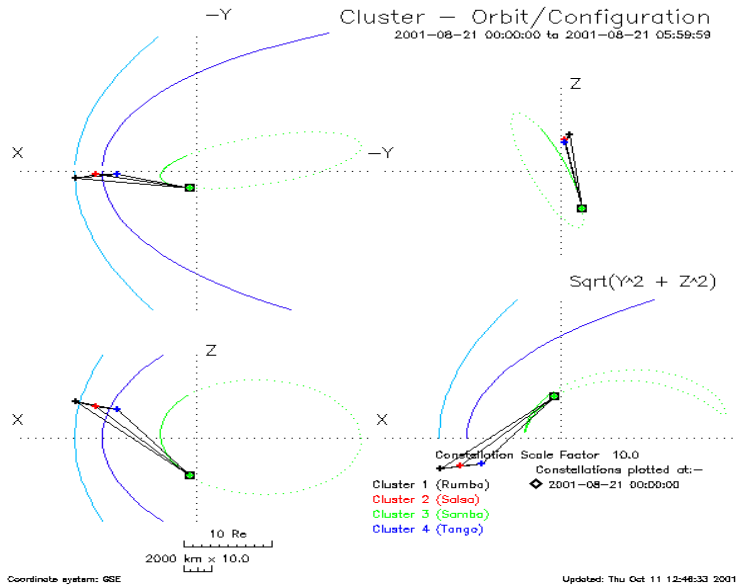

The 4 Cluster spacecraft: detailed 3D map of magnetosphere:

- elliptical polar orbit
- perigee: 19 000 km, apogee: 119 000 km
- period: 57 hours

CIS (Cluster Ion Spectrometry) experiment:
full 3D ion distributions (about 0 to 40 keV), time resolution of 4 sec
COmposition and DIstribution Function analyser (CIS1/CODIF), mass per charge composition with 22.5° angular resolution,
Hot Ion Analyser (CIS2/HIA), no mass resolution but angular resolution (5.6°)

Wedge-like structures: Cluster CIS observations

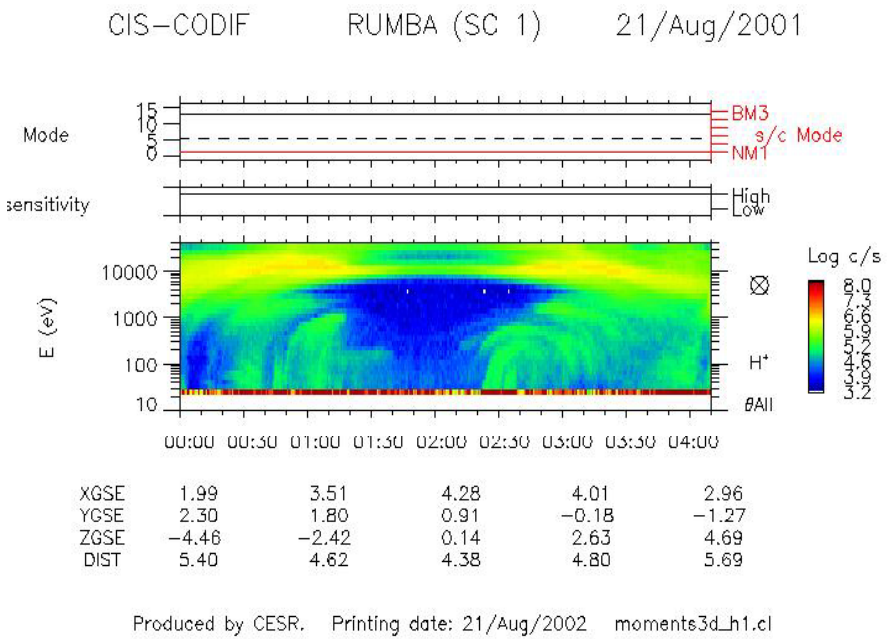

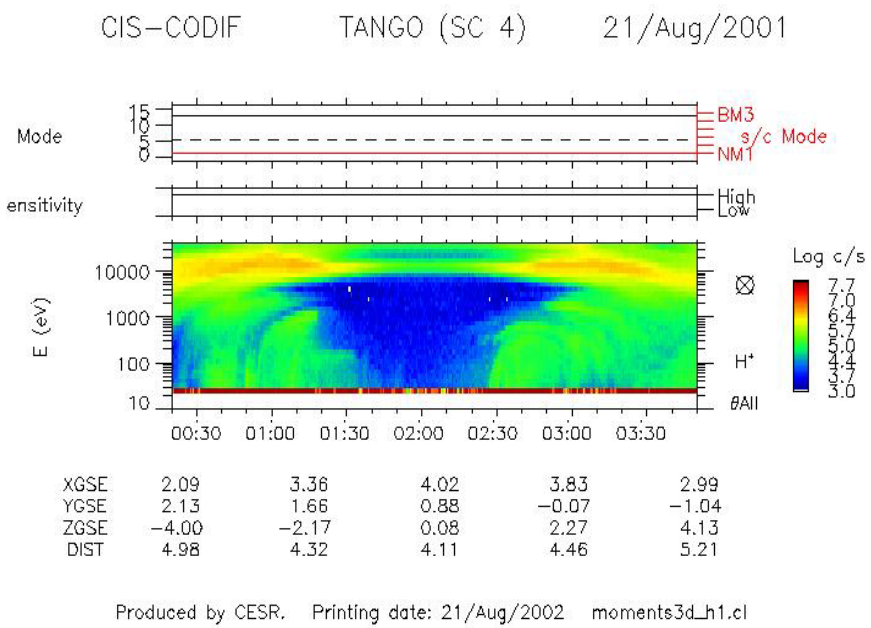

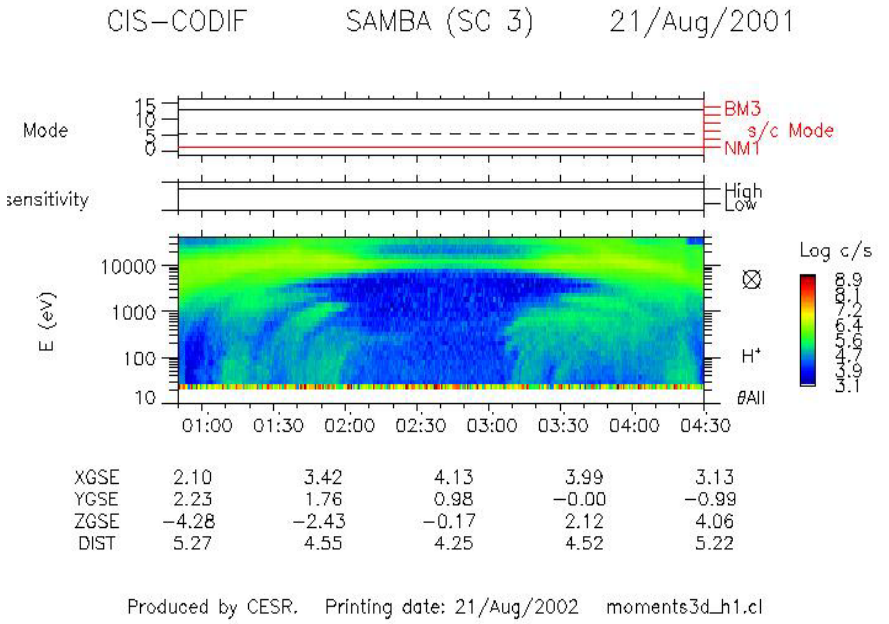

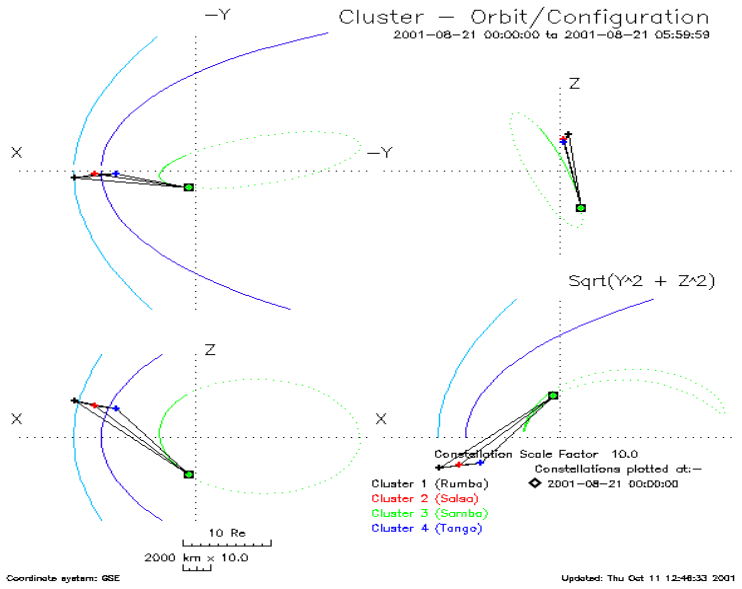

Wedge-like structures: Modeling of Cluster CIS observations (1)

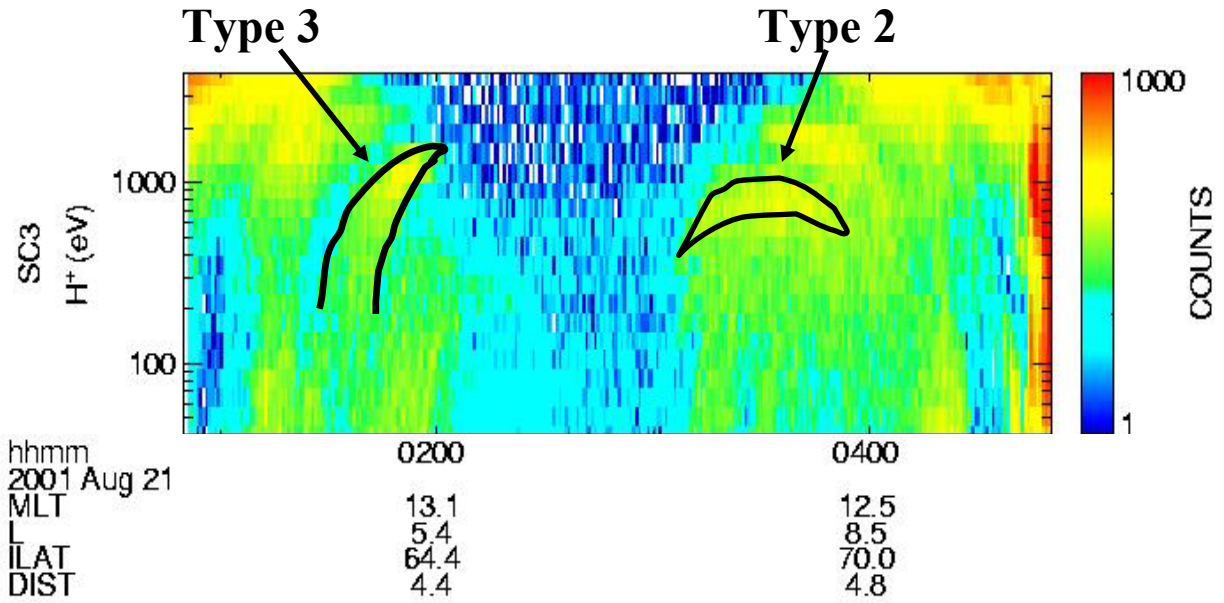

Type 3, observe
0145-0200 UT
67.1-64.6 MLA
13.2 MLT
L=6.6-5.4

Backward tracir
22.4-22.8 MLT
at L=10

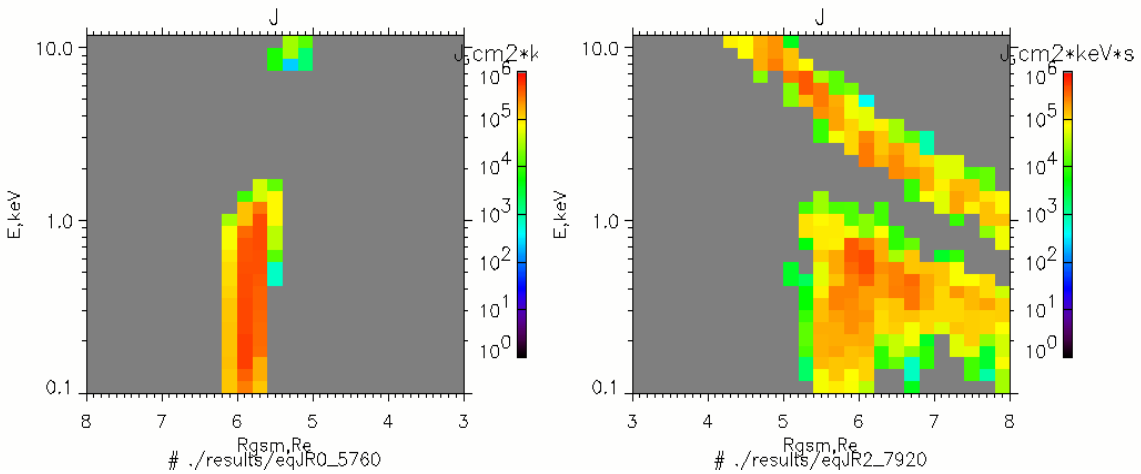

Type 2, observed:
0310-0400 UT
59.0-65.7 MLAT
12.0 MLT
L=4.6-8.5

Injection of 1 hour
duration

Wedge-like structures: Modeling of Cluster CIS observations (2)

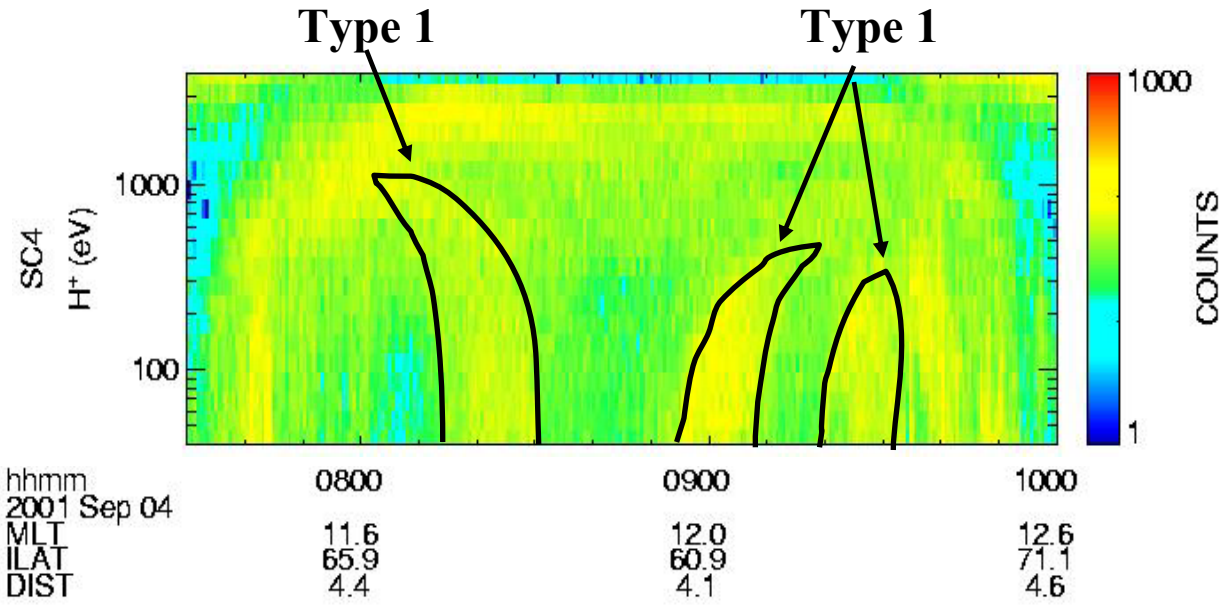

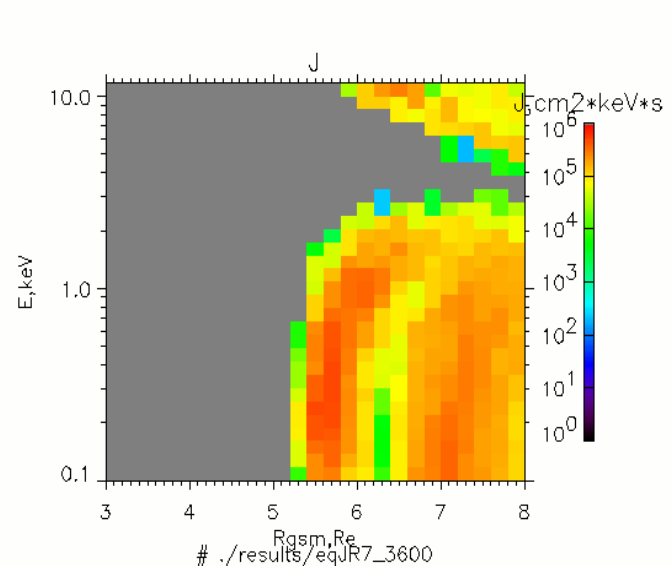

Type 1, observed:
0855-0910 UT
60.2-61.8 MLAT
12. MLT
L=5.4

2 injections of 1 hour duration each 2 hours apart

Akebono LEP measurements

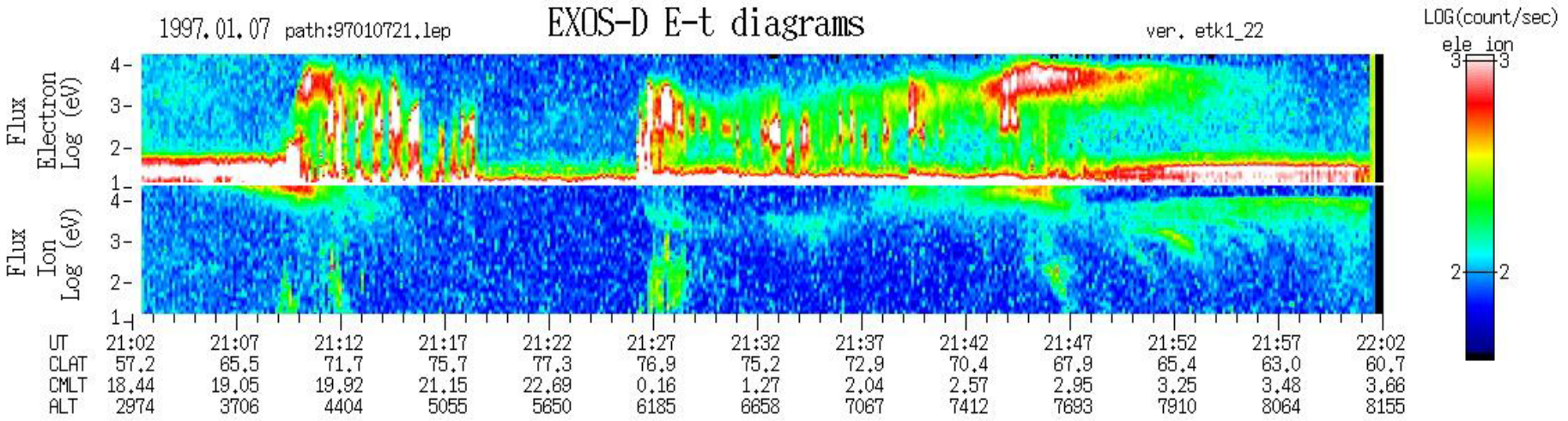

Akebono satellite:

- **elliptical orbit**
- **with inclination of 75.1 deg**
- **initial perigee of 272 km,**
- **apogee of 10482 km,**
- **evolution period of 212 min**

LEP (Low Energy Particles)

- **electrons, 10 eV-16 keV**
- **ions, 13 eV/q-20 keV/q.**

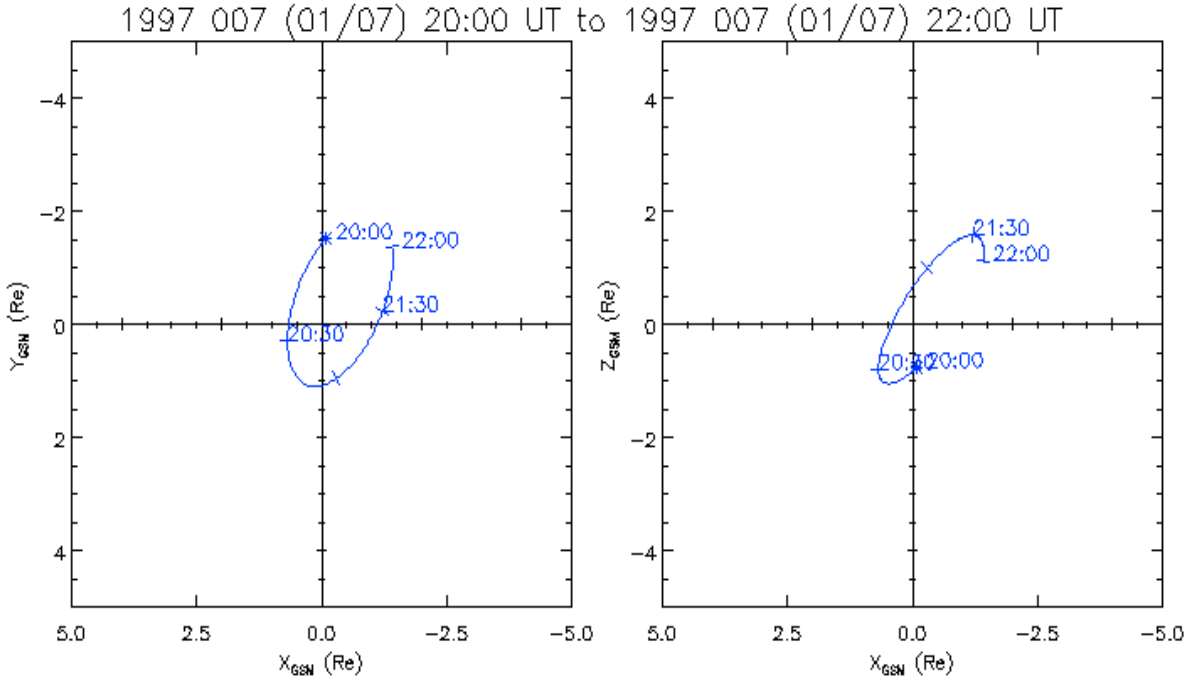

Akebono LEP measurements

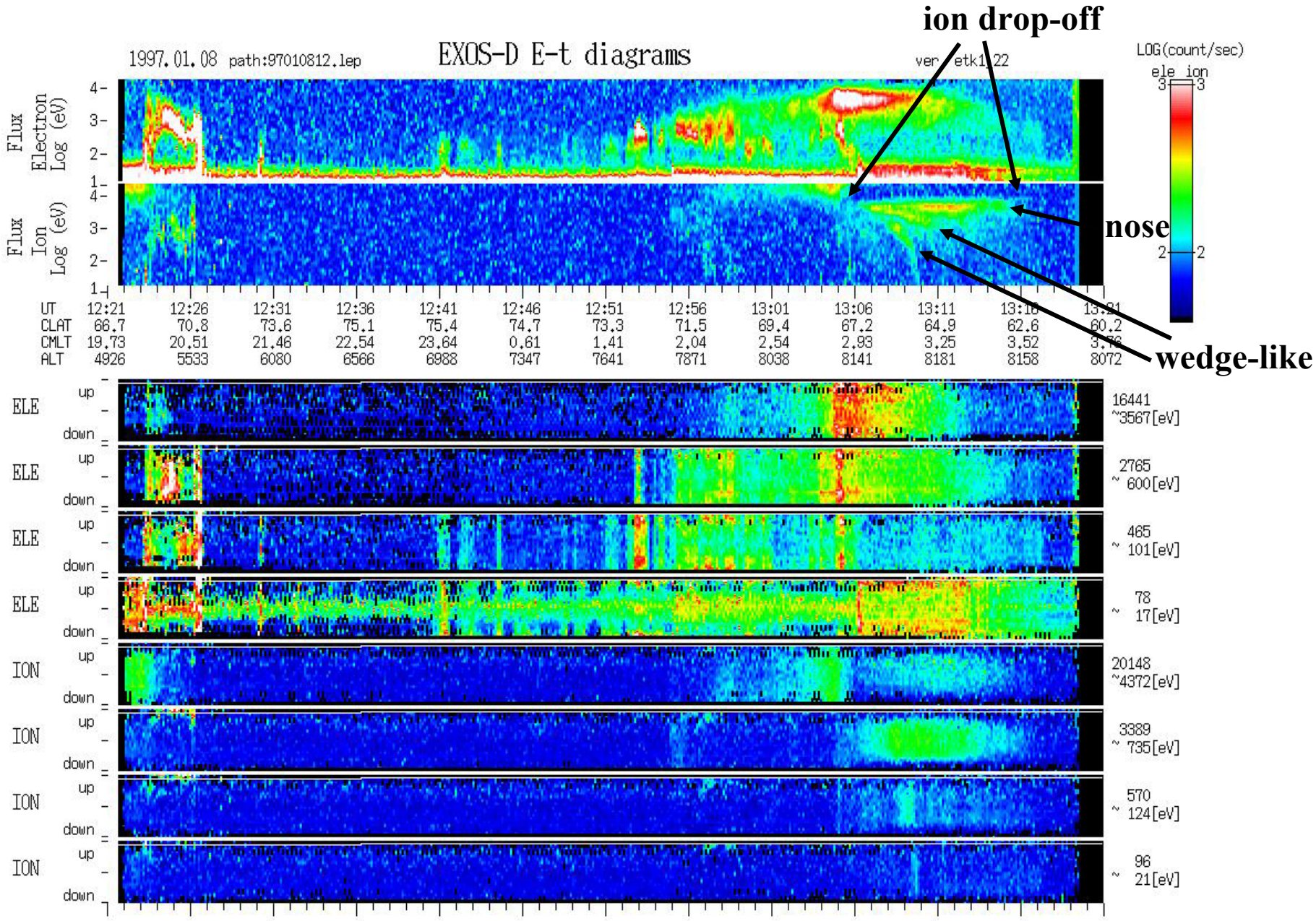

Wedge-like structures: Statistical results

Courtesy of Dr. Yu. Ebihara

Viking

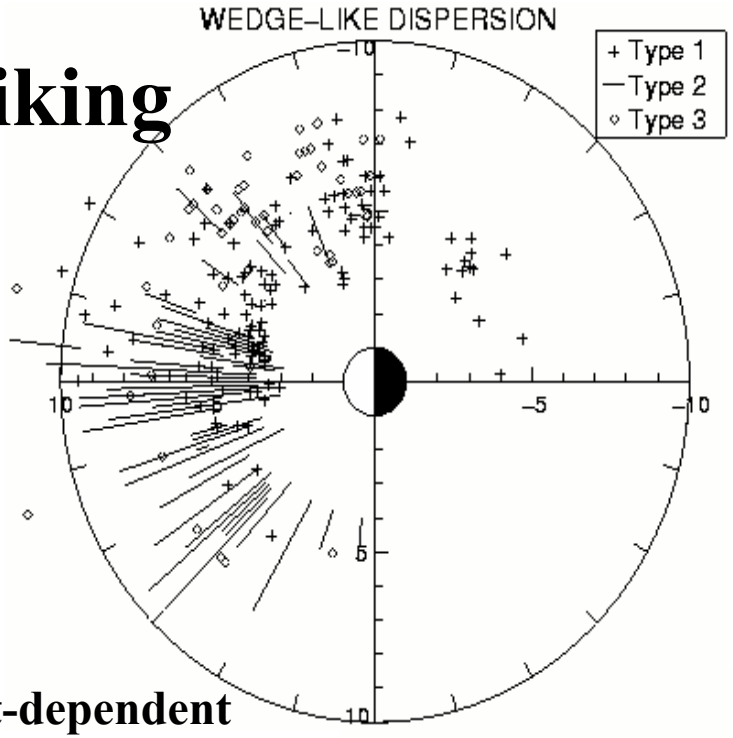

Orbit-dependent

Akebono

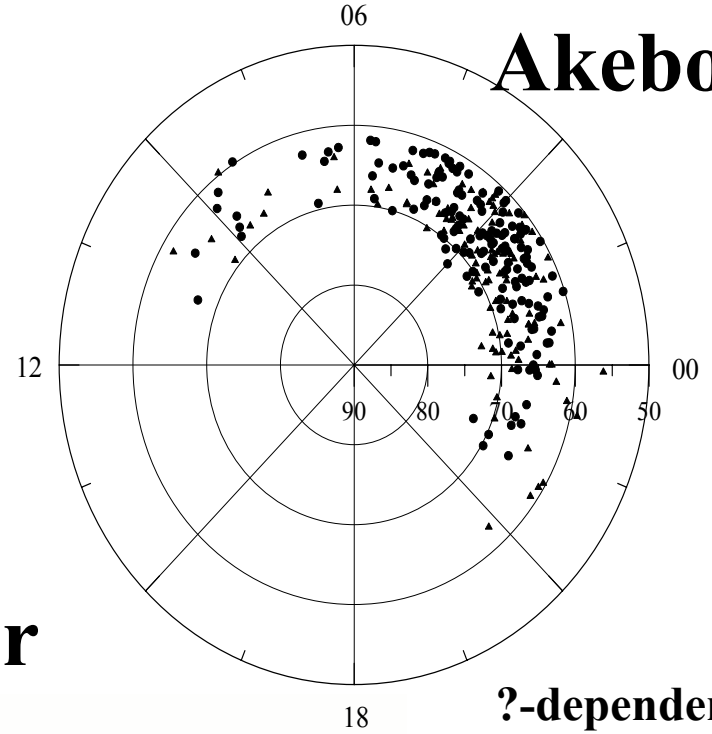

?-dependent

Cluster

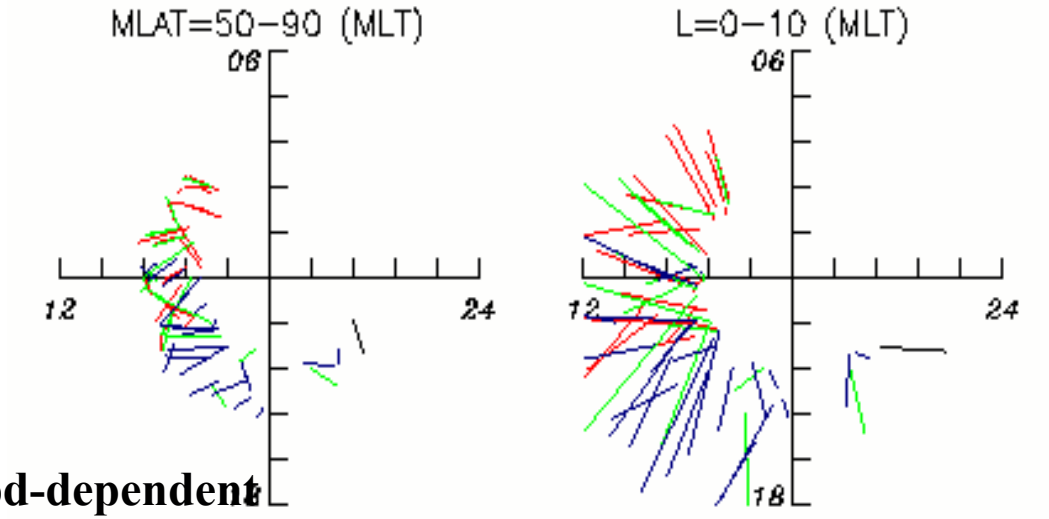

Analyzed period-dependent

Akebono LEP observations during January 6-7, 1997

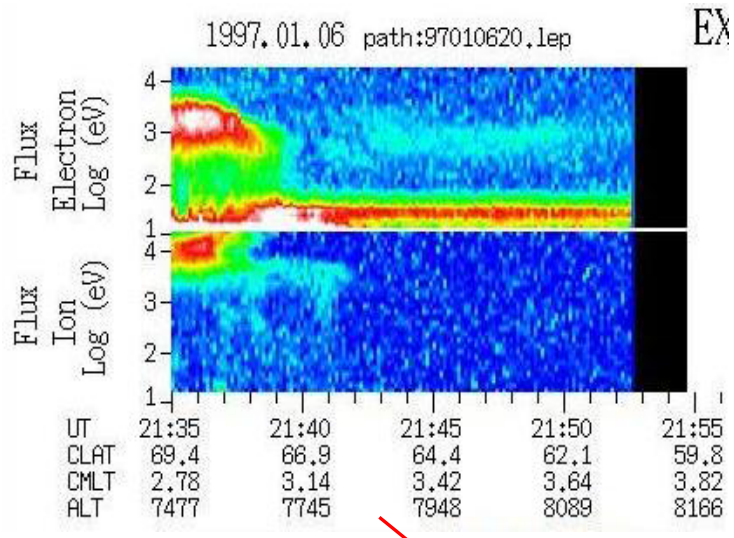

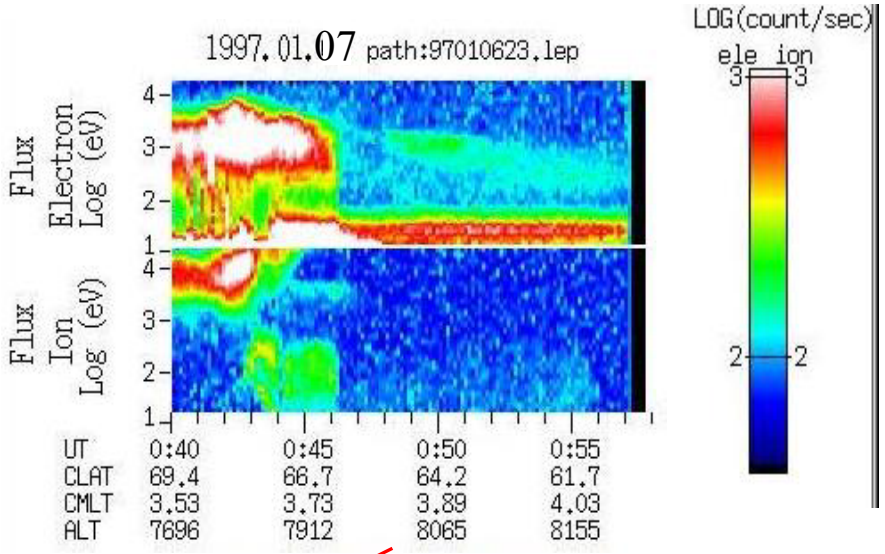

January 6, 1997 Kp: 1-1-0+1-1+1-0+0+

Kp: 2+4 2 2+3-3-2+2- January 7, 1997

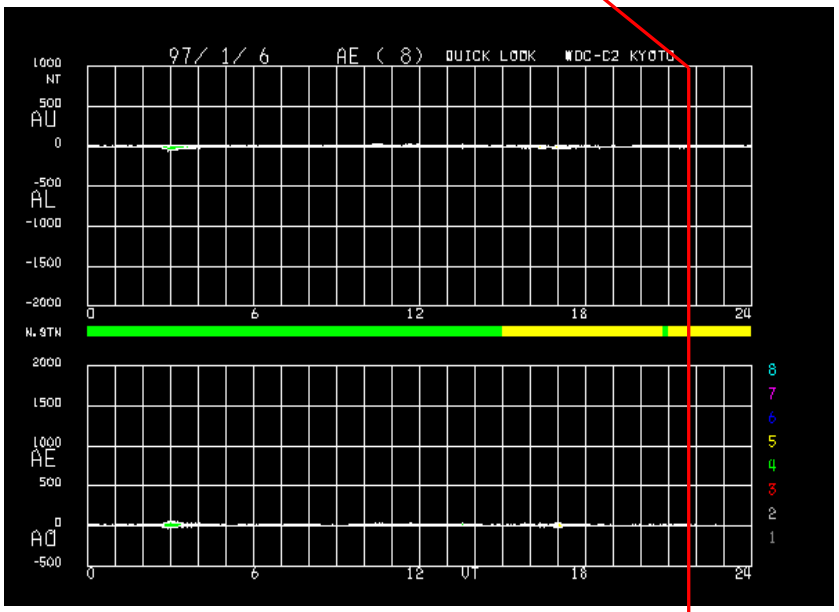

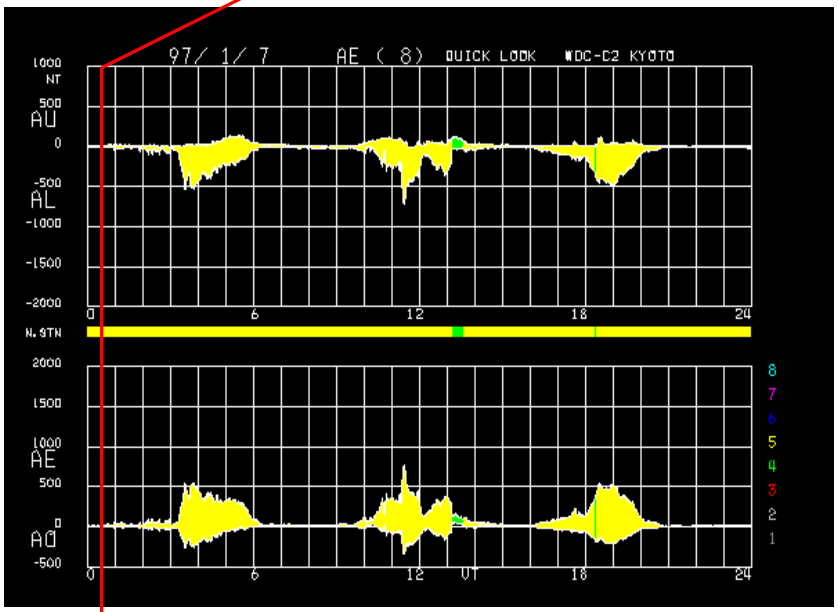

Akebono LEP observations during January 7, 1997

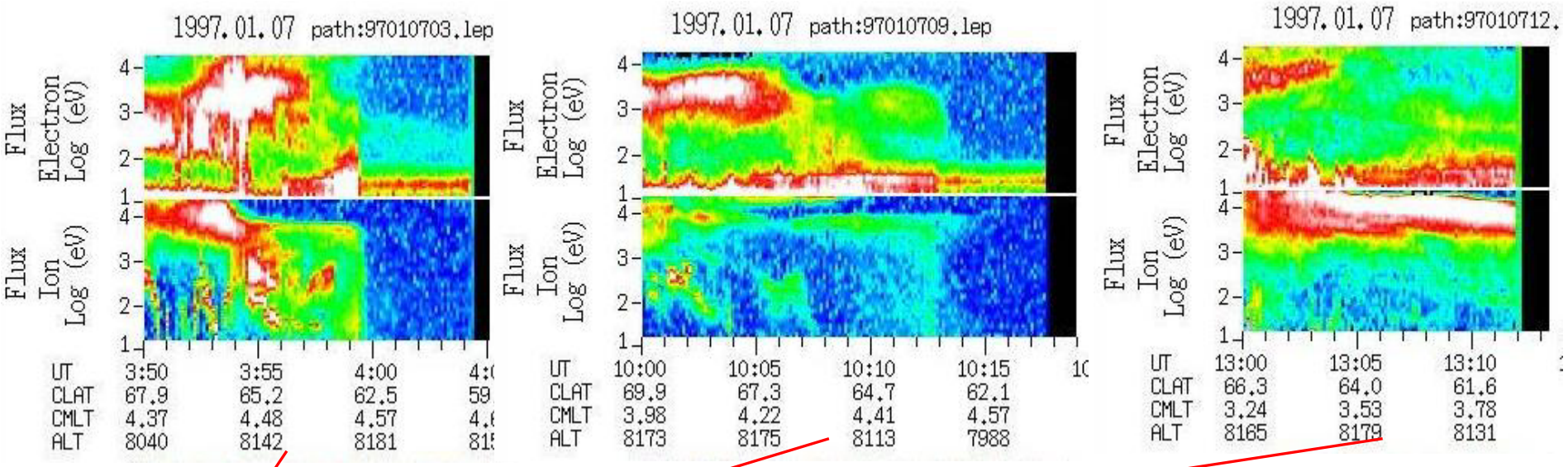

Kp: 2+4 2 2+3-3-2+2-

WL appeared after substorm was over, about 1.5 ho

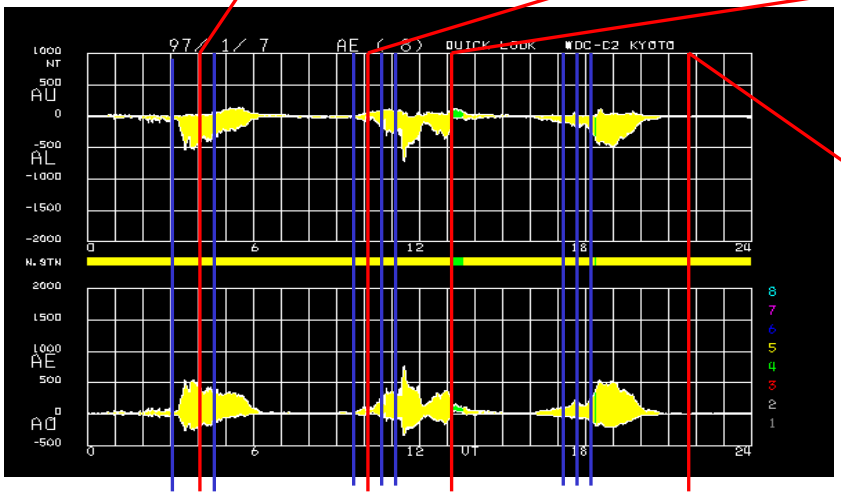

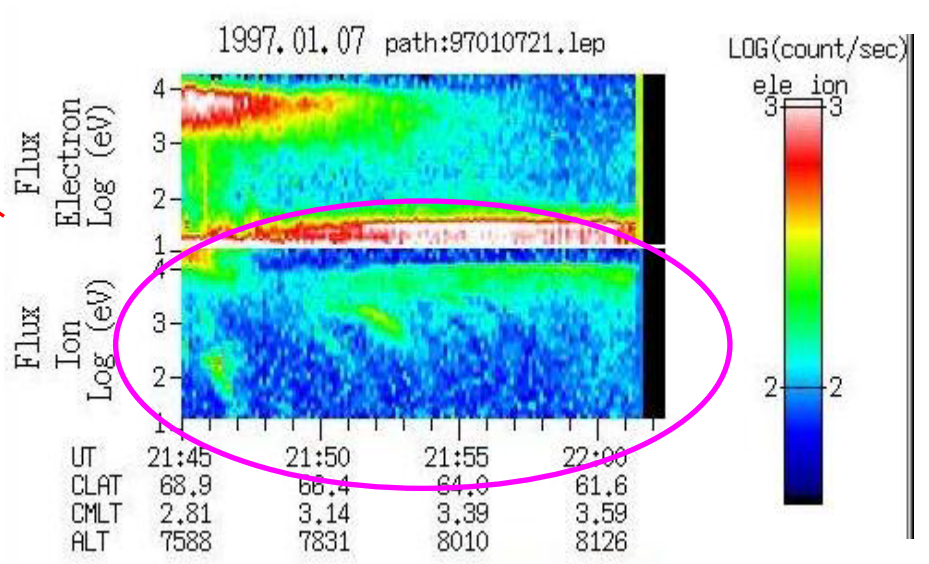

0308 0422 0955 1035 1707 1729 1819

LANL 1990-095 1115 Honolulu Kakioka Pi2

LANL 1994-084

Akebono LEP observations during January 8, 1997

After 4.5 hours - no WL

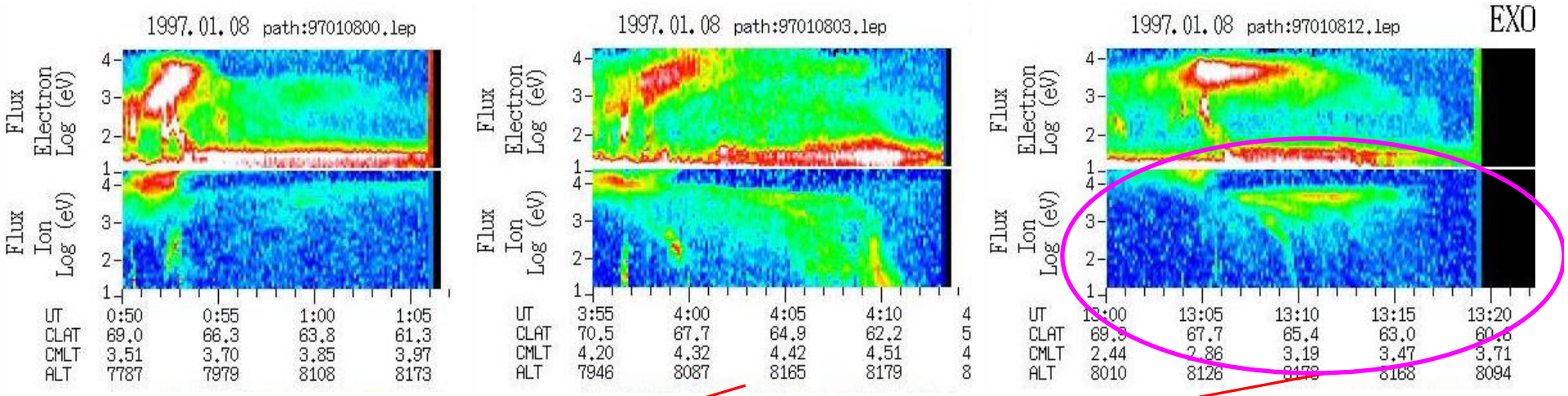

Kp: 3-3+1+1 2 1+1+2-

very clear WL after 8 hours after substorm

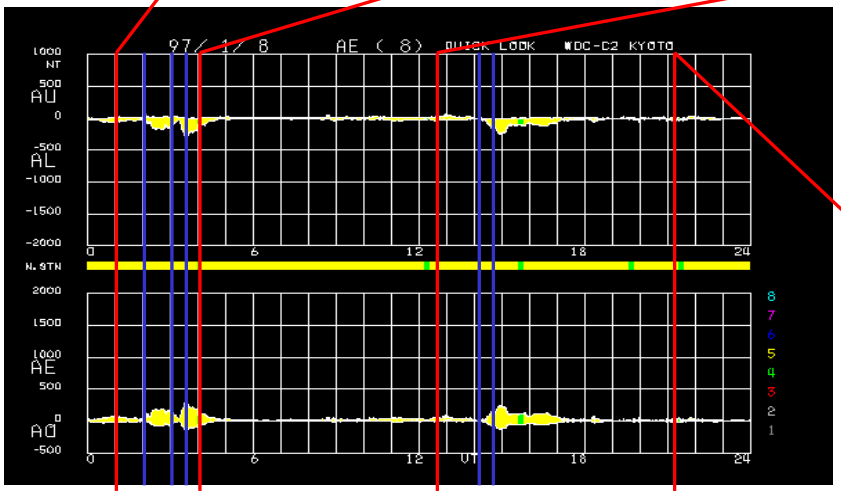

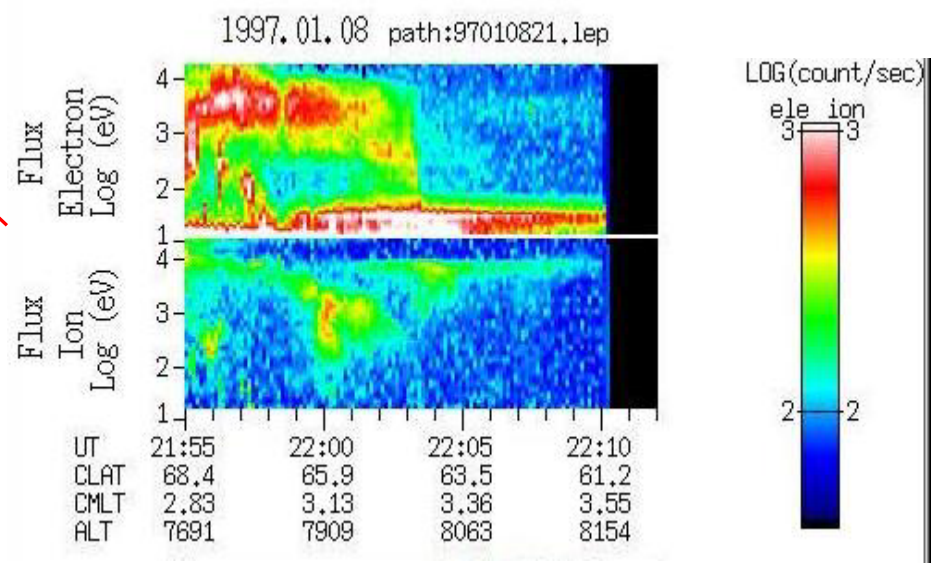

0315 0330
LANL 1990-095

1415 1440
Kakioka Pi2

0200
Fredericksburg

Akebono LEP observations during January 9, 1997

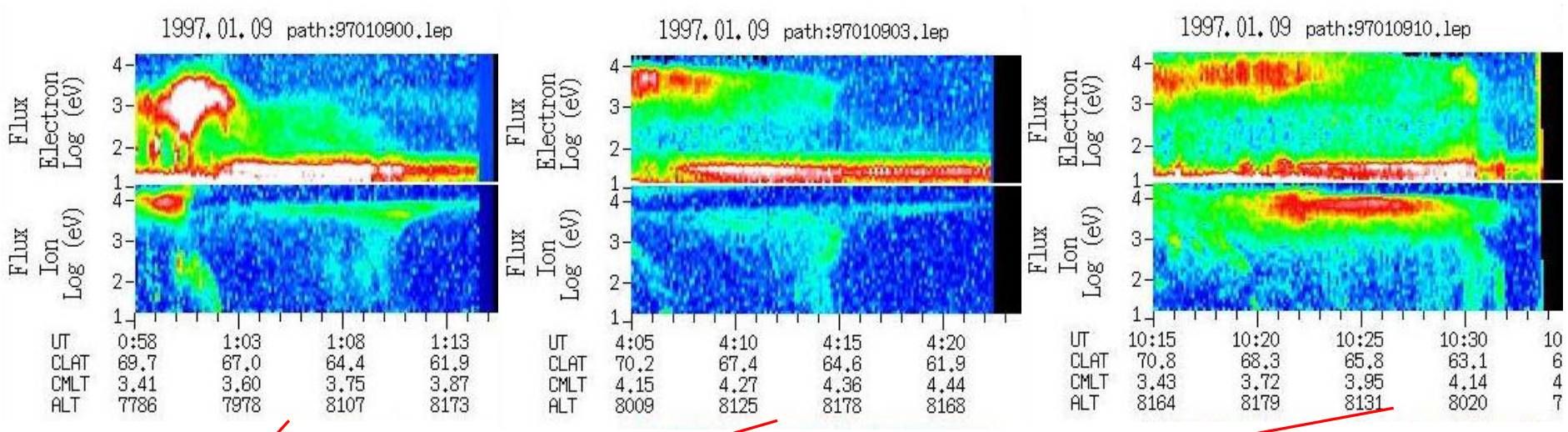

Kp: 2 1+2+1 1-0+1+2

WL appeared after small disturbance in AE

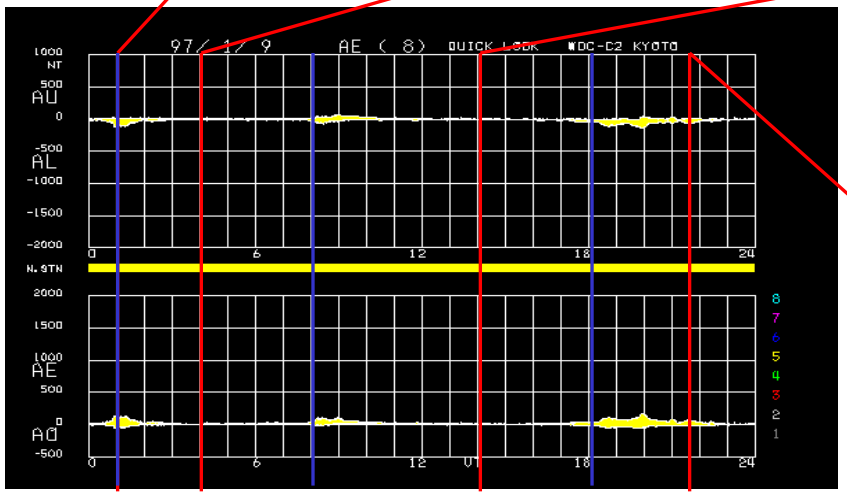

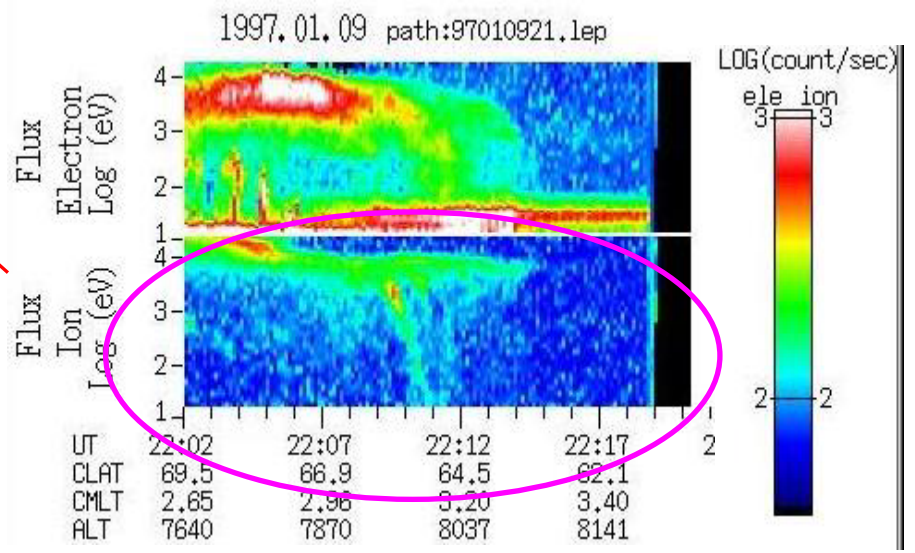

0100 LANL 1991-080

0750 LANL 1990-095

1815 Kotel'nyy

Clear wedge-like structures observed by Akebono LEP

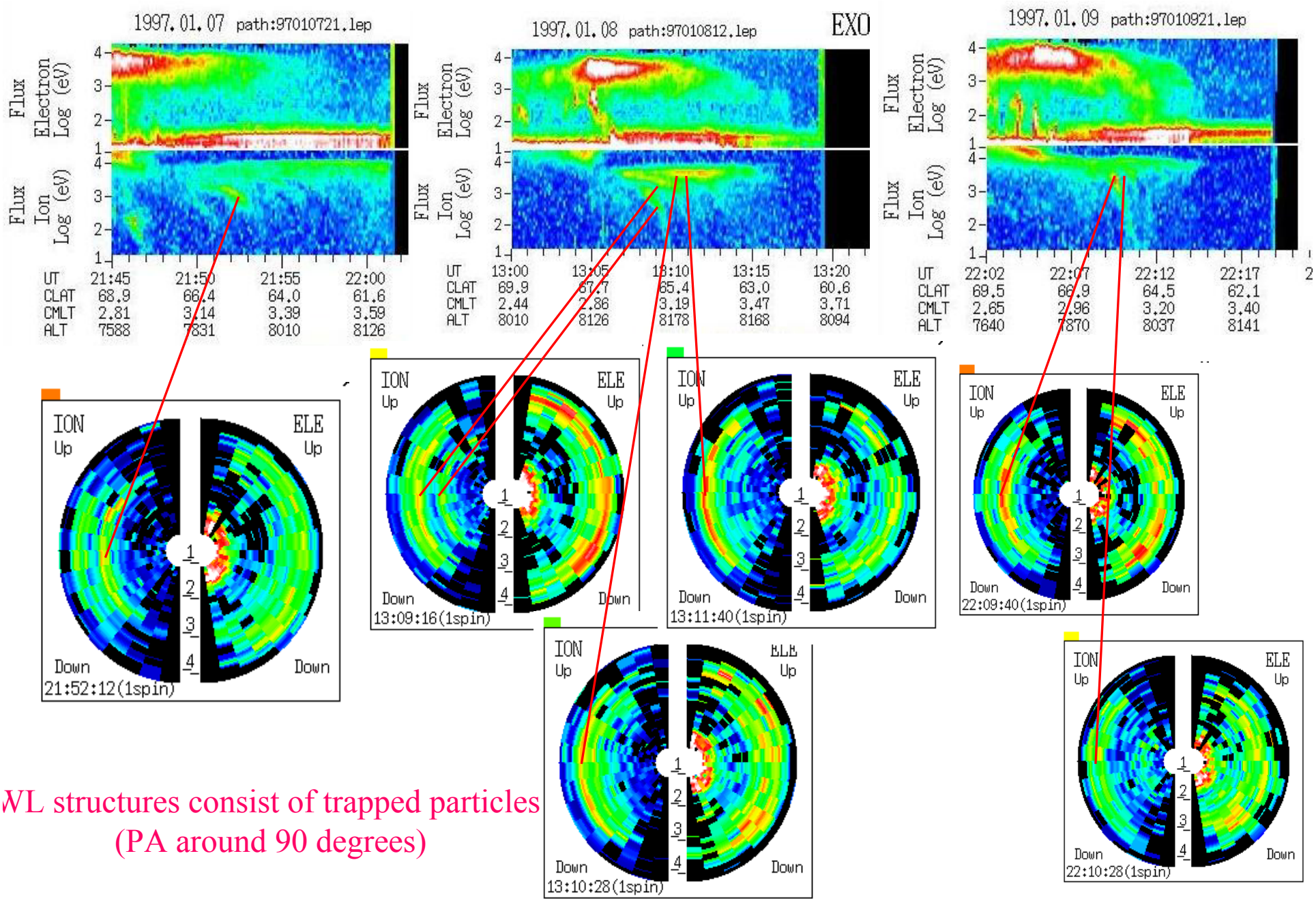

WL structures consist of trapped particles
(PA around 90 degrees)

Modelling of Akebono LEP observations of WL on January 7, 1997

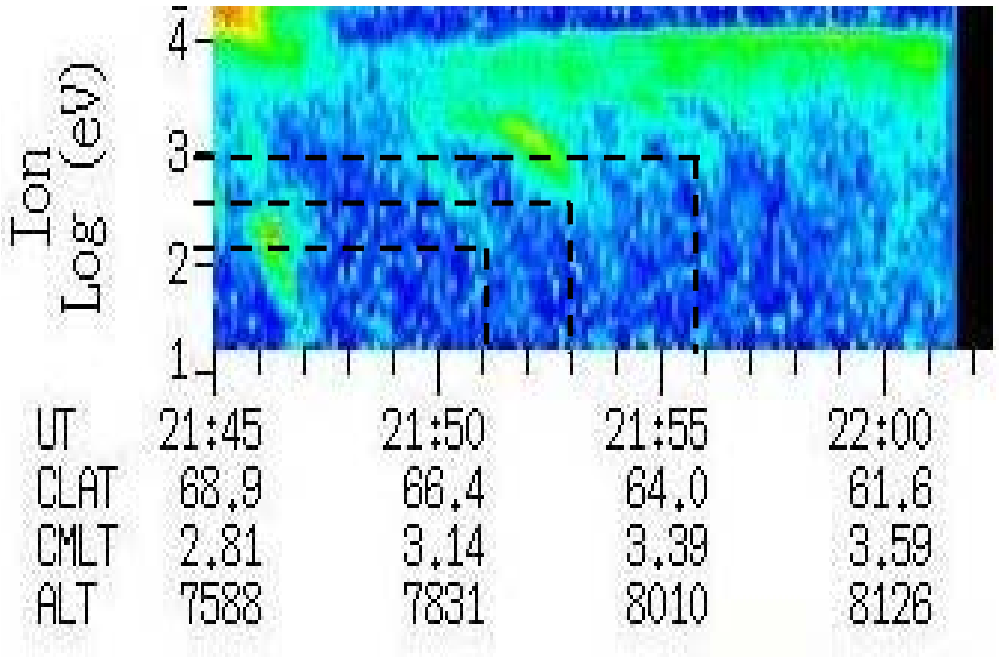

3 WL structures identified, lowest energies at:
2151 UT, 0.1 keV, L = 5.6, 0320 MLT, 11° PA
2153 UT, 0.3 keV, L = 5.2, 0325 MLT, 12° PA
2156 UT, 0.6 keV, L = 4.7, 0332 MLT, 15° PA

backward tracing in time, reaching L = 8:
2151 UT, 0.1 keV, after 2.78 hours, at 1904 UT
2153 UT, 0.3 keV, after 4 hours, at 1753 UT
2156 UT, 0.6 keV, after 5.65 hours, at 1617 UT

Forward tracing with 1 minute increase of n in initial distribution at L = 8 at 1617, 1753 and 1904 UTs.

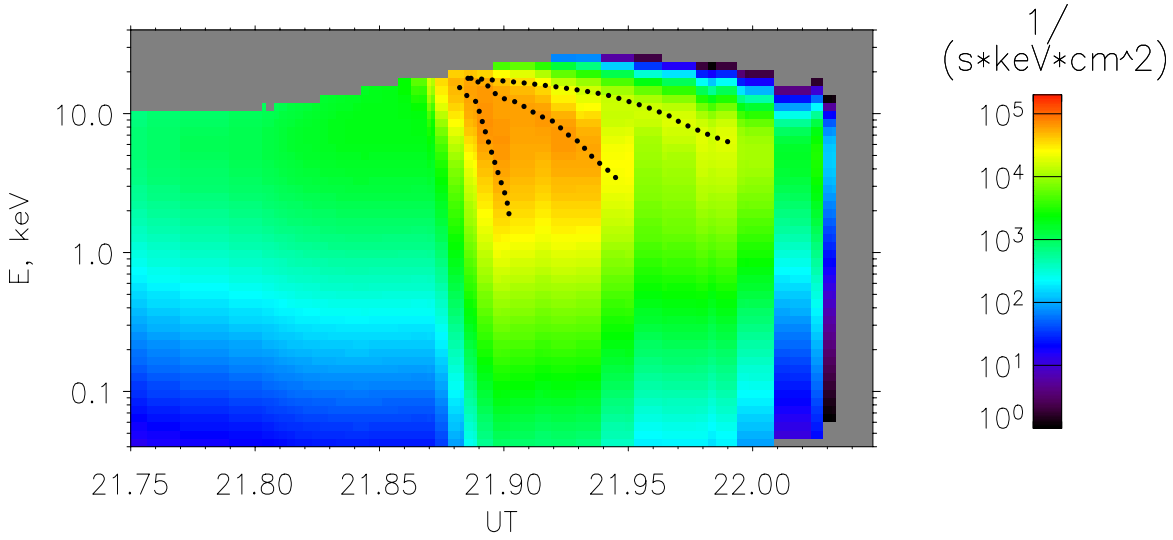

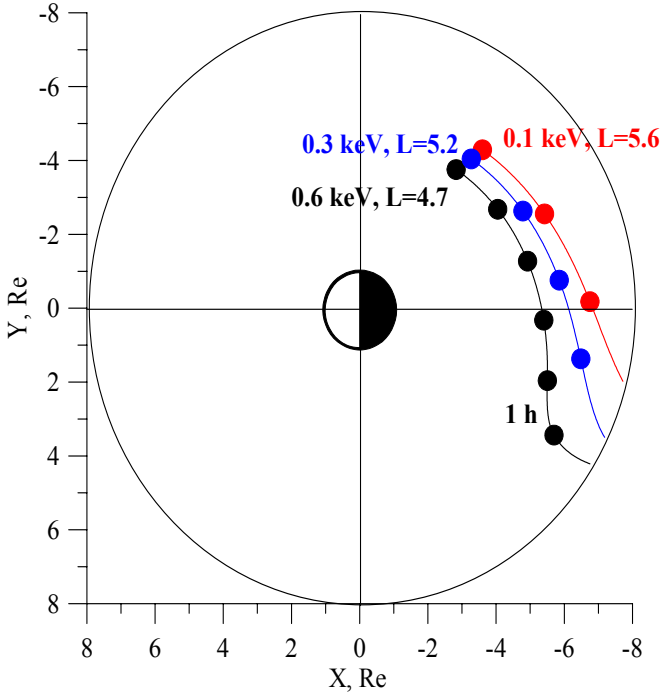

Variations of source distribution and substorm onsets in the tail

Onsets:
LANL SOPA
magnetograms

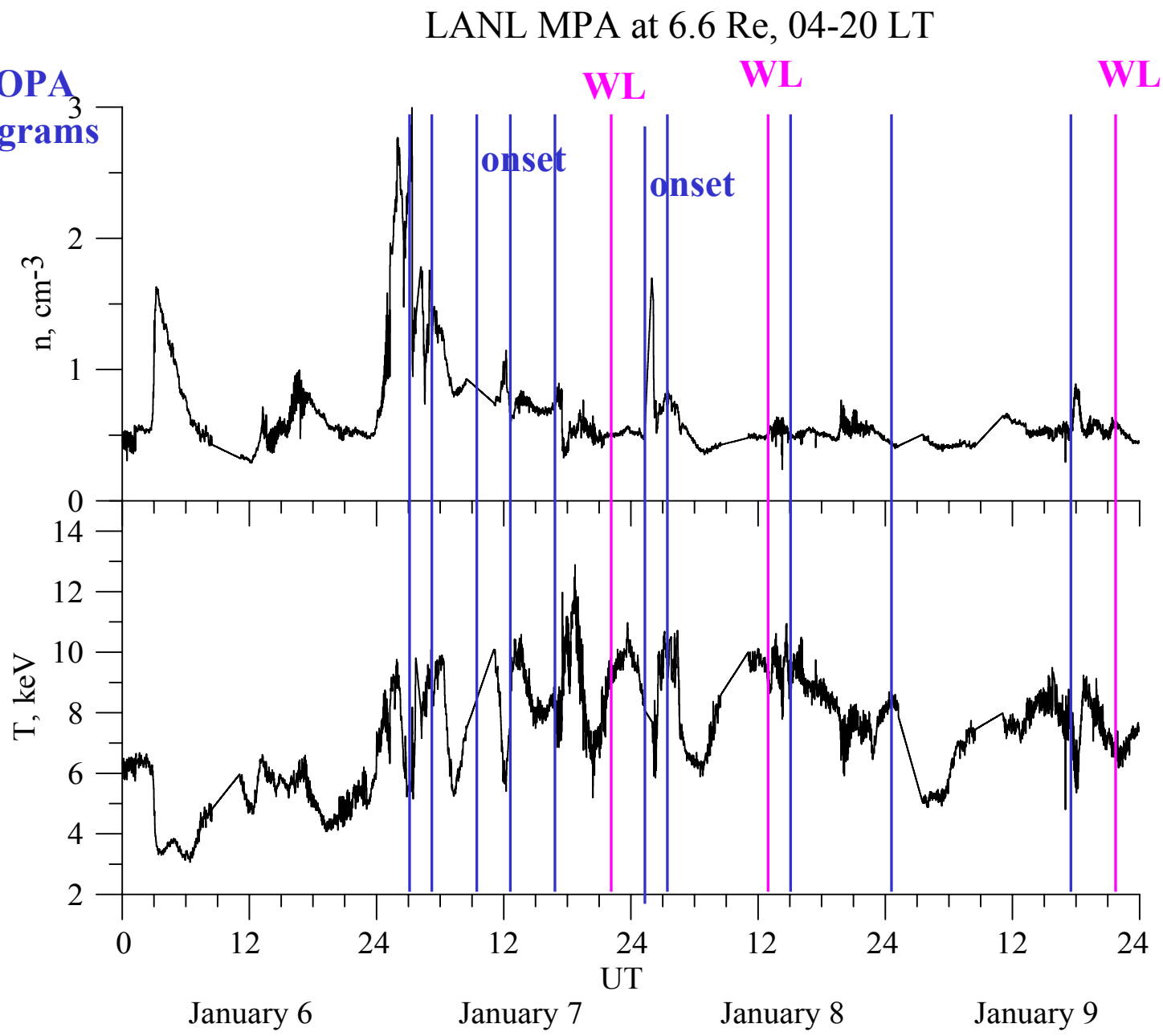

Modelling of Akebono LEP observations of WL on January 6-7, 199

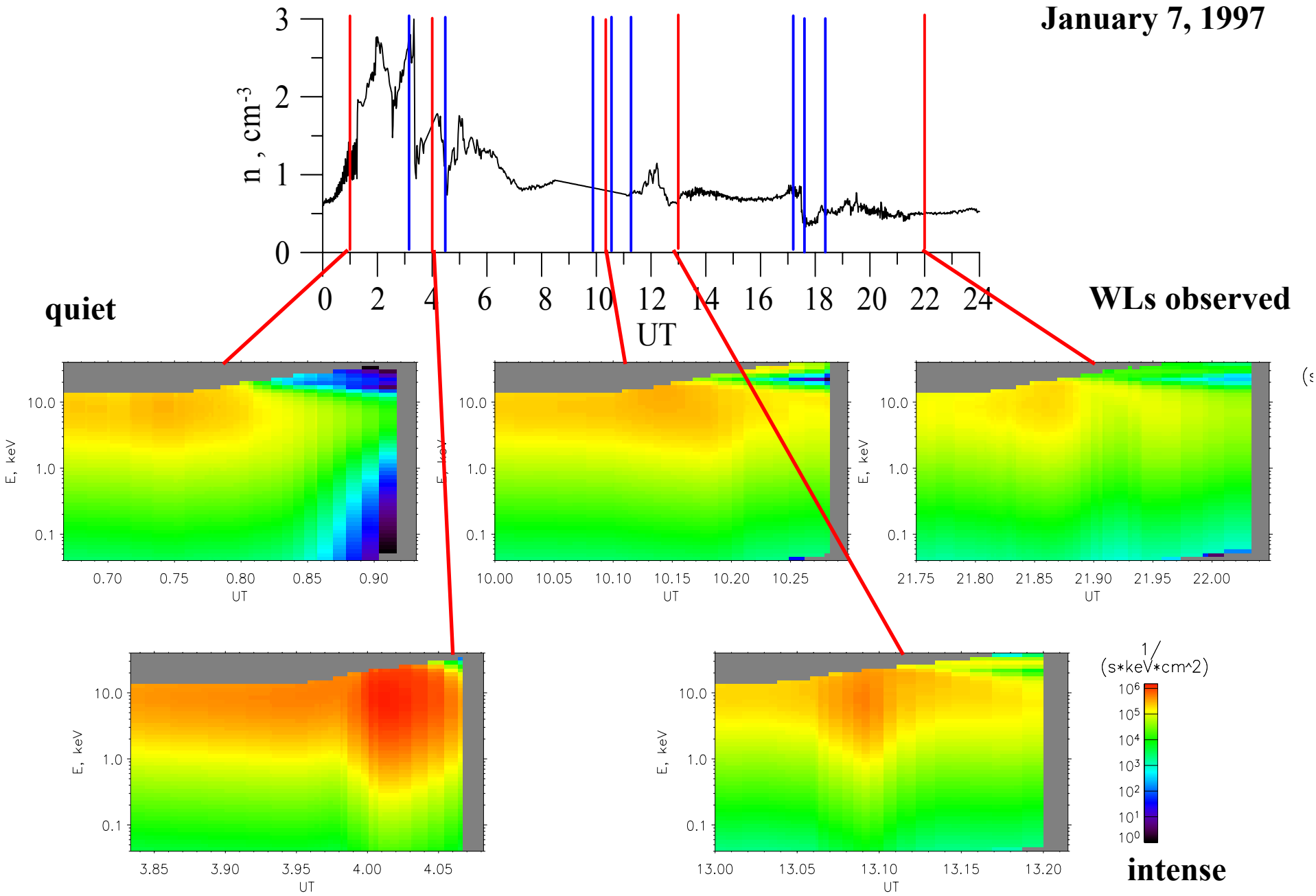

Summary for wedge-like structures

- We studied energy-dispersed ion structures, called wedge-like structures (WL), observed by Akebono LEP instrument.

- The observed ion structures are trapped ions extended in energies from 100 eV up to few keV in Type 1 sense, with maximum flux at above 1 keV at inv. lat within 60-70 deg.

- They are mainly concentrated in the dawn LT sector, Viking and CLUSTER observations are in dayside sector – orbit-dependent statistics

- January 6-9, 1997 observations analysed in details: January 6 was very quiet day, later each WL observatic was after a small substorm, time differs.

- Backward tracing of lowest energies in WLs seen on LEP spectrograms in Kp-dependent large-scale electr and magnetic fields showed easy access of plasma sheet particles to Akebono orbit with longest time of 5 ho

- Artificial increase of source number density in the plasma sheet with 1 minute duration was successful to reproduce the observed WLs (similar to Ebihara et al, 2001).

- Introducing the observed (LANL MPA) variations of number density and temperature did not result in reproducing the observed spectrograms, no observations of large 1 minute variations necessary for WL forma

- Role of substorm-associated fields should be considered

Dynamical inner magnetosphere: fields, currents and particles

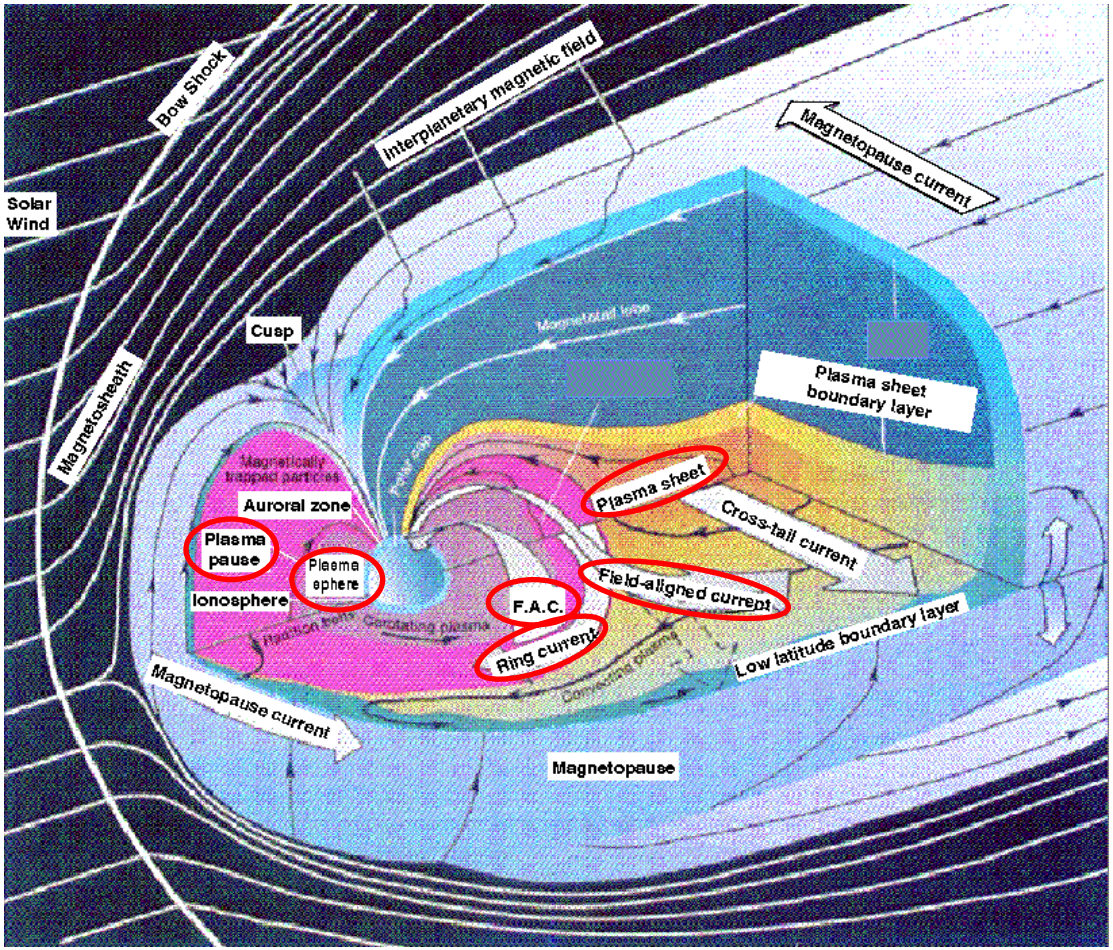

- ***Particles*** carrying currents move in electromagnetic fields
WELL-KNOWN

- ***Magnetic fields***: model accuracy and applicability
OPEN QUESTION

- ***Electric fields***: scales, nature, models for disturbed times
OPEN QUESTIONS

- ***Ring current***: storm key element,
- ***Space weather***: damage to space- and ground-based technological systems and danger to human
WELL-KNOWN

- ***Ring current formation*** during storms:
MANY OPEN QUESTIONS..